The Role of HEXIM1 in the Transcriptional Regulation of Neural Crest Differentiation and Melanoma

The Role of HEXIM1 in the Transcriptional Regulation of Neural Crest Differentiation and Melanoma

A dissertation presented

by

Justin Lee Hong Tan

to

The Committee on Higher Degrees in Chemical Biology

in partial fulfillment of the requirements
for the degree of
Doctor of Philosophy
in the subject of
Chemical Biology

Harvard University
Cambridge, Massachusetts

April 2014

Dissertation Advisor:

Professor Leonard Ira Zon

Author:

Justin Lee Hong Tan

The Role of HEXIM1 in the Transcriptional Regulation of Neural Crest Differentiation and Melanoma

Abstract

Recent evidence suggests that leflunomide, a dihydroorotate dehydrogenase (DHODH) inhibitor, disrupts neural crest development and melanoma pathogenesis via inhibiting transcription elongation. DHODH is an enzyme in the pyrimidine biosynthetic pathway and inhibition of this enzyme by leflunomide triggers a low nucleotide state. Leflunomide effectively ablates the neural crest lineage in embryonic zebrafish, preventing the formation of mature melanocytes, among other neural crest lineages. This drug also effectively suppresses melanoma and is in a clinical trial, administered in combination with the BRAF inhibitor vemurafenib, for metastatic melanoma. Despite knowing that leflunomide targets transcription elongation, the mechanism by which low nucleotides directly regulates transcription is unknown.

Here, we provide evidence that a transcriptional regulator, HEXIM1, is upregulated in response to leflunomide. HEXIM1 is assembled into the 7SK snRNP complex to sequester and inhibit the kinase P-TEFb. P-TEFb triggers elongation by phosphorylating RNA polymerase II and other pausing factors. Knockdown of *hexim* in zebrafish rescues the effects of leflunomide. HEXIM1 expression is low in human melanoma and overexpression of this gene can suppress melanoma onset *in vivo* in zebrafish. Increased HEXIM1 expression, in response to low nucleotides triggered by DHODH inhibition, sequesters P-TEFb away from genes associated

with melanoma pathogenesis, proliferation and cell cycle based on ChIP-seq and GRO-seq analyses. This inhibits productive transcription elongation at genes that maintain the tumorigenic state. Our study illustrates that HEXIM1 responds to cell stress to suppress tumorigenesis by inhibiting productive elongation of proliferative genes in melanoma. Targeting HEXIM1 can therefore prove useful in treating melanoma.

Contents

Citations to Submitted Work

Parts of chapter 2 and 3 have been written as one manuscript and submitted for publication as:

Tan, J.L., Fogley, R.D., Santoriello, C., Saint-André, V., Yang, S., Fan, Z.P., Laga, A.C., van Rooijen, E., Greer, C.B., Kim, Y.J., Fujinaga, K., Brogie, J.E., Price, D.H., Peterlin, B.M., Zhou, Y., Kim, T.H., Asara, J.M., Young, R.A., Zon, L.I. (2014). Inducing HEXIM1 by pyrimidine nucleotide depletion suppresses neural crest development and melanoma. Cell.

Acknowledgements

Embarking on a graduate career in Chemical Biology is a long and challenging road, but I am glad that I have met many along the way who have made the journey more manageable and fulfilling. Firstly, I would like to thank my wife Amanda Teow for being highly supportive throughout my career as a graduate student. She has always been there during the ups and downs, and has been so patient with our long distance relationship. I appreciate her love and encouragement, which have gone a long way in making me what I am today. I would also like to thank my parents and brothers, whom I have been apart from for many years, but who have been very supportive throughout my education since my undergraduate studies. They always ensure that I enjoy what little time I spend back home for the holidays.

Other than my family, I also have many to thank who have directly contributed to my success in graduate school. First and foremost, I would like to thank Prof. Leonard Zon, my caring and kind mentor. Len is an exceptional mentor who cares a lot about his graduate students. He believes strongly in work-life balance that has made my time in lab fruitful and enjoyable. Secondly but no less important, I would like to thank my talented and caring technician Rachel Fogley. Rachel is a fast learner who is highly motivated, and her skill and perfectionism has contributed greatly to all aspects of my work. Thirdly, I would like to thank Cristina Santoriello, who has worked closely with me on both our projects, and has contributed greatly to my work. Fourthly, I would like to thank Ellen van Rooijen, who has taught me many techniques and has generously shared her boundless knowledge on zebrafish biology with me. Last but not least, I would like to thank all my other fellow lab mates, who have helped and encouraged me along the way, and who have made work and personal life so much more worthwhile.

The next group I would like to extend my appreciation to is my collaborators. For metabolomics, I would like to thank Dr. Shyh Chang Ng, Min Yuan and Prof. John Asara for their

help with these experiments and analyses. For sequencing, I would also like to thank Celeste Greer, Yoon Jung Kim and Prof. Tae Hoon Kim for performing the GRO-seq experiment, as well as Dr. Song Yang, Dr. Violaine Saint-André, Zi Peng Fan and Prof. Richard Young for their analysis of the ChIP-seq, RNA-seq and GRO-seq data. For pathology, I would like to thank Dr. Alvaro Laga for performing and analyzing immunohistochemical staining on human melanoma tissue. For biochemistry, I would like to thank Dr. Koh Fujinaga, John Brogie, Prof. Matija Peterlin and Prof. David Price for performing and analyzing the glycerol gradients and HEXIM1-luciferase report assay.

I also would like to thank the Chemical Biology program for accepting me and giving me valuable training for my dissertation work and for my future endeavors. The program has been very receptive to feedback and has improved by leaps and bounds over the years. I would like to thank the faculty members who have been closely involved in running the program successfully, especially our former co-directors Prof. John Clardy and Prof. David Liu, and our current co-directors, Prof. Daniel Kahne and Prof. Suzanne Walker. I also like to thank Samantha Reed, KeyAnna Wright and Jason Millberg for being such amazing program coordinators. The program would not run smoothly without them.

My Dissertation Advisory Committee has been very supportive of my research and I would like to thank them wholeheartedly. Prof. James Bradner has been an excellent committee chair and has lead many productive discussions on furthering my research. Prof. Thomas Look and Prof. Alan Cantor have also contributed substantially to my progress, giving me many suggestions and leads to work on. I am glad to have had such a supportive and nurturing committee, whose guidance has allowed me to graduate in a timely fashion with a strong skill set.

Last but not least, I would like to thank my funding sources. I first like to thank the Agency for Science, Technology and Research for funding my studies from undergraduate to

graduate school. I would not be here without this generous funding. Also, I would like to thank the Howard Hughes Medical Institute and the National Institutes of Health for their generous grants that have enabled me to conduct my doctoral research.

Chapter 1:

Introduction

Introduction

Melanoma is a malignant form of skin cancer that is responsible for about 75% of skin cancer deaths (Schadendorf and Hauschild, 2014). Activating mutations in *BRAF*, *NRAS* and *CKIT* are found in 60-70% of cutaneous melanomas and these mutations result in an over-activation of MAP kinase signaling that drives pathological cell proliferation (Schadendorf and Hauschild, 2014; Sullivan and Flaherty, 2013). Recently, there have been a number of advancements in anti-melanoma targeted therapeutics based on melanoma genetics. The FDA has recently approved two BRAF inhibitors and one MEK inhibitor to target the MAP kinase pathway, based on excellent patient responses in clinical trials (Eggermont et al., 2014). However, drug resistance is common and has limited the effectiveness of these targeted therapies (Schadendorf and Hauschild, 2014; Trunzer et al., 2013). There is a need to further investigate melanoma for other molecular mechanisms that can be exploited for therapeutic intervention.

Targeted Therapies for Melanoma

Current targeted therapies have been limited to targeting the MAPK pathway (Schadendorf and Hauschild, 2014; Sullivan and Flaherty, 2013). This is both due to vigorous studies on mutations in *RAS* GTPases and *RAF* kinases as reviewed by Sullivan and Flaherty (Sullivan and Flaherty, 2013), as well as the ease of developing inhibitors to kinase members of the MAPK pathways (BRAF and MEK) that have well-defined enzymatic active sites. *NRAS* is mutated in 15-30% of melanoma and the predominant mutation prevents the enzyme from hydrolyzing GTP to GDP, thereby keeping RAS in an active conformation to constitutively activate BRAF and CRAF (Bardeesy et al., 2005; Jakob et al., 2012; Marquette et al., 2011). Other than being aberrantly activated by mutated NRAS, *BRAF* itself is also mutated in 40-60% of melanomas (Davies et al., 2002), with the most frequent mutation being the V600E amino

acid substitution in the kinase domain (Pollock et al., 2003). This mutation results in constitutive BRAF activation and initiates MEK phosphorylation (Beeram et al., 2005; Pollock et al., 2003). MEK consequently phosphorylates ERK, which in turn upregulates transcription in pro-growth and transformation genes (Beeram et al., 2005; Sullivan and Flaherty, 2013). In addition to being significantly mutated in melanoma, both *BRAF* and *NRAS* mutations are associated with poor prognosis for melanoma survival (Jakob et al., 2012; Long et al., 2011).

Since the MAPK pathway features as an important signal transduction pathway in melanoma oncogenesis, there have been numerous efforts to design targeted therapies to members of the pathway. Selective BRAF inhibitors vemurafenib and dabrafenib have been developed and are currently approved for use in melanoma (Schadendorf and Hauschild, 2014). Treatment of patient tumors containing the $BRAF^{V600E}$ mutation with either drug caused a reduction in phospho-ERK levels that correlates with significant clinical responses (Bollag et al., 2010; Joseph et al., 2010). A second type of MAPK pathway drug approved for melanoma is MEK inhibitor trametinib (Schadendorf and Hauschild, 2014). Although this drug shows more modest patient response compared to the aforementioned BRAF inhibitors (Ascierto et al., 2012; Flaherty et al., 2012), it still provides an alternative means to target the MAPK pathway should tumors become resistant to BRAF inhibitors. Unfortunately, virtually all patients treated with these drugs will relapse, even after initial strong clinical responses, due to the MAPK pathway being reactivated by alternative means such as activation of RAS or upregulation of CRAF (Chapman et al., 2011; Sullivan and Flaherty, 2013). More work has to be done to discover novel pathways that can be therapeutically targeted in melanoma and hopefully, which will be more resistant to being bypassed by the tumor.

Zebrafish as a Melanoma Model

The zebrafish model has proved particularly useful for melanoma research. In a proof-of-principle study, the role of human *BRAF* was examined via melanocyte-specific overexpression in zebrafish under the mitfa promoter (Patton et al., 2005). As mentioned previously, $BRAF^{V600E}$ is the most frequent mutation in human nevi and melanoma that makes this kinase constitutively active (Pollock et al., 2003). Since this mutation had not been functionally validated *in vivo* for its relevance in melanoma, Patton et. al. examined if zebrafish could be used as an appropriate model to study the effects of human $BRAF^{V600E}$ on melanoma. Interestingly, they demonstrate that overexpressing human mutated but not wild-type BRAF induced ectopic melanocyte patches (Patton et al., 2005). In addition, the overexpression of mutated BRAF in a p53-deficient zebrafish line induced invasive melanoma (Patton et al., 2005). It must be emphasized that the human *BRAF* gene and not the zebrafish version of *braf* was examined, demonstrating that zebrafish and human melanoma biology are likely conserved. This study pioneered the use of zebrafish as an effective melanoma model, owing to its ability to recapitulate human phenotypes.

Other than recapitulating human melanoma biology, zebrafish are advantageous as a cancer model over the more commonplace mouse model. Mice, being a mammalian system, are currently preferred for cancer research as they are closer to humans from an evolutionary standpoint. As a result, there have been a number of melanoma studies focused on transgenic mouse models as reviewed by Walker et. al. (Walker et al., 2011). However, the cost of generating and maintaining mouse strains is prohibitive to performing large-scale genetics experiments (White et al., 2013). As a result, mice have primarily been used to test a small number of candidate melanoma genes as well as potential melanoma therapeutics which have first been evaluated in cell culture systems (Walker et al., 2011). Zebrafish, on the other hand, can overcome these obstacles in mouse melanoma modeling. Compared to mice, zebrafish

are much cheaper to maintain and easier to handle. There is no risk of user injury caused by fish unlike bites received from mice, which can result in infection. In addition, zebrafish can be generated in large numbers, with each mating pair capable of laying up to 200-300 embryos (Tan and Zon, 2011). Since zebrafish embryos develop *ex vivo*, genetic manipulation such as gene knockdown or transgenesis is also straightforward, which is performed via injection of DNA or RNA into the one-cell stage embryo. Since mice develop *in utero*, the generation of transgenic lines requires genetic modification in mouse embryonic stem cells, followed by injection of cells into mouse blastocysts which are then transplanted into a pseudo pregnant female (Thomas and Capecchi, 1987). This gives zebrafish a huge advantage in terms of the ease and rate of transgenesis, and has enabled the use of zebrafish in genetic screens to probe melanoma biology (Ceol et al., 2011).

The zebrafish have been particularly valuable in genetic screens for novel drivers of melanoma based on mutational data obtained from sequencing melanoma genomes (Ceol et al., 2011; White et al., 2013). Since current sequencing technologies have advanced to the point where melanoma genomes can be sequenced rapidly and cost-effectively, large volumes of mutational data have been obtained (Berger et al., 2012; White et al., 2013). There is a need to systematically test these newfound mutations *in vivo* in order to discover relevant mutations to oncogenesis. A genetic screen performed in zebrafish has demonstrated the potential of zebrafish to rapidly screen through candidate oncogenes to determine the ones that are relevant (Ceol et al., 2011). In this study, Ceol et. al. generate a zebrafish strain which is mitfa- and p53-deficient, and which also expresses the human $BRAF^{V600E}$ gene under the control of the mitfa promoter. They also generated a vector called MiniCoopR that contains an *mitfa* minigene and an *mitfa* promoter controlling expression of any candidate gene-of-interest. The plasmid also contains Tol2 sites for Tol2 transposase-mediated transgenesis for efficient insertion into the fish genome. Using this system, they tested candidate human genes

from a region on chromosome 1 that was significantly amplified in human melanoma (Curtin et al., 2005) and identified *SETDB1* amplification as a novel driver of melanoma. Results were statistically significant as a large number of fish could be easily generated for each candidate gene and analyzed for phenotypes. Such a study relies on the conservation of zebrafish and human biology, as well as the ease and cost-effectiveness of this system. This type of screening strategy would be unfeasible in mice. One can foresee future zebrafish-based screening studies that examine other mutated regions in melanoma to discover novel oncogenes and tumor suppressors.

In addition to genetic screening, the zebrafish are highly amenable to chemical screening (Tan and Zon, 2011), as demonstrated by a recent melanoma study (White et al., 2011). In this study, synchronized zebrafish embryos were screened with 2,000 chemicals to ascertain changes in neural crest marker *crestin* expression by *in situ* hybridization. This screen is possible owing to technology and low cost, that allows for the generation of large numbers of synchronized embryos for chemical treatment (Tan and Zon, 2011). A potent DHODH inhibitor, leflunomide that targets pyrimidine biosynthesis, was found to specifically downregulate *crestin* expression. The drug did not appear to be nonselectively toxic since the primary target of the drug appeared to be the neural crest lineage, as the rest of the embryo seemed morphologically intact. Interestingly, the drug could significantly debulk tumors in a melanoma mouse xenograft model and synergized with the FDA-approved BRAF inhibitor vemurafenib (Bollag et al., 2010) to suppress melanoma. A combination therapy of leflunomide and vemurafenib is currently in clinical trials for metastatic melanoma. This study demonstrates the feasibility of utilizing zebrafish to not only screen for novel melanoma therapeutics, but also assess *in vivo* toxicity at the same time.

Based on current work, the zebrafish is a valuable model organism for studying melanoma. The advantages of low cost, ease of breeding and handling, ease of transgenesis

and amenability to screening make the zebrafish an attractive system to study melanoma with. In addition, the zebrafish can recapitulate human melanoma biology similar to the mouse model, without the inherent limitations of this mammalian model. The zebrafish will likely prove to be useful in filtering through the large amount of genetic data for melanoma for relevant oncogenes and tumor suppressors.

The Neural Crest and Melanoma

Melanoma is a cancer of the melanocyte lineage, which are melanin pigment-producing cells residing in the epidermis. Melanin protects our skin from ultra violet radiation damage from the sun by attenuating this radiation (Kollias et al., 1991). Melanocytes are differentiated from the neural crest stem cells (NCSCs), which arise in the ectoderm at the margins of the neural tube in the developing embryo (Shakhova, 2014). The NCSCs are a transient and migratory cell population that gives rise to the melanocytes, among other lineages including smooth muscle cells, adipocytes, neurons, glial cells, chondrocytes and osteoblasts (Shakhova, 2014). Recent studies have shown that melanoma possesses neural crest-like characteristics (Boiko et al., 2010; Civenni et al., 2011; Schatton et al., 2008), suggesting that tumor cells could have undergone de-differentiation to acquire the migratory and self-renewal properties of the NCSCs. Not surprisingly, melanoma has been shown to possess similar genetic regulatory networks to NCSCs, being critically dependent on the transcription factor SOX10 for self-renewal and survival (Shakhova, 2014; Shakhova et al., 2012). SOX10 is regulated by NRAS (Shakhova, 2014), which was mentioned previously as being commonly mutated in melanoma. Therefore, there is strong evidence that transcriptional regulation of differentiation plays an important role in melanoma malignancy, and more work has to be done to further understand this relationship.

The Significance of Transcription Elongation in Differentiation

Control of the elongation phase of RNA polymerase II (RNA Pol II) transcription plays a significant role in regulating gene expression in specific cell types and during differentiation as reviewed in Guo and Price (Guo and Price, 2013). A summary of the process is shown in Figure 1.1. After initiation, RNA Pol II comes under the control of negative transcription elongation factors that include DSIF, NELF, Gdown1 and GNAF and becomes paused close to the promoter (Cheng et al., 2012a; Rahl et al., 2010). Release of these promoter proximal paused polymerases into productive elongation requires the kinase activity of the positive transcription elongation factor P-TEFb (Marshall et al., 1996). P-TEFb comprising cyclin-dependent kinase 9 (Cdk9) and either cyclin T1 or T2 (CCNT1/CCNT2) in humans is able to phosphorylate RNA Pol II (Marshall et al., 1996), and phosphorylation of DSIF (Wada et al., 1998; Yamada et al., 2006) and NELF (Fujinaga et al., 2004) leads to the release of NELF from the elongation complex and the transition into productive elongation (Rahl et al., 2010). RNA Pol II elongation control is prevalent in metazoan species (Adelman and Lis, 2012). In many cell types over half of human (Rahl et al., 2010) and drosophila (Muse et al., 2007) genes are occupied by promoter proximal paused RNA Pol II and synthesis of essentially all mRNAs requires P-TEFb.

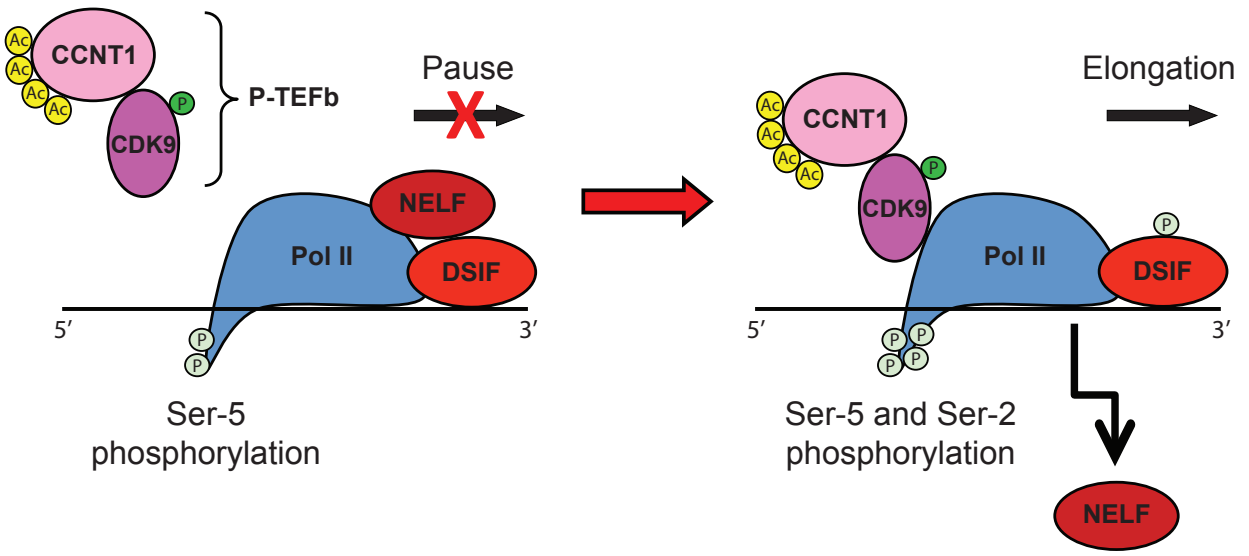

Figure 1.1 Regulation of Transcription Elongation

During the initiation step, RNA Pol II is recruited to the promoters of highly regulated genes and is held in a paused position by the binding of pausing factors such as NELF and DSIF. The arrival of P-TEFb, comprising CDK9 and either CCNT1 or CCNT2, is required to phosphorylate RNA Pol II at Ser-2 in the C terminal domain, DSIF and NELF. This causes dissociation of NELF, converts DSIF into a positive elongation factor, and shifts RNA Pol II into a state of productive elongation.

Transcriptional Regulation in the Neural Crest and Melanoma

Transcriptional elongation has been shown to be an important regulator of neural crest differentiation and melanoma (Keegan et al., 2002; White et al., 2011). Zebrafish mutants in transcription elongation factors *spt5* and *spt6* possess pigmentation defects possibly due to the absence of mature melanocytes (Keegan et al., 2002). Spt5 and spt6 promote transcription elongation and their loss seemingly inhibits productive elongation that hinders melanocyte differentiation (Keegan et al., 2002).

In a related study, a chemical *in situ* hybridization screen for modulators of neural crest marker crestin expression discovered that a DHODH inhibitor called leflunomide (Kaplan, 2001) can ablate *crestin* expression and melanocytes in zebrafish embryos (White et al., 2011). DHODH is an enzyme in the nucleotide *de novo* biosynthesis pathway and its inhibition impairs pyrimidine nucleotide biosynthesis (Löffler et al., 1997). This inhibits elongation in key genes necessary for

melanoma tumorigenesis (White et al., 2011). The loss of melanocytes and pigmentation induced by leflunomide phenocopies the pigmentation defects in the *spt5* and *spt6* mutants (Keegan et al., 2002; White et al., 2011). In addition, leflunomide synergizes with a hypomorphic allele of *spt5* in zebrafish, causing complete ablation of the melanocytes at a sub-optimal dose in these mutants (White et al., 2011). The *spt5* hypomorph experiences less severe transcriptional defects, so a low dose of leflunomide is sufficient to further inhibit elongation to similar effect as the *spt5* null alleles (White et al., 2011). More importantly, leflunomide causes melanoma regression in a mouse xenograft model (White et al., 2011). These studies posit an important role for elongation in neural crest differentiation and melanoma. However, it is unclear how leflunomide directly pauses elongation. It is possible that the action of leflunomide involves a negative regulator of elongation.

HEXIM1, a Negative Regulator of Transcription Elongation

One such factor that is known to negatively regulate elongation is HEXIM1, a component of the 7SK small nuclear ribonuclear protein (7SK snRNP), which might play a role in the effects of leflunomide. HEXIM1 has been shown to negatively regulate transcription in cell culture by sequestering P-TEFb and inhibiting its kinase activity (Yik et al., 2003). Sequestering and inhibiting P-TEFb allows for regulation of transcriptional pause release, which in turn regulates differentiation (Guo and Price, 2013; Zhou et al., 2012). HEXIM1 protein domains are highly conserved among humans, mice and zebrafish (Figure 1.2A). Phylogenetic analysis of *HEXIM* orthologues demonstrates that human and mouse *HEXIM1* are closely related, while zebrafish *hexim* relates more closely with human and mouse *HEXIM2* (Figure 1.2B). The *HEXIM* gene is also highly syntenic among humans, mice and zebrafish (Figure 1.2C). This suggests identical functioning of *HEXIM* in all three species.

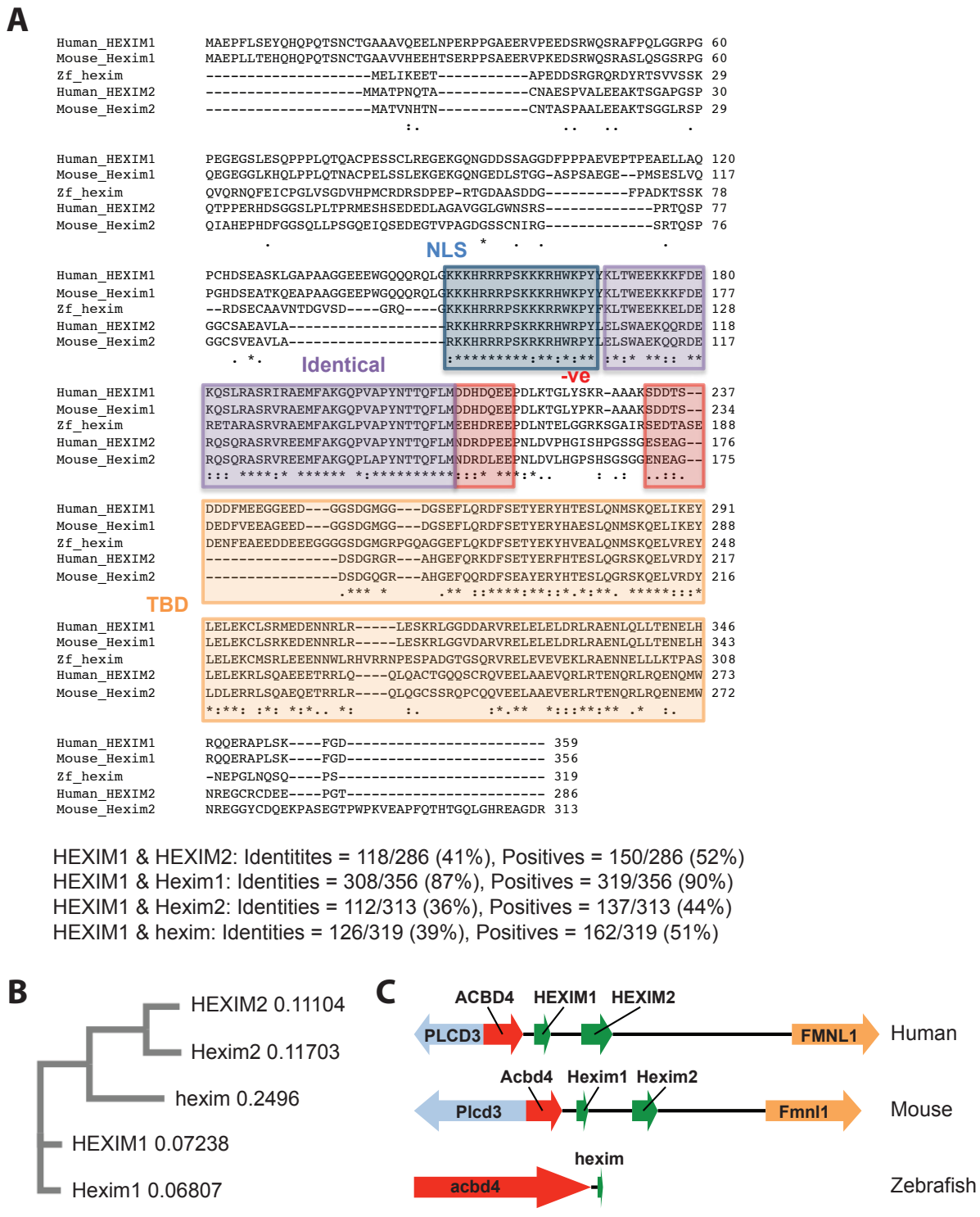

HEXIM1 & HEXIM2: Identitites = 118/286 (41%), Positives = 150/286 (52%)
HEXIM1 & Hexim1: Identities = 308/356 (87%), Positives = 319/356 (90%)
HEXIM1 & Hexim2: Identities = 112/313 (36%), Positives = 137/313 (44%)
HEXIM1 & hexim: Identities = 126/319 (39%), Positives = 162/319 (51%)

Figure 1.2 HEXIM1 is Highly Homologous in Humans, Mice and Zebrafish

(A) Alignment of HEXIM orthologues in humans, mice and zebrafish using Clustal Omega. The conserved regions of the nuclear localization signal (NLS), identical region, negatively charged

(Continued) region (-ve) and cyclin T binding domain (TBD) are highlighted. (B) HEXIM orthologue phylogenetic tree by Clustal Omega. (C) HEXIM orthologue synteny analysis.

A fraction of HEXIM1 is found a form of the 7SK snRNP that contains P-TEFb (Figure 1.3) (Michels and Bensaude, 2008; Nguyen et al., 2001; Yang et al., 2001; Yik et al., 2003). The 7SK snRNP consists of non-coding RNA, the 7SK snRNA, the 5' methylphosphate capping protein MEPCE (also known as BCDIN3) and the 3' end binding protein LARP7 (He et al., 2008; Jeronimo et al., 2007). Incorporation of dimeric HEXIM1 into the 7SK snRNP induces a conformational change in HEXIM1 that allows for P-TEFb binding (Barboric et al., 2005; Blazek et al., 2005; Li et al., 2005). The 7SK snRNP is also tightly regulated by calcium/calmodulin phosphatases (PP1α and PP2B), AKT, P300 and PKC (Chen et al., 2008; Cho et al., 2009; Contreras et al., 2007; Fujinaga et al., 2012).

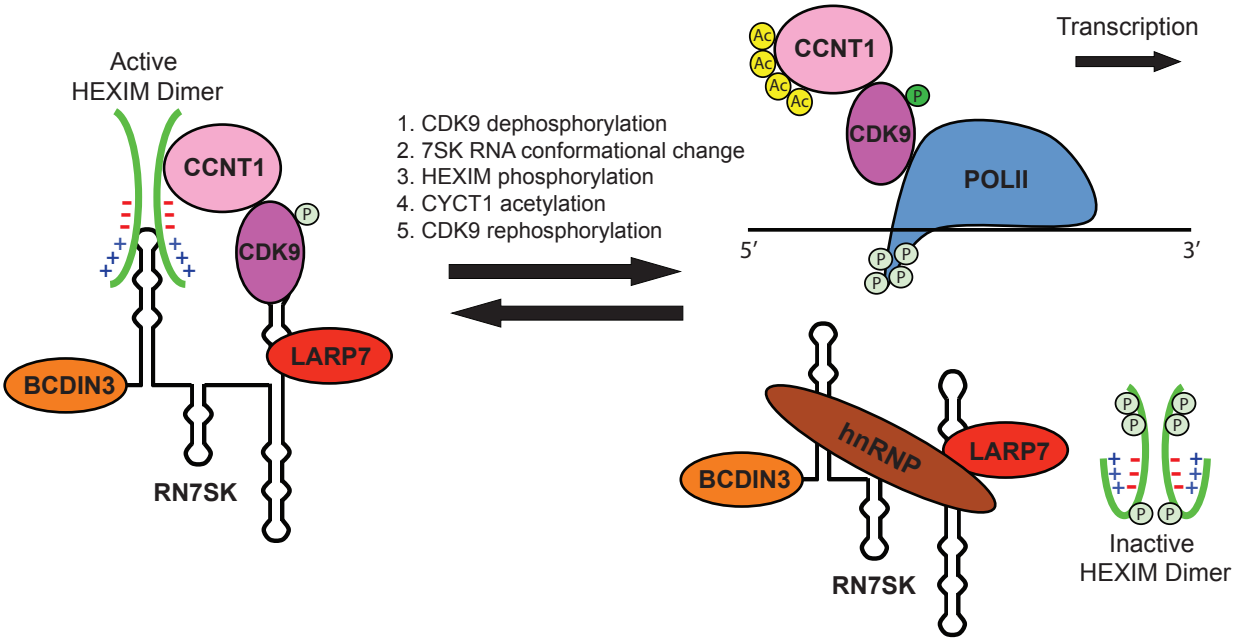

Figure 1.3 Regulation of the 7SK snRNP

HEXIM, as part of the 7SK snRNP complex, sequesters and inhibits P-TEFb activity. Complex association and dissociation is modulated by a series of complex phosphorylation, dephosphorylation, acetylation and conformational change events.

Tumor Suppressing Activity of HEXIM1

In addition to being an essential regulatory component of gene expression, there is evidence that the inability of the 7SK snRNP to function is relevant to cancer. HEXIM1, which is responsible for direct interaction with P-TEFb, is downregulated by estrogen to relieve negative regulation on genes involved in cell proliferation, possibly exacerbating breast cancer proliferation (Ogba et al., 2008; Wittmann et al., 2005). In prostate cancer, HEXIM1 modulates androgen receptor and TGF-β signaling (Mascareno et al., 2012). LARP7, the 3' binding protein of the 7SK RNA, was found to be truncated and non-functional in gastric cancer (Cheng et al., 2012b). This truncation prevented the formation of the functional 7SK snRNP to suppress tumorigenic gene expression (Cheng et al., 2012b). Through a poorly understood feedback loop, any treatment or condition that inhibits the elongation by RNA Pol II causes release of P-TEFb from the 7SK snRNP and a subsequent increase in HEXIM1 gene expression (Guo and Price, 2013; Liu et al., 2014a). These treatments include a number of cancer drugs and investigational anti-cancer agents, suggesting a role for HEXIM1 in suppressing tumorigenesis.

Since both leflunomide and HEXIM1 negatively regulate transcription elongation, we investigated if HEXIM1 is responsible for the effects of leflunomide on the neural crest and melanoma. Our genetic and biochemical studies demonstrate that HEXIM1 is required for leflunomide-induced phenotypes through its sequestration of P-TEFb. HEXIM1 levels are modulated by nucleotide perturbations induced by leflunomide. Furthermore, HEXIM1 can suppress melanoma, independent of leflunomide, by modulating tumorigenic genes associated with melanoma. These results illustrate the importance of HEXIM1 induction as a stress response to nucleotide shortage. HEXIM1 induction inhibits transcription in cells, and consequently cell cycle and proliferation, until the stress is alleviated. This pathway can be targeted to suppress melanoma by initiating a non-proliferative state in tumors.

Chapter 2:

HEXIM1 is Induced by DHODH Inhibition to Suppress Melanoma

Justin L. Tan[1,2], Rachel D. Fogley[1,2], Cristina Santoriello[1,2], Violaine Saint-André[3], Song Yang[1,2], Zi Peng Fan[3], Alvaro C. Laga[4], Ellen van Rooijen[1,2], Celeste B. Greer[5], Yoon Jung Kim[6], Koh Fujinaga[7], John E. Brogie[8], David H. Price[8], B. Matija Peterlin[7,9], Yi Zhou[1,2], Tae Hoon Kim[6], John M. Asara[10], Richard A. Young[3], Leonard I. Zon[1,2]*

[1]Howard Hughes Medical Institute, Stem Cell Program and Division of Pediatric Hematology/ Oncology, Boston Children's Hospital, Dana-Farber Cancer Institute, Harvard Medical School, Boston MA 02115, USA. [2]Department of Stem Cell and Regenerative Biology, Harvard Stem Cell Institute, Cambridge, MA 02138, USA. [3]Whitehead Institute for Biomedical Research and Department of Biology, Massachusetts Institute of Technology, Cambridge, MA 02142, USA. [4]Department of Pathology, Brigham & Women's Hospital, Boston, MA 02215, USA. [5]Department of Pharmacology, Yale University, School of Medicine, New Haven, CT 06520, USA. [6]Department of Genetics, Yale University, School of Medicine, New Haven, CT 06520, USA. [7]Departments of Medicine, Microbiology and Immunology, Rosalind Russell Medical Research Center, University of California, San Francisco, CA 94143, USA. [8]Department of Biochemistry, University of Iowa, Iowa City, IO 52242, USA. [9]Department of Virology, Haartman Institute, University of Helsinki, FIN-00014 Helsinki, Finland. [10]Department of Medicine, Division of Signal Transduction, Beth Israel Deaconess Medical Center and Harvard Medical School, Boston, MA 02215, USA

*To whom correspondence should be addressed
Address: 300 Longwood Ave, Boston, MA 02115
Email: zon@enders.tch.harvard.edu

Attributions

L. I. Zon and I conceived the project to determine the relevance of HEXIM1 in the context of DHODH inhibition in melanoma. I designed and performed the morpholino knockdown assays in zebrafish embryos. I also designed the *in situ* hybridization primers for *hexim*. I performed all *in situ* hybridization experiments. I performed all western blots and real time RT-PCR analysis with technical assistance from R. D. Fogley. K. Fujinaga performed the *HEXIM1*-Luciferase assay and together with J. E. Brogie, performed the glycerol gradient experiments. K. Fujinaga, J. E. Brogie and myself analyzed the luciferase and glycerol gradient assays. I performed the co-immunoprecipitation assay with technical assistance from R. D. Fogley. I analyzed human melanoma expression data from previously published studies. A. C. Laga performed immunohistochemistry on human melanoma tissue microarrays and analyzed them together with myself. I designed and performed the HEXIM1 MiniCoopR tumor assays with technical assistance from R. D. Fogley. I cloned all constructs required for the project. I performed the siRNA knockdown experiments with technical assistance from R. D. Fogley. C. B. Greer and Y. J. Kim performed the GRO-seq experiment. V. Saint-André and S. Yang analyzed the GRO-seq data together with myself. E. van Rooijen generated the list of neural crest-associated genes. I performed gene overlap, Ingenuity Pathway Analysis and literature-based analysis on all generated gene sets. I performed the ChIP-seq assays with technical assistance from R. D. Fogley. S. Yang, Z. P. Fan and I performed the analysis of the ChIP-seq results.

Introduction

Control of the elongation phase of RNA polymerase II (RNA Pol II) transcription plays a significant role in regulating gene expression in specific cell types and during differentiation as reviewed in Guo and Price (Guo and Price, 2013). After initiation, RNA Pol II comes under the control of negative transcription elongation factors that include DSIF, NELF, Gdown1 and GNAF and becomes paused close to the promoter (Cheng et al., 2012a; Rahl et al., 2010). Release of these promoter proximal paused polymerases into productive elongation requires the kinase activity of the positive transcription elongation factor P-TEFb (Marshall et al., 1996). P-TEFb comprising cyclin-dependent kinase 9 (Cdk9) and either cyclin T1 or T2 (CCNT1/CCNT2) in humans is able to phosphorylate RNA Pol II (Marshall et al., 1996), and phosphorylation of DSIF (Wada et al., 1998; Yamada et al., 2006) and NELF (Fujinaga et al., 2004) leads to the release of NELF from the elongation complex and the transition into productive elongation (Rahl et al., 2010). RNA Pol II elongation control is prevalent in metazoan species (Adelman and Lis, 2012). In many cell types over half of human (Rahl et al., 2010) and drosophila (Muse et al., 2007) genes are occupied by promoter proximal paused RNA Pol II and synthesis of essentially all mRNAs requires P-TEFb.

Transcriptional elongation has been shown to be an important regulator of neural crest differentiation and melanoma (Keegan et al., 2002; White et al., 2011). Zebrafish mutants in transcription elongation factors *spt5* and *spt6* possess pigmentation defects possibly due to the absence of mature melanocytes (Keegan et al., 2002). *Spt5* and *spt6* promote transcription elongation and their loss seemingly inhibits productive elongation that hinders melanocyte differentiation (Keegan et al., 2002). In a related study, a chemical *in situ* hybridization screen for modulators of neural crest marker *crestin* expression discovered that a dihydro-orotate dehydrogenase (DHODH) inhibitor called leflunomide (Kaplan, 2001) can ablate *crestin* expression and melanocytes in zebrafish embryos (White et al., 2011). DHODH is an enzyme in the nucleotide

de novo biosynthesis pathway and its inhibition impairs pyrimidine nucleotide biosynthesis (Löffler et al., 1997). This inhibits elongation in key genes necessary for melanoma tumorigenesis (White et al., 2011). The loss of melanocytes and pigmentation induced by leflunomide phenocopies the pigmentation defects in the *spt5* and *spt6* mutants (Keegan et al., 2002; White et al., 2011). In addition, leflunomide synergizes with a hypomorphic allele of *spt5* in zebrafish, causing complete ablation of the melanocytes at a sub-optimal dose in these mutants (White et al., 2011). The *spt5* hypomorph experiences less severe transcriptional defects, so a low dose of leflunomide is sufficient to further inhibit elongation to similar effect as the *spt5* null alleles (White et al., 2011). More importantly, leflunomide causes melanoma regression in a mouse xenograft model (White et al., 2011). These studies posit an important role for elongation in neural crest differentiation and melanoma. However, it is unclear how leflunomide directly pauses elongation. It is possible that the action of leflunomide involves a negative regulator of elongation. One such factor that is known to negatively regulate elongation is HEXIM1, a component of the 7SK small nuclear ribonuclear protein (7SK snRNP) (Yik et al., 2003), which might play a role in the effects of leflunomide.

HEXIM1 has been shown to negatively regulate transcription in cell culture by sequestering P-TEFb and inhibiting its kinase activity (Yik et al., 2003). Sequestering and inhibiting P-TEFb allows for regulation of transcriptional pause release, which in turn regulates differentiation (Guo and Price, 2013; Zhou et al., 2012). HEXIM1 protein domains are highly conserved among humans, mice and zebrafish. A fraction of HEXIM1 is found a form of the 7SK snRNP that contains P-TEFb (Michels and Bensaude, 2008; Nguyen et al., 2001; Yang et al., 2001; Yik et al., 2003). The 7SK snRNP consists of non-coding RNA, the 7SK snRNA, the 5’ methylphosphate capping protein MEPCE (also known as BCDIN3) and the 3’ end binding protein LARP7 (He et al., 2008; Jeronimo et al., 2007). Incorporation of dimeric HEXIM1 into the 7SK snRNP induces a conformational change in HEXIM1 that allows for P-TEFb binding (Barboric et al., 2005; Blazek et al., 2005; Li et al., 2005). The 7SK snRNP is also tightly regulated by calcium/calmodulin phosphatases (PP1α

and PP2B), AKT, P300 and PKC (Chen et al., 2008; Cho et al., 2009; Contreras et al., 2007; Fujinaga et al., 2012).

Since both leflunomide and HEXIM1 negatively regulate transcription elongation, we investigated if HEXIM1 is responsible for the effects of leflunomide on the neural crest and melanoma. Our genetic and biochemical studies demonstrate that HEXIM1 is required for leflunomide-induced phenotypes through its sequestration of P-TEFb. HEXIM1 levels are modulated by nucleotide perturbations induced by leflunomide. Furthermore, HEXIM1 can suppress melanoma, independent of leflunomide, by modulating tumorigenic genes associated with melanoma. These results illustrate the importance of HEXIM1 induction as a stress response to nucleotide shortage. HEXIM1 induction inhibits transcription in cells, and consequently cell cycle and proliferation, until the stress is alleviated. This pathway can be targeted to suppress melanoma by initiating a non-proliferative state in tumors.

Results

Knockdown of *hexim* and Other Protein Members of the 7SK snRNP Rescues Neural Crest Phenotypes Associated with DHODH Inhibition.

Leflunomide is a potent DHODH inhibitor and treatment of developing zebrafish embryos with the drug ablates *crestin* and *mitfa* gene expression at 24 hours post fertilization (hpf) (White et al., 2011). *Crestin* is a zebrafish specific pan-neural crest marker (Luo et al., 2001) while *mitfa* is the master regulator of the melanocyte cell fate (Levy et al., 2006), indicating that leflunomide specifically represses these genes. In addition to the loss of gene expression, leflunomide also inhibits melanocyte differentiation from 24 to 48 hpf. The pausing of *crestin* and *mitfa* transcripts might be induced by the 7SK snRNP.

Morpholino knockdown of *hexim* rescues *crestin* and *mitfa* expression in leflunomide-treated zebrafish embryos at 24 hpf (Figure 2.1A). Melanocytes are also rescued at 48 hpf (Figures 2.1B and 2.1C). A *hexim* mismatch morpholino control did not rescue leflunomide phenotypes. Also, overexpressing human *HEXIM1* via mRNA injection in conjunction with zebrafish *hexim* knockdown ablated the rescue. We validated hexim protein knockdown via western blot (Figure 2.1D). In addition, knockdown of either *larp7* or *bcdin3*, both members of the active 7SK snRNP together with hexim, also recapitulated the rescue of melanocytic gene expression and melanocytes (Figures 2.2A and 2.2B). These results suggest a role for the 7SK snRNP in maintaining RNA Pol II in its paused state in the neural crest lineage in response to DHODH inhibition, thereby leading to transcriptional pausing of neural crest and melanocytic genes.

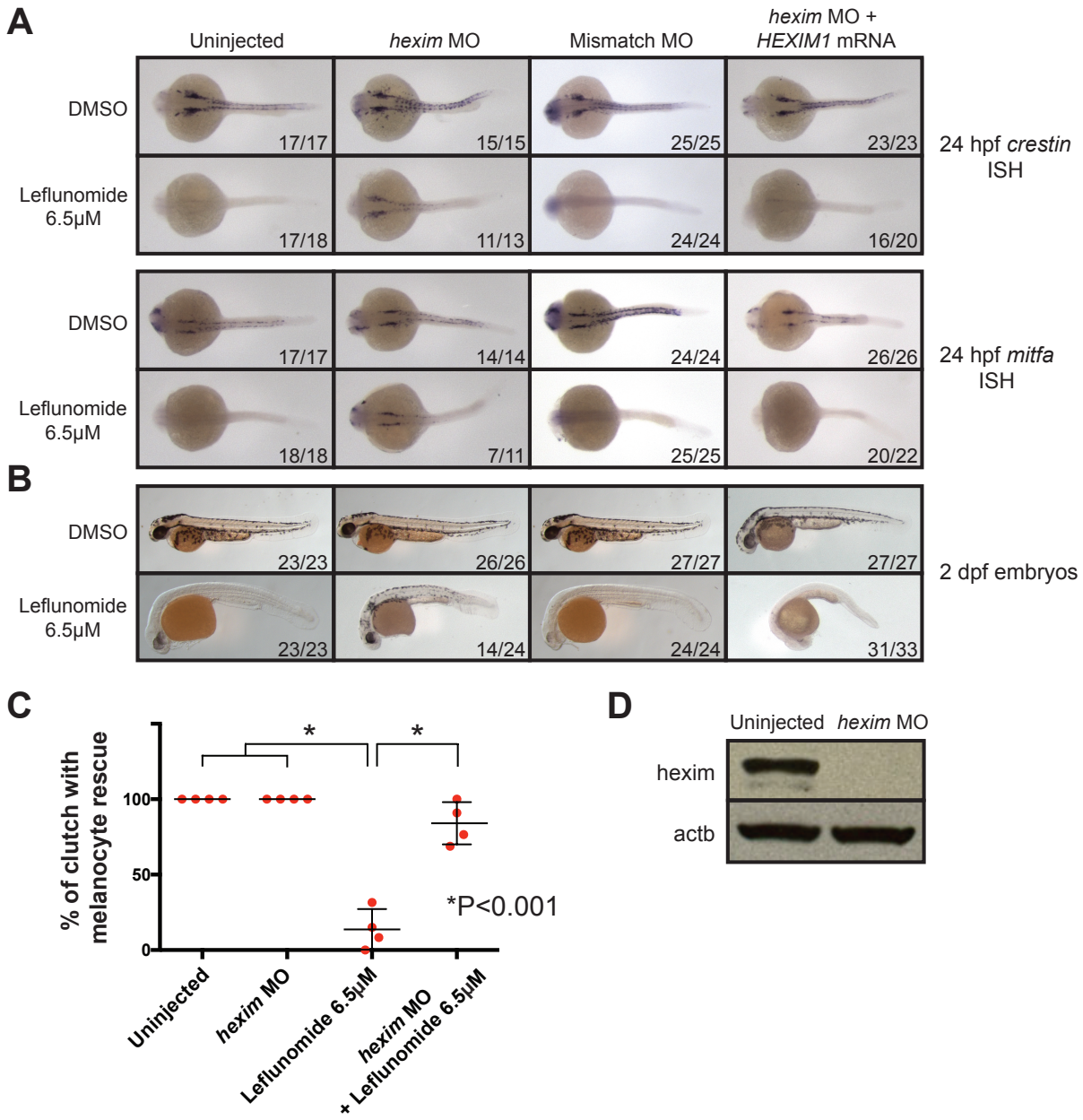

Figure 2.1 Knockdown of hexim Rescues Leflunomide-associated Neural Crest Phenotypes

(A) Zebrafish embryos were injected with 8 ng of *hexim* or control morpholino (MO), as well as a combination of *hexim* MO and 300 pg of human *HEXIM1* mRNA. Embryos were treated with either DMSO or 6.5 μM leflunomide at 50% epiboly and were subjected to *in situ* hybridization at 24 hpf for *crestin* and *mitfa* expression. Dorsal views of embryos are shown. (B) Embryos treated as described in (A) were also scored for melanocytes at 2 dpf. (C) Four separate clutches of embryos were analyzed for rescue of melanocytes under the conditions of uninjected, *hexim* MO injected, leflunomide treatment or *hexim* MO injected with leflunomide treatment. Percentages of the number of embryos rescued in each clutch are plotted. (D) Western blot for hexim and β-actin (actb) in uninjected and *hexim* MO injected embryos at 24 hpf.

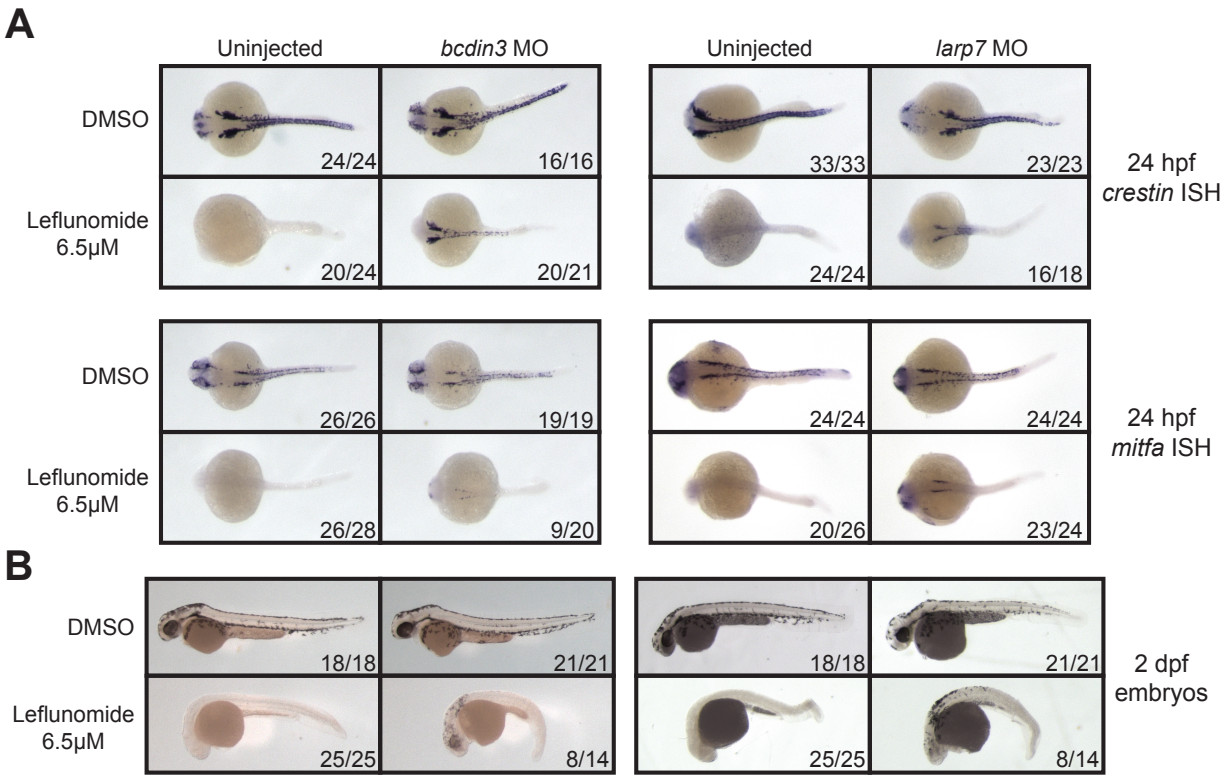

Figure 2.2 Knockdown of *bcdin3* and *larp7* Rescues Leflunomide-induced Phenotypes

(A) Zebrafish embryos were injected with 10 ng of *bcdin3* or 12 ng of *larp7* MOs that were previously published. Embryos were treated with either DMSO or 6.5 μM leflunomide at 50% epiboly and subjected to *in situ* hybridization at 24 hpf for *crestin* and *mitfa* expression. Dorsal views of embryos are shown. (B) Embryos treated as described in (A) were also scored for melanocytes at 2 dpf.

Hexim is Ubiquitously Expressed in Early Development.

Leflunomide treatment primarily affects the neural crest lineage of developing zebrafish embryos. Hence, we first investigated if *hexim* is expressed in the neural crest and melanocytes in these embryos. We developed two anti-sense *in situ* hybridization (ISH) RNA probes targeting the 5' or the 3' end of the mature *hexim* transcript which were validated for specificity by sense control probes (Figures 2.3A and 2.3B). ISH was then performed on zebrafish embryos at different developmental stages. *Hexim* is ubiquitously expressed at early developmental stages (Figure 2.3C) before 24 hpf. After 24 hpf, expression is observed mostly in the head. Ubiquitous *hexim*

expression is similarly observed in developing mouse embryos from E9.5 to E11.5 (Huang et al., 2004; Montano et al., 2008). *Hexim* is therefore expressed in the neural crest lineage at early developmental stages, albeit non-specifically.

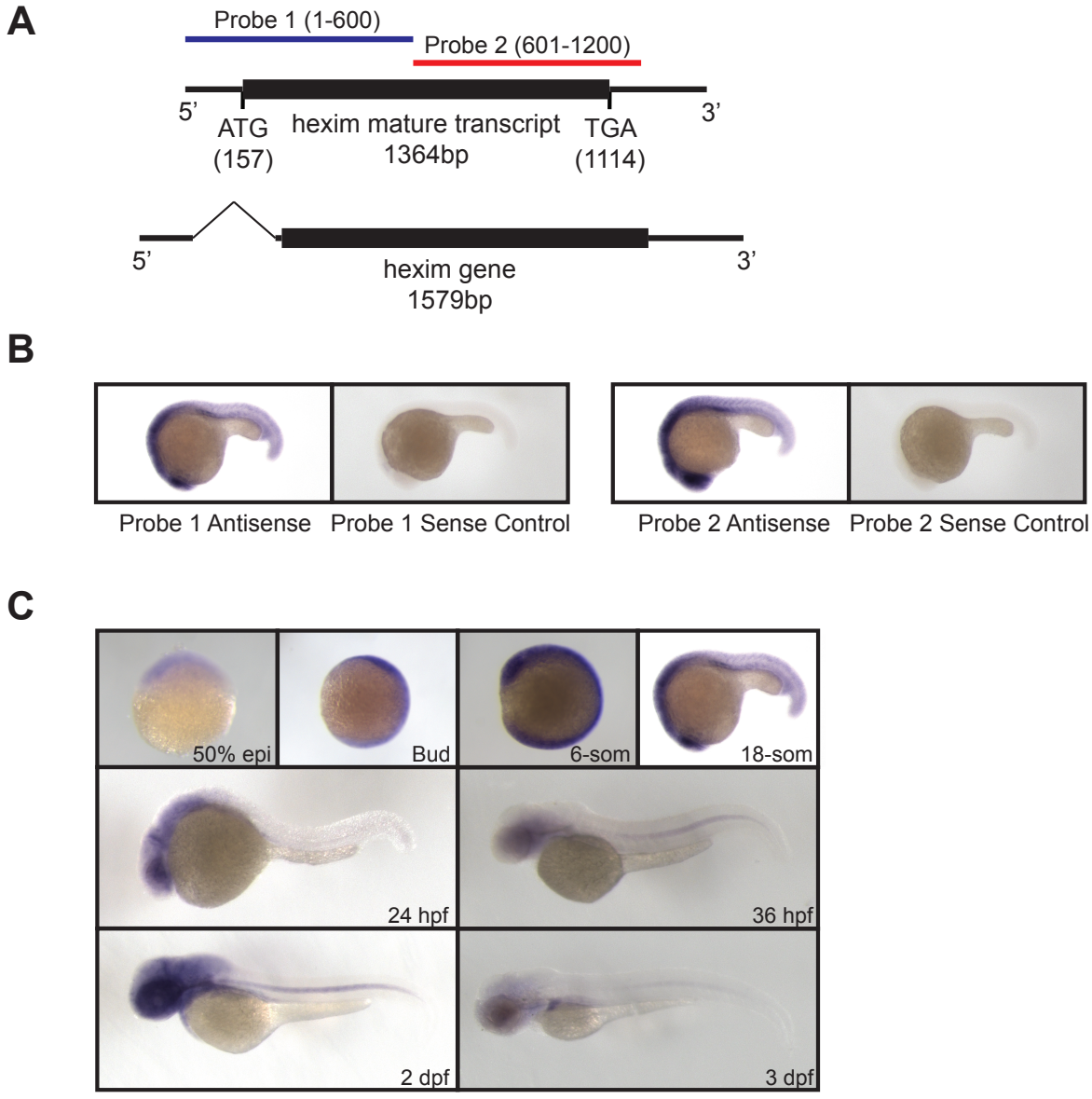

Figure 2.3 *Hexim* is Ubiquitously Expressed in Developing Zebrafish Embryos

(A) Two 600bp *in situ* hybridization probes to the *hexim* mature transcript were designed. (B) Both antisense probes and their corresponding sense controls were tested on 18-somite stage zebrafish embryos. (C) *Hexim* expression at various zebrafish developmental stages with probe 1. Results were identical for probe 2.

HEXIM is Upregulated in Zebrafish Embryos and Human Melanoma in Response to DHODH Inhibition.

Since hexim seems to be responsible for leflunomide-induced phenotypes in the zebrafish, we investigated if leflunomide has an effect on *HEXIM* expression. We performed real time RT-PCR on leflunomide-treated embryos and observed that *hexim* expression is upregulated by 2-fold (Figure 2.4A). In addition, hexim protein levels are upregulated by leflunomide (Figure 2.4C). Treatment of A375 human melanoma cells with A771726, the metabolized and functional form of leflunomide (Magne et al., 2006), also increases HEXIM1 mRNA and protein levels in a dose response manner (Figures 2.4B and 2.4D). Furthermore, we tested A771726 in our *HEXIM1*-luciferase reporter system (Liu et al., 2014b), which we had previously shown to have an excellent response to *HEXIM1* inducing drugs, in the A375 cells. As expected, A771726 significantly increased *HEXIM1* expression over time, similar to our positive control HMBA that is known to upregulate *HEXIM1* (Figure 2.4E). This indicates that both human *HEXIM1* and zebrafish *hexim* respond to DHODH inhibition by increasing their mRNA and protein levels.

Since we previously showed that drugs HMBA, SAHA and JQ1 can upregulate *HEXIM1* transcription via a transient release of P-TEFb from the 7SK snRNP that triggers elongation at the *HEXIM1* locus (Bartholomeeusen et al., 2012; Contreras et al., 2007, 2009; Lenasi et al., 2008), we examined if leflunomide upregulates *HEXIM1* by this mechanism as well. We performed glycerol gradient sedimentation experiments on A771726-treated A375 cell lysates at early time points and determined that P-TEFb component CCNT1 is indeed released from the 7SK snRNP fraction into the free P-TEFb fraction in the first 6 hrs of drug treatment (Figure 2.4F). At 24 hrs of drug treatment however, there was a decrease in the amount of CCNT1 in the free P-TEFb fraction (Figure 2.4F). Quantification of the ratio of the amount of CCNT1 protein in the free P-TEFb fraction over the 7SK snRNP-bound P-TEFb fraction reveals a linear increase in the ratio from 0 to 6 hrs, followed by a drop to the 0 hr level by 24 hrs (Figure 2.4G). This demonstrates an

initial increase in the amount of free P-TEFb versus bound P-TEFb, followed by a reincorporation of P-TEFb into the 7SK snRNP. To complement the glycerol gradient studies, we performed co-immunoprecipitation for endogenous HEXIM1 in A375 cells treated with A771726 for 72 hrs and assessed the levels of the components of the 7SK snRNP that are co-bound. We detected not only more HEXIM1 in the A771726 treatment as expected, but also more LARP7, BCDIN3, CCNT1 and CDK9 that are co-bound to HEXIM1 (Figure 2.4H).

Taken together, these experiments provide evidence that DHODH inhibition first causes an initial increase in HEXIM1 protein levels due to a transient release of P-TEFb from the 7SK snRNP, which can upregulate *HEXIM1* transcription. In this way, leflunomide functions similarly to HMBA, SAHA and JQ1 by transiently releasing active P-TEFb from the 7SK snRNP to upregulate transcription elongation in *HEXIM1*, among other genes (Bartholomeeusen et al., 2012a; Contreras et al., 2007, 2009; Lenasi et al., 2008; Liu et al., 2014b). Increased *HEXIM1* transcription and protein synthesis following the initial release of P-TEFb from the 7SK snRNP means there is now more new HEXIM1 to consequently sequester and inactivate P-TEFb, inhibiting the transition from a transcriptional pause to productive elongation (Bartholomeeusen et al., 2012; Contreras et al., 2007, 2009).

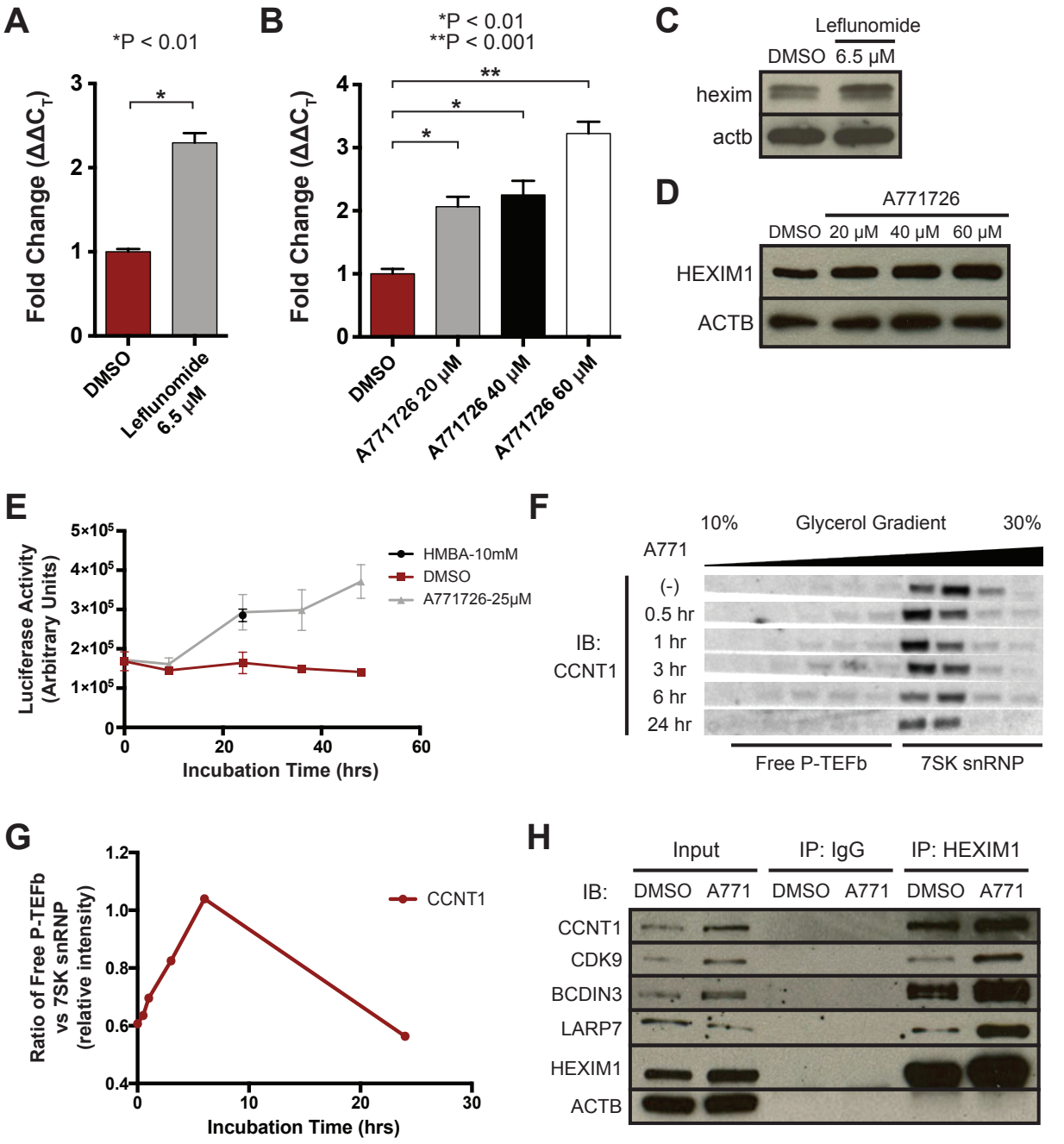

Figure 2.4 DHODH Inhibition Upregulates HEXIM to Sequester P-TEFb

(A) Real time RT-PCR on 24 hpf zebrafish embryos treated with leflunomide to examine *hexim* expression, normalized to *gapdh*. (B) Real time RT-PCR on A375 cells treated with A771726 for 72 hrs to examine *HEXIM1* expression, normalized to *GAPDH*. (C) Western blot for hexim on 24 hpf zebrafish embryos treated with leflunomide from 50% epiboly to 24 hpf. (D) Western blot for HEXIM1 on A375 cells treated with A771726 for 72 hrs. (E) *HEXIM1*-luciferase reporter assay in A375 cells treated with DMSO or 25 μM A771726 and monitored over time. 10 mM HMBA treatment at 24 hrs, which is known to induce *HEXIM1* expression, was the positive control.

(Continued) (F) Cell lysates of A375 cells treated with 50 μM A771726 at various time points were subjected to 10-30% glycerol gradient sedimentation. CCNT1 in fractions containing free P-TEFb and 7SK snRNP-bound P-TEFb was detected by western blotting. (G) Quantification of the ratio of the amount of CCNT1 protein in the free P-TEFb fraction versus the 7SK snRNP-bound P-TEFb fraction based on western band intensities in (F). (H) Co-immunoprecipitation of HEXIM1 was performed on A375 cells treated with DMSO or 60 μM A771726 for 72 hrs. Input, IgG and HEXIM1 IP samples were analyzed by western blotting for 7SK snRNP members and β-Actin (ACTB).

HEXIM1 Expression is Low in Melanoma.

As leflunomide causes a proliferation defect in the A375 human melanoma line that correlates with increased HEXIM1 mRNA and protein levels, we looked for evidence of alterations in *HEXIM1* expression in human melanoma. We analyzed two existing human melanoma microarray datasets for *HEXIM1* expression (Lin et al., 2008; Talantov et al., 2005). The Talantov et al. study examines gene expression from primary melanoma and benign skin nevi tissues, while the Lin et al. study examines gene expression in melanoma short-term cultures and cell lines. We found that *HEXIM1* is significantly downregulated by at least 2-fold in 78% of human nevi compared to normal skin controls (Figures 2.5A and 2.6A). When comparing human melanoma and skin, 100% of melanoma cases are downregulated by at least 2-fold (Figures 2.5A and 2.6A). Considering short-term cultures and cell lines versus normal melanocyte lines, 44% of melanoma cases have *HEXIM1* downregulated by at least 2-fold (Figures 2.5B and 2.6A). Hence by expression, *HEXIM1* levels seem to be downregulated in melanoma.

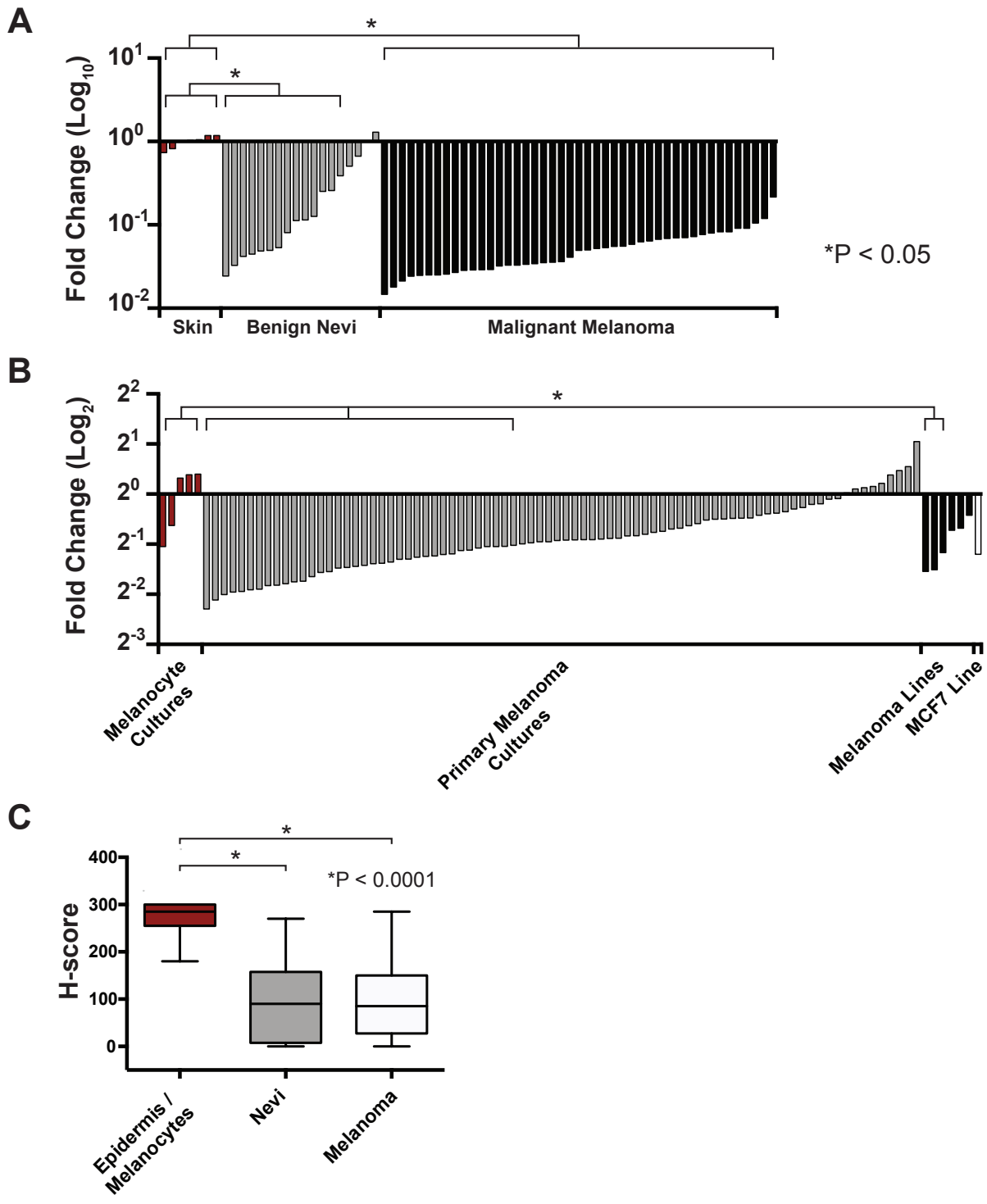

Figure 2.5 HEXIM1 is Downregulated in Human Melanoma

(A) Gene expression plot of *HEXIM1* microarray data from the Talantov et al. melanoma study showing fold change of nevi/tumor samples versus normal skin controls, which are set to 1-fold. (B) Gene expression plot of *HEXIM1* microarray data from the Lin et al. melanoma study

(Continued) showing fold change of primary melanoma cultures, melanoma cell lines and a breast cancer cell line versus melanocyte culture controls, which are set to 1-fold. (C) Bar graph summarizing overall H-scores for normal epidermis, nevi and melanoma samples.

In addition to gene expression analyses, we performed immunohistochemistry for HEXIM1 on human melanoma tissue microarrays and scored them by the H-score method (McClelland et al., 1990). Remarkably, 66% of nevi and 72% of human melanoma samples showed low H-scores of < 100, which corresponds to low HEXIM1 protein levels (Figures 2.5C and 2.6B). 6% of nevi and 13% of melanoma showed high HEXIM1 levels with H-scores of > 200 (Figures 2.6B and 2.6D). 100% of normal epidermal samples scored high for HEXIM1 expression, with 94% of samples possessing H-scores of > 200 (Figures 2.6B and 2.6D). Since melanoma is derived from melanocytes, we examined normal epidermal sections co-stained for HEXIM1 and MART1, a melanocyte specific cell surface antigen (Coulie et al., 1994; Kawakami et al., 1994). As expected, melanocytes expressing high levels of MART1 also express high levels of HEXIM1, meaning that HEXIM1 protein is high in normal melanocytes compared to nevi and melanoma (Figure 2.6C). These results mirror both our analyses of HEXIM1 expression in the Talantov et. al. and Lin et. al. studies. The aforementioned mRNA and protein analyses therefore suggest that HEXIM1 can functionally suppress tumors, and is therefore downregulated in melanoma.

A

Gene	Comparison	% of samples > 2-fold downregulated	P-value[1]	Mean fold change	P-value[2]	Reference
HEXIM1	Nevi vs. normal skin	78%	<0.05	-3.53	<0.05	Talantov *et al.*
	Melanoma vs. normal skin	100%	<0.05	-18.6	<0.05	
	Melanoma vs. melanocyte cultures	44%	<0.05	-1.69	0.0854	Lin *et al.*

[1]P-value of comparison between samples > 2-fold downregulated vs. controls.
[2]P-value of mean fold change of all samples vs. controls.

B

Sample Type	H-score	No. of Samples	% of Samples
Epidermis (n=17)	0	0	0
	1 - 100	0	0
	101 - 200	1	6
	201 - 300	16	94
Nevi (n=18)	0	4	22
	1 - 100	8	44
	101 - 200	5	28
	201 - 300	1	6
Melanoma (n=82)	0	8	10
	1 - 100	51	62
	101 - 200	12	15
	201 - 300	11	13

C

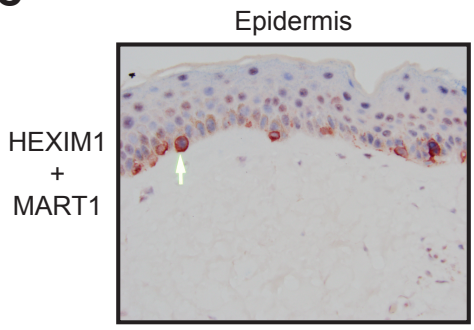

D

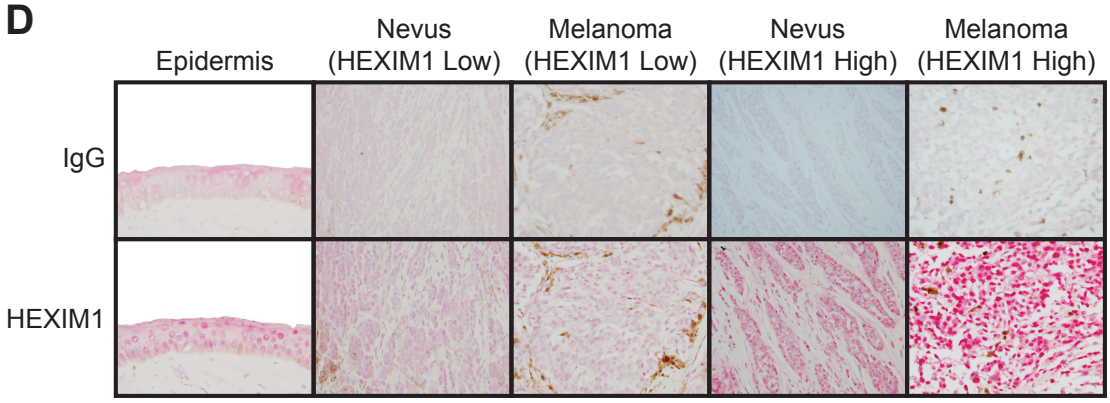

Figure 2.6 HEXIM1 mRNA and Protein Levels are Downregulated in Melanoma

(A) Microarray *HEXIM1* data from the Talantov et al. and Lin et al. studies are presented in two ways. Firstly, the percentage of nevi/melanoma samples with *HEXIM1* expression more than 2-fold downregulated versus the average expression level of the controls is tabulated. The associated p-value is calculated by comparing only samples with more than 2-fold downregulation with control samples using Student's two-tailed t-test. Secondly, the mean fold change of all nevi/melanoma samples versus controls is tabulated with its associated p-value. (B) Tabulation of H-scores from a human melanoma tissue microarray immuno-stained for HEXIM1 protein. A lower H-score corresponds to lower HEXIM1 protein levels. (C) Immunohistochemical co-staining of HEXIM1 (blue) and MART1 (brown) in a normal human epidermis section at 400x magnification. The white arrow indicates a normal melanocyte that is positively co-stained by both HEXIM1 and MART1. (D) Immunohistochemical staining of HEXIM1 (pink) in normal epidermis, nevi and

(Continued) melanoma samples with low (H-score < 100) or high (H-score > 100) HEXIM1 levels from a human tissue microarray at 400x magnification.

HEXIM Overexpression Suppresses Melanoma Onset *in vivo*.

Decreased HEXIM1 expression in human melanoma suggests that HEXIM1 can suppress tumorigenesis and is consequently downregulated in tumors so they can gain a competitive growth advantage. To investigate the *in vivo* action of HEXIM on melanoma directly, we overexpressed human *HEXIM1* and zebrafish *hexim* in the MiniCoopR zebrafish melanoma assay system (Ceol et al., 2011). This system allows for melanocyte-specific expression of genes-of-interest, and enables the tracking of tumorigenesis over time. Compared to the *EGFP* background control and the *SETDB1* positive control, which accelerates tumor onset, both human *HEXIM1* and fish *hexim* effectively suppress melanoma onset (Figures 2.7A and 2.7B). 80% of *HEXIM1/hexim* fish remain tumor-free at the 25-week endpoint, while only 30% of *EGFP* fish and 10% of *SETDB1* fish are tumor-free. HEXIM1 can therefore robustly suppress melanoma in our zebrafish *in vivo* system.

We next investigated if HEXIM1 suppression of tumorigenesis is dependent on its P-TEFb sequestration function. It has been shown that the HEXIM1/P-TEFb interaction is modulated by mutating HEXIM1 amino acid residues at S268, T270, T276 and S278, located at the P-TEFb binding domain (Contreras et al., 2007). Mutating these sites to aspartate generates *HEXIM1-4D*, which ablates P-TEFb binding and renders HEXIM1 non-functional for inhibiting transcription elongation. Conversely, mutating these sites to alanine generates *HEXIM1-4A*, which can efficiently sequester P-TEFb. Overexpressing *HEXIM1-4A* suppresses tumors to a similar extent as *HEXIM1* and *hexim* (Figure 2.7C). Conversely, overexpressing *HEXIM1-4D* did not suppress tumors and tumorigenesis continued at the background rate similar to *EGFP* (Figure 2.7C).

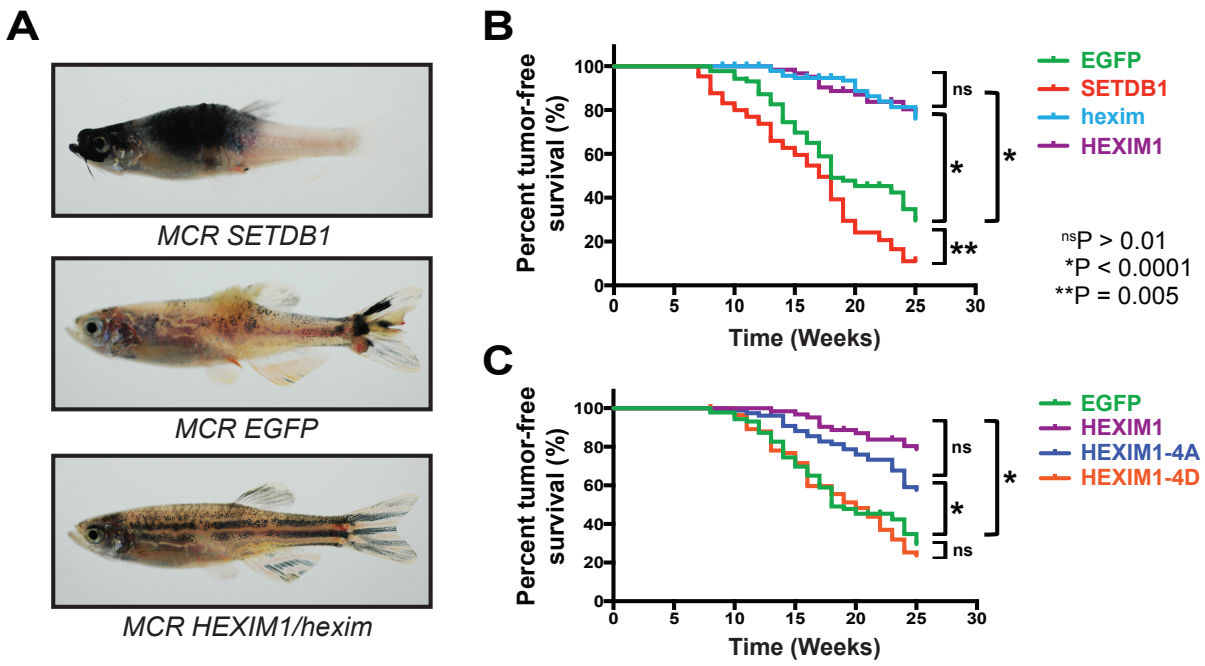

Figure 2.7 *HEXIM* Overexpression Suppresses Melanoma

(A) 19 week old *Tg(mitfa:BRAF^{V600E});p53$^{-/-}$;mitfa$^{-/-}$* zebrafish with rescued melanocytes expressing tumor accelerator *SETDB1*, background control *EGFP* or *HEXIM1/hexim* in the MiniCoopR system. (B) Tumor-free survival curves were generated for MiniCoopR zebrafish over a 25-week time period. Percentages of the total numbers of zebrafish that were tumor-free each week are plotted. We tested both human *HEXIM1* and zebrafish *hexim* overexpression in this system. The positive and background controls are known tumor accelerator *SETDB1* and *EGFP* respectively. (C) Tumor-free survival curves were also generated for overexpression of human *HEXIM1-4A*, which can efficiently bind P-TEFb, and human *HEXIM1-4D*, which does not bind P-TEFb, in this system.

To validate MiniCoopR integration and expression of the appropriate transgenes in our fish, we genotyped transgenic fish from tail fin clips containing melanocytes. We used PCR primers specific for human *HEXIM1* to amplify a 212 bp region containing the *HEXIM1-4A* and *-4D* mutations (Figure 2.8A). The PCR yielded products only for fish containing human *HEXIM1* constructs and not for those containing *EGFP* or zebrafish *hexim* (Figure 2.8A). The products were then sequenced to confirm that fish of each strain had the appropriate *HEXIM1* construct integrated (Figure 2.8B). We also performed HEXIM1 western blots on representative tumor and skin samples harvested from fish of each genotype to ensure that construct integration resulted

in the production of functional protein (Figure 2.8C). As expected, skin and tumor samples from *SETDB1* and *EGFP* transgenic fish did not express human HEXIM1 protein while all *HEXIM1* transgenic fish expressed significant levels of human HEXIM1 protein (Figure 2.8C). We did not detect any appreciable zebrafish hexim protein in the adult MiniCoopR fish skin and tumor samples, unlike in the 24 hpf embryo, where hexim protein is highly expressed. Zebrafish hexim is detected at the ~45 kD mark unlike human HEXIM1, which is larger and is detected at ~60 kD.

In addition to the effects in adult zebrafish, we also investigated the effects of *HEXIM1* overexpression in melanocytes during development. To this end, we generated stable lines from transient fish that were validated for MiniCoopR integration and HEXIM1 protein expression as mentioned previously (Figures 2.8A, 2.8B and 2.8C). Validated *HEXIM1*, *HEXIM1-4A* and *-4D* MiniCoopR transgenic fish were outcrossed to the *Tg(mitfa:BRAF^{V600E});p53$^{-/-}$;mitfa$^{-/-}$* strain to generate the stable lines. We outcrossed these stables to the *Tg(mitfa:BRAF^{V600E});p53$^{-/-}$;mitfa$^{-/-}$* strain and examined the melanocytes at 2 dpf, using a Tu wildtype strain incross as control (Figure 2.8D). These outcrosses produced offspring with an embryonic decrease in melanocytes similar to the effects of leflunomide, in the case of *HEXIM1* and *HEXIM1-4A*, but not *EGFP* or *HEXIM1-4D*, which maintain melanocytes comparable to the wildtype Tu strain. This is only a partial phenocopy of leflunomide since crestin expression is unchanged (data not shown). *HEXIM1* is being specifically overexpressed in melanocytes under the control of the mitfa promoter, so the early neural crest cells affected by leflunomide are still present in the transgenic embryos.

With transient and stable expression of HEXIM1 and its mutated forms in zebrafish melanocytes, we provide *in vivo* evidence for the tumor suppressing function of HEXIM independent of leflunomide, and show that the ability of HEXIM to sequester P-TEFb is required for this function.

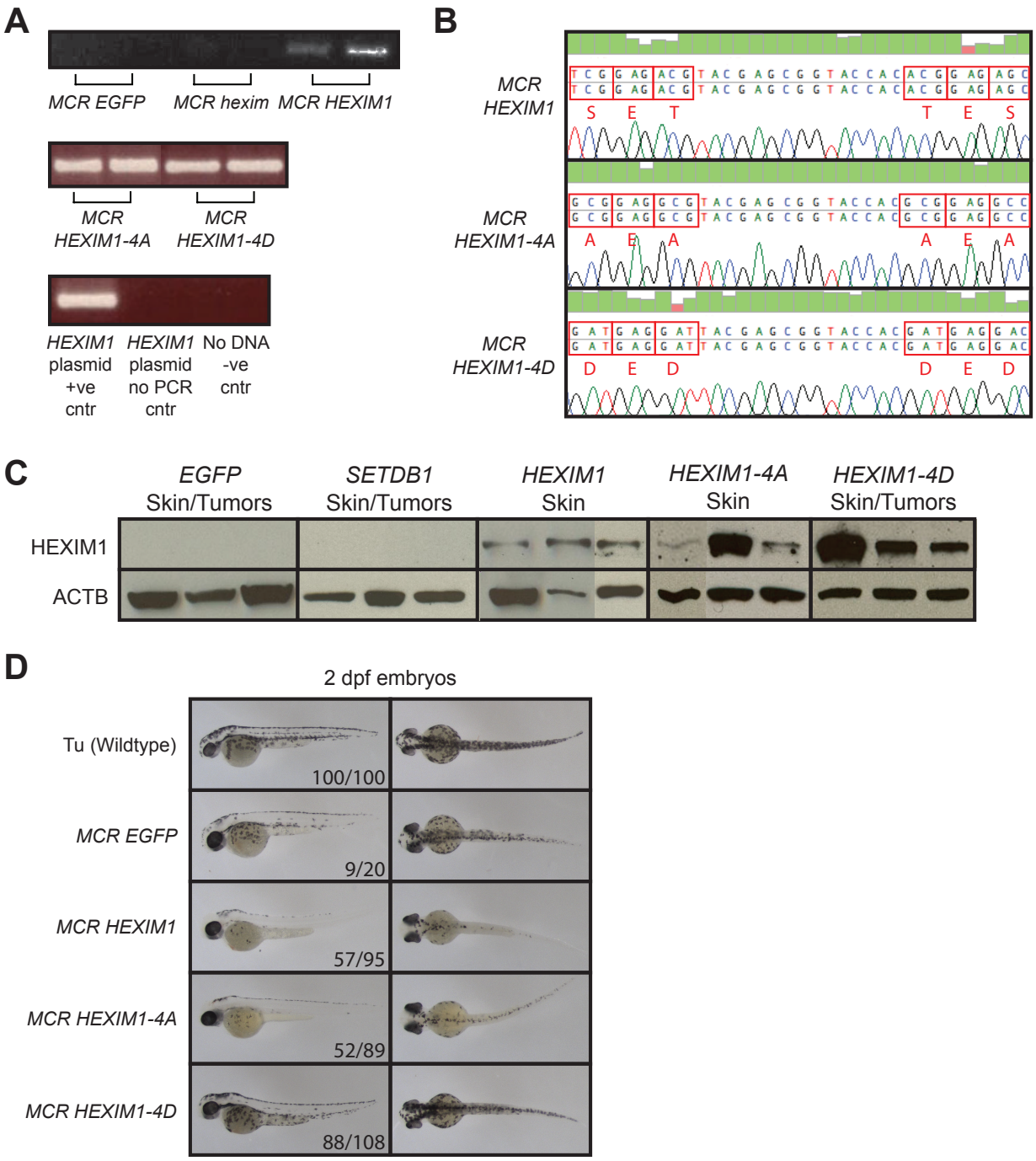

Figure 2.8 Validation of MiniCoopR HEXIM1 Integration and Overexpression in Adult *Tg(mitfa:BRAF^{V600E});p53$^{-/-}$;mitfa$^{-/-}$* Zebrafish, and Examination of Embryonic Phenotypes in Transgenic Zebrafish

(A) MiniCoopR transient and stable lines were validated by extracting genomic DNA from tail fin clips of adult zebrafish. The region of human *HEXIM1* that was mutated was then amplified by PCR. PCR was run on fin clips from *MCR EGFP* fish, *MCR hexim* fish, a *HEXIM1* plasmid, a no-DNA control and *HEXIM1* plasmid with no-PCR for comparison. (B) PCR amplification products

(Continued) from (A) were sequenced to confirm strains containing WT *HEXIM1*, *HEXIM-4A* or *-4D*. A representative sequencing trace shows that amino acids S268, T270, T276 and S278 in human *HEXIM1* were mutated to alanine in *HEXIM1-4A* and aspartate in *HEXIM1-4D*. (C) Three representative adult MiniCoopR-integrated zebrafish for each strain were sacked and protein was isolated from their skin or tumors, if present. Western blots for HEXIM1 and β-Actin were then performed on these samples. (D) Side and dorsal views of 2 dpf zebrafish embryos produced from incrosses of the Tu wildtype strain and outcrosses of MiniCoopR transgenic stable lines of *EGFP*, *HEXIM1*, *HEXIM1-4A* and *HEXIM1-4D* with the *Tg(mitfa:BRAF^{V600E});p53$^{-/-}$;mitfa$^{-/-}$* strain.

Induction of HEXIM1 by Leflunomide Reduces Productive Elongation.

Since HEXIM1 upregulation by leflunomide is sufficient to suppress tumors by sequestering P-TEFb, we investigated the transcriptional mechanism of how leflunomide-induced HEXIM1 can suppress tumorigenesis. We first performed Global Run-On sequencing (GRO-seq) on A375 cells treated with leflunomide or A771726 for 48 hrs to confirm the pausing phenotype observed by RNA Pol II ChIP-seq in our previous study. Only gene loci that were considered expressed in the DMSO condition were used in the GRO-seq analysis for DMSO, leflunomide and A771726 conditions. These genes are shortlisted based on a traveling ratio (TR) cutoff of less than 7.5 in the DMSO condition, similar to our previous study (White et al., 2011). TR is a measure of RNA Pol II transcription along a gene in which read density at the promoter is divided by read density along the gene body (Rahl et al., 2010). A higher TR corresponds to an increase in transcriptional pausing. Based on mapped reads, RNA Pol II occupancy at the promoters and gene bodies is plotted for the short-listed gene loci in all three conditions (Figure 2.9A). The overall traveling ratios obtained from Figure 2.9A demonstrate a significant increase in TR for both leflunomide and A771726 treatment (Figure 2.9B). Gene meta-analysis also shows that RNA Pol II density is significantly lower in the gene body with DHODH inhibition (Figure 2.9C). Example tracks of genes unaffected and affected by drug are shown in Figure 2.9D. An unaffected gene is housekeeping gene β-Actin (*ACTB*), while an affected gene is melanoma-associated transcription factor *HMGA2* (Raskin et al., 2013). The GRO-seq data supports the hypothesis that DHODH inhibition induces a transcriptional pause in these melanoma cells.

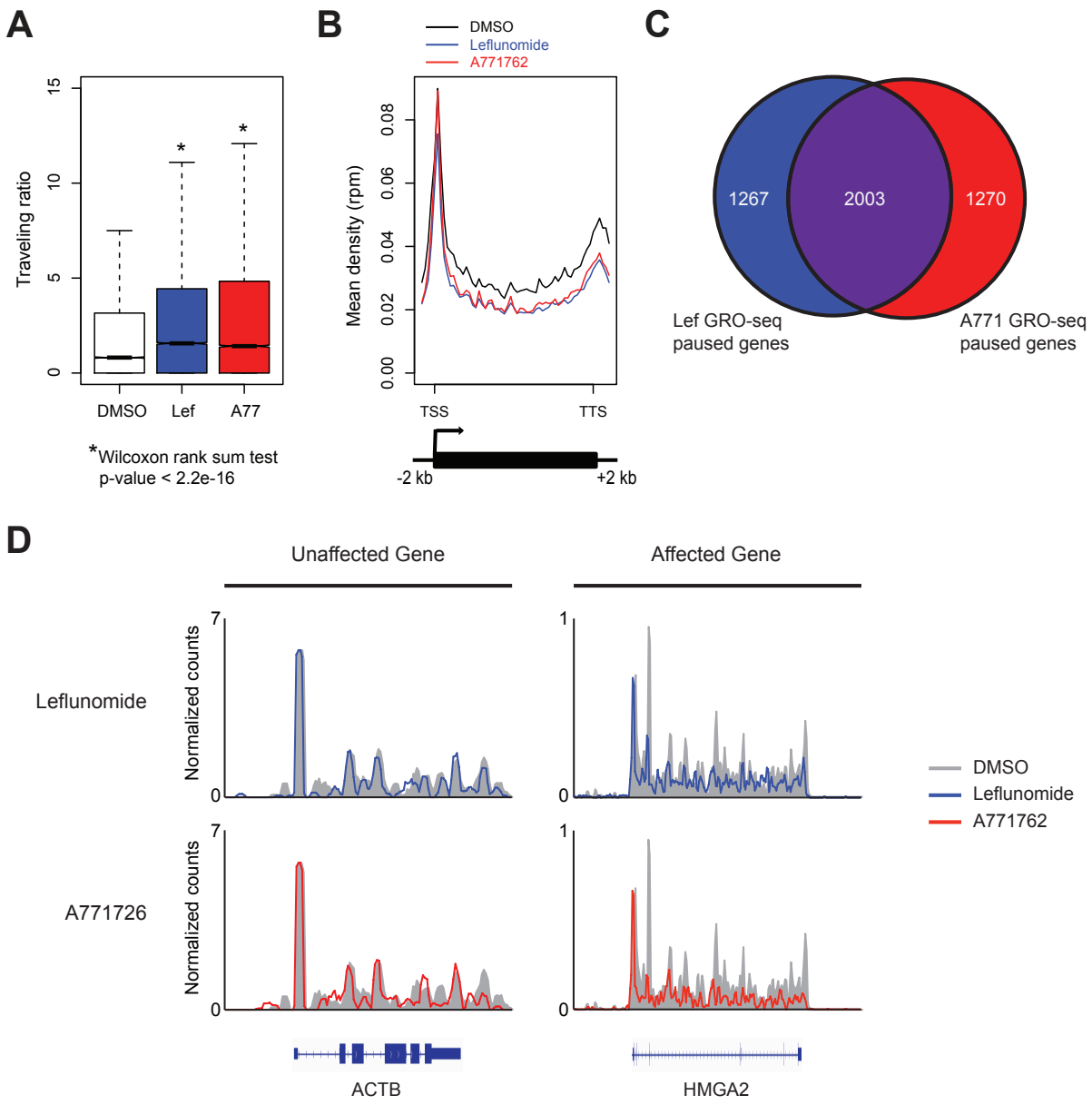

Figure 2.9 DHODH Inhibition Induces a Transcriptional Pause on Tumorigenic Genes

(A) GRO-seq read densities at the promoter (P) or within the Gene Body (GB) of genes with RNA Pol II traveling ratio (TR) < 7.5 from A375 human melanoma cells after 48 hr treatment with DMSO (white), 25 μM leflunomide (blue) or 25 μM A771762 (red) (mean of two replicates). (B) TR plots of genes from the GRO-seq experiment described in (A). (C) Metagene analysis of RNA Pol II occupancy +/-2 kb around transcription units from GRO-seq described in (A). (D) Representative traces of genes unaffected (*ACTB*) or affected (*HMGA2*) by leflunomide and A771726 treatment.

GRO-seq illustrates that DHODH inhibition is responsible for inducing a transcriptional pause, but does not provide any evidence for the involvement of HEXIM1. We therefore examined Ser-2 phosphorylation at the C-terminal domain (CTD) of RNA Pol II in A375 cells treated with A771726 in conjunction with HEXIM1 siRNA knockdown. The transition into productive elongation mediated by P-TEFb leads to increased Ser-2 phosphorylation in the CTD of the large subunit of RNA Pol II (Peng et al., 1998; Wei et al., 1998; Yang et al., 2001; Zhu et al., 1997). In cells with control siRNA, Ser-2 phosphorylation is decreased with a 48 hr drug treatment, along with a concomitant increase in HEXIM1 levels (Figure 2.10A). We expect this decrease in Ser-2 phosphorylation since the GRO-seq data shows there is a significant reduction in productive elongation at actively transcribed gene loci. This decrease in Ser-2 phosphorylation can be rescued by HEXIM1 knockdown (Figure 2.10A). DHODH inhibition also causes a previously undefined transcription initiation defect, evident from the decrease in Ser-5 phosphorylation caused by A771726 (Figure 2.10A). This is only partially rescued by HEXIM1 knockdown. These results provide support for a model that DHODH inhibition results in HEXIM1 induction and reduction of RNA Pol II Ser-2 phosphorylation.

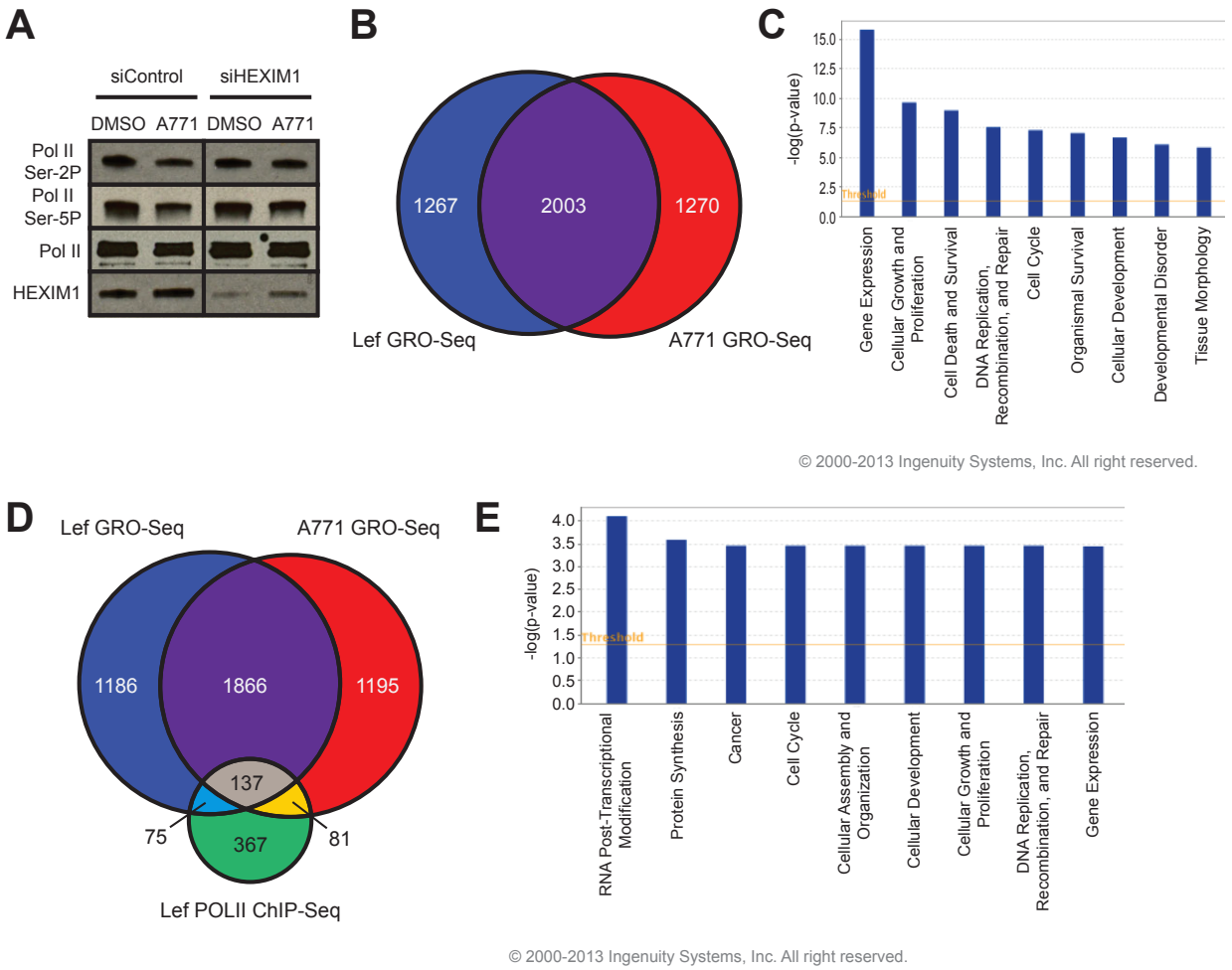

F

Transcription Factor	Motif	Leflunomide P-value (Paused/Unpaused)	A771726 P-value (Paused/Unpaused)
MYC/MAX		1.63E-08/1.26E-02	1.35E-06/2.88E-04
C-MYC		6.39E-08/5.12E-02	3.88E-04/3.46E-03
PAX3		1.91E-09/9.52E-03	2.89E-06/6.04E-03
ARNT		5.34E-08/3.78E-03	2.34E-08/2.09E-03
C-REL		2.01E-07/1.07E-03	7.78E-05/3.02E-04
PEA3		4.30E-06/4.19E-01	8.82E-06/7.74E-02

Figure 2.10 HEXIM1 Induction by Leflunomide Causes Transcriptional Pausing in Genes Associated with Cell Proliferation and Survival

(A) Western blot on A375 cells treated with 60 μM A771726 for 48 hrs combined with siRNA knockdown for HEXIM1. Proteins detected are RNA Pol II C-terminal domain Ser-2 and Ser-5 phosphorylation, total RNA Pol II and HEXIM1. (B) Venn diagram of the overlap of genes which transcripts have a RNA Pol II TR fold change > 1.3 in the leflunomide (blue) or A771762 (red) treated condition. (C) Ingenuity pathway analysis on the 2,003 overlapping genes from leflunomide and A771726 GRO-seq in (B) that are paused. (D) Venn diagram of the overlap of

(Continued) genes from (B) and the list of paused genes from our previously published RNA Pol II ChIP-seq data on A375 cells treated with leflunomide (White et al., 2011). (E) Ingenuity pathway analysis on the 137 overlapping genes among the data sets in (D). (F) Table of transcription factor motifs that are significantly enriched in genes paused by DHODH inhibition but not in unpaused genes. Motifs were shortlisted based on an enrichment p-value < 1.0E-04 in the paused gene list but not in the unpaused list.

To examine the genetic mechanism of how DHODH induced transcriptional pausing suppresses melanoma, we obtained a list of 2,003 overlapping significantly paused genes (fold change in TR > 1.3 drug versus DMSO) from the GRO-seq experiment to analyze in Ingenuity Pathway Analysis (Figure 2.10B). Genes involved in gene expression, cell proliferation, and cell death and survival are significantly enriched (Figure 2.10C). Also, we examined the overlap of the GRO-seq data with our previously published ChIP-seq paused gene list and analyzed this list of 137 genes via Ingenuity Pathway Analysis (Figure 2.10D). This gene list also showed enrichment in cell cycle and proliferation pathways, similar to the pathways enriched by examining only GRO-seq data (Figure 2.10E). In addition, we generated a list of 368 neural crest associated genes (Table 2.1) by gene expression and gene ontology analyses utilizing the zebrafish whole-mount mRNA expression database (http://zfin.org/cgi-bin/webdriver?MIval=aa-xpatselect.apg) and the gene ontology database AmiGO (Carbon et al., 2009) (http://amigo.geneontology.org). We compared this list to our GRO-seq paused gene list from Figure 2.10B and found that 33 neural crest associated genes are significantly paused in the GRO-seq experiment (Table 2.2). Of these genes, 5 are known to exacerbate melanoma. *GDNF*, *SMARCA4* and *STMN1* are upregulated in melanoma and contribute to melanoma pathogenesis (Chen et al., 2013; Lin et al., 2010; Ohshima et al., 2010). *CCDN1* is frequently mutated in melanoma and contributes to melanoma progression (Sauter et al., 2002). Elevation of *CTSB* contributes to the metastatic potential of melanoma (Sloane et al., 1982). Thus, DHODH inhibition seems to target melanoma by reducing productive elongation at genes associated with melanoma progression and metastasis, as well as general cell cycle and proliferation genes, negating their tumorigenic effect.

Table 2.1 List of Neural Crest-Associated Genes

Gene Symbol								
ABCC4	CHD7	EDNRA	GBX2	L1CAM	OVOL1	RADIL	SOX9	ZEB2
ACBD7	CHGA	EDNRB	GCH1	LAMA5	OVOL2	RALDH2	SPRY1	ZFP36L1
ACVR1	CHPF	EFNB1	GDF6	LATS2	PAH	RARA	SQSTM1	ZIC1
ACVR2A	CHSY3	EFNB2	GDNF	LEF1	PAICS	RARG	STAT3	ZIC2
ACVR2B	CITED2	EGR2	GIPC2	LEO1	PARP3	RASL11A	STMN1	ZIC3
AFAP1L1	CITED4	EIF2S1	GMPS	LHX6	PAX3	RAX	STX7	ZIC4
AK4	CNBP	ERBB2	GPD1	LIMD1	PAX7	RBP4	SUMO1	ZIC5
ALCAM	CNDP2	ERBB3	GPR143	LMO4	PAX9	RDH10	SUMO2	ZMAT1
ALDH16A1	CNN3	ERBB4	GREM1	LRAT	PBX1	RET	SUMO3	
ALDH1A2	COL11A1	FAM212A	GREM2	LRP5	PBX2	RGS14	SYNGR1	
ALDH2	COL15A1	FAM46B	GRHL2	LRP6	PBX3	RHOU	SYPL1	
ALK	COL2A1	FGF10	GRWD1	LRRC8D	PBX4	RNF41	TBC1D5	
ALX1	COL5A1	FGF15	GSC	MAFB	PCDH10	ROBO1	TBX1	
ALX4	COLEC11	FGF19	GSTP1	MARVELD1	PCDH18	RPE65	TBX22	
AMDHD2	CRABP1	FGF20	HAND2	MASP1	PCNA	RTF1	TES	
ANKRD50	CRABP2	FGF3	HDAC4	MDK	PDE7A	RUNX2	TFAP2A	
AOX1	CRIP2	FGF8	HES1	MECOM	PDGFRA	RXRA	TFAP2B	
AP2A1	CSF1R	FGFR1	HES3	MED12	PEPD	RXRG	TFAP2C	
AQP7	CTR9	FGFR2	HES4	MEF2A	PHACTR4	SALL4	TFAP2E	
ARG1	CTSB	FGFRL1	HHIP	MEF2C	PHLDA1	SDC4	TFEC	
ASPM	CTSC	FLNC	HIF1A	MEIS1	PHOX2B	SEMA3C	TGFB2	
ATIC	CXCR4	FLRT3	HOXA1	MEIS3	PIAS2	SEMA3D	TGFB3	
ATOH8	CYB5A	FMOD	HOXA2	MITF	PITX2	SEMA3F	TGFBI	
ATP1B3	CYP26A1	FMR1	HOXB1	MOCOS	PKNOX1	SFRP1	TMEM243	
ATP6V1A	CYP26C1	FOXC1	HOXB2	MPV17	PLCB3	SFRP5	TNC	
B3GAT1	CYTH1	FOXC2	HOXB3	MREG	PLCG2	SHH	TRAF4	
BARX1	D4ADT9	FOXD1	HTR2B	MSX1	PLSCR1	SKIDA1	TRPM3	
BCMO1	DACH1	FOXD2	ID2	MSX2	PMEL	SLC16A1	TSPAN8	
BHLHE40	DCT	FOXD3	ID3	MYC	PNP	SLC1A3	TTC8	
BHLHE41	DDX21	FOXD4	IGDCC3	MYCN	POLD1	SLC22A7	TWIST1	
BMP2	DEGS1	FOXD4L1	IGFBP3	NAV3	POU3F3	SLC24A4	TWIST2	
BMP4	DERA	FOXD4L2	IL17RD	NES	PPAT	SLC40A1	TWIST3	
BMPER	DFNA5	FOXD4L4	IMPDH1	NEUROD4	PRDM1	SLC45A2	UBE2I	
BMPR1A	DISC1	FOXD4L5	IRX1	NEUROG1	PRDM12	SLC4A1	VENTX	
BTBD6	DLG1	FOXD4L6	ISL1	NRARP	PRDX1	SLC4A2	VGLL2	
C10orf11	DLL1	FOXD5	ITGA9	NRG1	PRIM1	SLMAP	WNT1	
CCND1	DLX2	FOXI1	ITGB1	NRG2	PROM1	SMAD4	WNT10A	
CD200	DPYSL2	FOXS1	ITPKC	NRP1	PTGIS	SMARCA4	WNT11	
CDCA7	DPYSL3	FRZB	JUNB	NRP2	PTRH2	SMO	WNT3A	
CDH2	DPYSL4	FSCN1	KAT6A	NRTN	PTTG1IP	SNAI1	WNT5A	
CDH6	DPYSL5	FZD3	KCTD15	NUSAP1	RAB11FIP2	SNAI2	WNT5B	
CDON	DSTN	FZD7	KIT	OCRL	RAB12	SOX10	WNT8A	
CERS1	DTNBP1	GADD45B	KITLG	olfm2a	RAB32	SOX11	WTIP	
CFL1	EDN1	GART	KLF2	OSR1	RAB3C	SOX4	XBP1	
CFL2	EDN3	GATA3	KRT18	OSR2	RAB7A	SOX8	ZBTB10	

Table 2.2 Traveling Ratios of Paused Neural Crest-Associated Genes

Table 2.2 (Continued)

RefSeq.ID	Gene Symbol	Average DMSO TR	Average Leflunomide TR	Average A77726 TR	TR Fold Change Leflunomide	TR Fold Change A771726
NM_001167882	ANKRD50	1.84	7.78	6.62	4.24	3.61
NM_020337	ANKRD50	1.84	7.78	6.62	4.24	3.61
NM_053056	CCND1	0.86	1.87	2.50	2.18	2.91
NM_001792	CDH2	2.21	9.23	11.65	4.17	5.27
NM_017780	CHD7	0.83	4.62	17.51	5.56	21.07
NM_133467	CITED4	3.60	4.76	8.51	1.32	2.36
NM_001908	CTSB	0.30	2.01	0.54	6.81	1.81
NM_147780	CTSB	0.30	2.01	0.54	6.81	1.81
NM_147781	CTSB	0.30	2.01	0.54	6.81	1.81
NM_147782	CTSB	0.30	2.01	0.54	6.81	1.81
NM_147783	CTSB	0.30	2.01	0.54	6.81	1.81
NM_001127453	DFNA5	2.77	4.30	4.33	1.55	1.56
NM_001127454	DFNA5	2.97	5.22	3.19	1.76	1.08
NM_004403	DFNA5	2.97	5.22	3.19	1.76	1.08
NM_000399	EGR2	0.54	1.81	2.41	3.38	4.51
NM_001136177	EGR2	0.54	1.81	2.41	3.38	4.51
NM_001136179	EGR2	0.54	1.81	2.41	3.38	4.51
NM_052943	FAM46B	0.37	0.83	1.35	2.26	3.69
NM_001004356	FGFRL1	0.41	0.00	1.90	0.00	4.63
NM_001004358	FGFRL1	0.41	0.00	1.89	0.00	4.62
NM_021923	FGFRL1	0.41	0.87	0.00	2.12	0.00
NM_004472	FOXD1	2.28	6.54	3.37	2.87	1.48
NM_000514	GDNF	0.33	1.02	1.35	3.10	4.10
NM_001190468	GDNF	3.59	1.03	0.41	0.29	0.11
NM_001190469	GDNF	3.59	1.03	0.41	0.29	0.11
NM_199231	GDNF	0.97	0.32	0.00	0.33	0.00
NM_002167	ID3	0.16	0.74	0.36	4.62	2.26
NM_000598	IGFBP3	0.75	1.96	6.02	2.60	8.00
NM_001013398	IGFBP3	0.75	1.96	6.02	2.60	8.00
NM_001142573	IMPDH1	2.23	8.26	4.78	3.70	2.14
NM_001142574	IMPDH1	2.23	8.26	4.78	3.70	2.14
NM_001142575	IMPDH1	2.23	8.26	4.78	3.70	2.14
NM_001099412	KAT6A	1.47	4.47	6.49	3.04	4.42
NM_001099413	KAT6A	1.47	4.47	6.49	3.04	4.42
NM_006766	KAT6A	1.47	4.47	6.49	3.04	4.42
NM_000224	KRT18	3.99	4.50	13.59	1.13	3.40
NM_199187	KRT18	2.04	3.44	11.23	1.69	5.51
NM_017947	MOCOS	3.66	5.34	9.30	1.46	2.54
NM_002449	MSX2	0.94	12.55	8.46	13.32	8.98
NM_003872	NRP2	2.39	7.55	5.54	3.17	2.32
NM_018534	NRP2	2.19	6.78	5.19	3.10	2.37
NM_201264	NRP2	1.92	6.91	4.92	3.61	2.57
NM_201266	NRP2	2.39	7.55	5.54	3.17	2.32
NM_201267	NRP2	2.19	6.78	5.19	3.10	2.37
NM_201279	NRP2	2.39	7.55	5.54	3.17	2.32
NM_023923	PHACTR4	2.14	38.32	8.86	17.87	4.13
NM_006928	PMEL	5.20	14.95	12.33	2.88	2.37
NM_014904	RAB11FIP2	1.12	11.32	8.10	10.10	7.22

Table 2.2 (Continued)

RefSeq.ID	Gene Symbol	Average DMSO TR	Average Leflunomide TR	Average A77726 TR	TR Fold Change Leflunomide	TR Fold Change A771726
NM_001242826	RNF41	6.31	10.73	15.27	1.70	2.42
NM_005785	RNF41	7.44	19.46	18.60	2.61	2.50
NM_194358	RNF41	7.44	19.46	18.60	2.61	2.50
NR_040053	RNF41	7.44	19.46	18.60	2.61	2.50
NM_001199692	SLC4A2	0.83	1.09	1.46	1.32	1.77
NM_001199693	SLC4A2	0.54	2.06	0.28	3.79	0.52
NM_003040	SLC4A2	0.26	2.56	1.13	9.83	4.34
NM_007159	SLMAP	1.39	3.43	3.97	2.47	2.86
NM_001128844	SMARCA4	4.01	9.01	8.04	2.25	2.01
NM_001128849	SMARCA4	0.27	0.84	2.13	3.08	7.84
NM_003072	SMARCA4	4.01	9.01	8.04	2.25	2.01
NM_001142298	SQSTM1	0.23	0.30	0.47	1.32	2.08
NM_001142299	SQSTM1	0.27	0.63	0.80	2.38	2.99
NM_001145454	STMN1	0.74	7.02	1.89	9.43	2.54
NM_005563	STMN1	0.34	4.19	0.89	12.16	2.59
NM_203401	STMN1	0.33	7.66	0.86	23.12	2.58
NM_001032280	TFAP2A	3.65	2.00	12.79	0.55	3.51
NM_003220	TFAP2A	0.61	1.82	0.48	2.97	0.79
NM_003222	TFAP2C	0.45	2.04	0.96	4.53	2.13
NM_004295	TRAF4	0.46	0.90	3.48	1.95	7.57
NM_003412	ZIC1	3.58	13.64	17.25	3.81	4.82

We also examined how paused genes might be differentially regulated from unpaused genes (fold change in TR < 0.7 drug versus DMSO). From each gene list, we determined enrichment scores for transcription factor binding motifs using the Transcription Factor Affinity Prediction (TRAP) program (Thomas-Chollier et al., 2011). After which, we shortlisted motifs that were significantly enriched for paused genes in both the A771726 and leflunomide GRO-seq data set, but were not enriched in the unpaused genes from these two data sets. We obtained motifs for a number of transcription factors that are enriched in the paused versus unpaused gene sets (Figure 2.10F). As expected, we found that MYC target genes are preferentially paused, as highlighted by the pioneering study on leflunomide and melanoma (White et al., 2011). MYC is required for neural crest development and regulates transcriptional pause release in embryonic stem cells (Hong et al., 2008; Rahl et al., 2010). In addition, PAX3 targets also seem to be preferentially paused. Mutations in *PAX3* in humans results in Waardenburg syndrome, a disease

characterized by deafness and pigment defects caused by problems in the embryonic neural crest (Baldwin et al., 1992; Tassabehji et al., 1992; Wollnik et al., 2003). PEA3, the targets of which are also paused, upregulates FAK to induce melanoma metastasis and regulates smooth muscle cell differentiation from the neural crest (Huang et al., 2011; Li et al., 2013b). DHODH inhibition seems to preferentially pause genes regulated by key neural crest-associated transcription factors.

Leflunomide Induces HEXIM1 to Sequester P-TEFb Away From Paused Gene Promoters

HEXIM1 has recently been shown to bind gene promoter regions on chromatin (Ji et al., 2013), so we investigated if HEXIM1 occupancy is modulated by leflunomide. We performed ChIP-seq for HEXIM1 and CDK9 to determine their respective binding regions in the A375 cells treated with either DMSO or A771726 for 48 hrs. Meta-gene analysis on the 2,003 paused genes from GRO-seq (Figure 2.10B) demonstrates that HEXIM1 and CDK9 are co-localized at the promoters in the A375 cells (Figures 2.11A and 2.11B). Furthermore, ChIP-seq region plots for HEXIM1 and CDK9 binding throughout the genome based on the union of HEXIM1 and CDK9 binding regions in the DMSO control show co-binding of HEXIM1 with CDK9 at the same regions (Figure 2.11C). HEXIM1 seems to poise CDK9 at gene promoters for a quick release to the transcriptional machinery when required. Drug treatment causes a decrease in both HEXIM1 and CDK9 occupancy on chromatin (Figures 2.11A, 2.11B and 2.11C). This postulates that the drug induces the 7SK snRNP to sequester P-TEFb away from chromatin to inhibit the transition from a paused state to productive elongation.

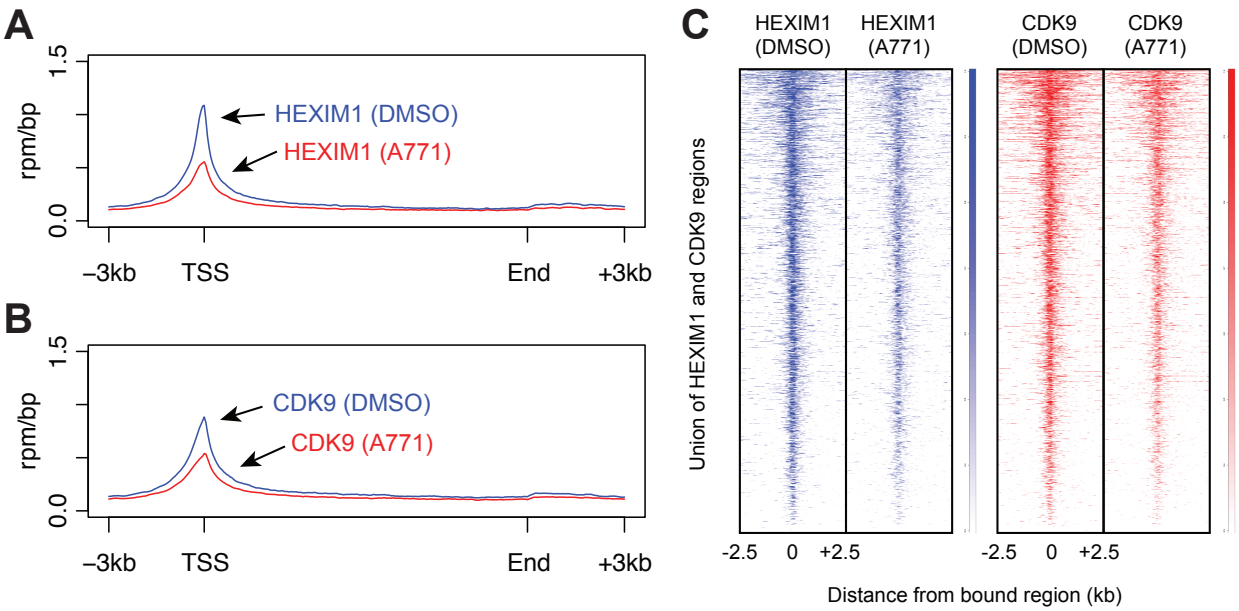

Figure 2.11 HEXIM1 Responds to DHODH Inhibition by Sequestering P-TEFb Away from Promoters

(A) Metagene analysis of genes with TR < 7.5 in the GRO-seq experiment for HEXIM1 binding regions determined by HEXIM1 ChIP-seq in DMSO or A771726 (25 μM for 48 hrs) conditions in the A375 cells. (B) Metagene analysis of genes described in (A) for CDK9 binding regions determined by CDK9 ChIP-seq in DMSO or A771726 (25 μM for 48 hrs) conditions in the A375 cells. (C) ChIP-seq region plots representing the distribution of regions bound by HEXIM1 and CDK9 in A375 cells, treated with either DMSO or 25 μM A771726 for 48 hrs, −2.5 and +2.5 kb relative to all HEXIM1 bound sites in the DMSO-treated A375 cells.

Discussion

Leflunomide can act as an efficient anti-melanoma drug, both on its own and in synergy with vemurafenib (White et al., 2011). The combination of these two drugs is currently in a Phase II clinical trial for metastatic melanoma. Leflunomide is a DHODH inhibitor that affects pyrimidine biosynthesis, resulting in a reduction in productive transcription elongation. A significant transcriptional reduction is induced in genes involved in cell proliferation and cell cycle, thereby slowing the growth and proliferation of the neural crest and melanoma. However, the mechanism of how a shortage of nucleotides through DHODH inhibition can eventually lead to a transcriptional pause is unclear. Our work presented here demonstrates an important role for HEXIM1 in regulating the transition of paused RNA Pol II to a state of productive elongation.

HEXIM1 can suppress melanoma

Even though we established that HEXIM1 is largely responsible for leflunomide's anti-melanoma effect through inhibiting productive transcription elongation, HEXIM1 alone has the ability to effectively suppress melanoma regardless of DHODH inhibition. HEXIM1 was previously discovered as a significantly upregulated gene upon treatment of cells with hexamethylene bis-acetamide (HMBA) (Ouchida et al., 2003). HMBA is a bipolar compound that was found to induce differentiation in a variety of cancer cell lines and primary human cancer cell cultures, instead of the usual cytotoxicity caused by prominent chemotherapies (Marks and Rifkind, 1989). Upregulation of HEXIM1 therefore seems to be involved in the transition of cancer cells from the proliferative to a differentiating state. Since then, there have been a number of studies illustrating the importance of upregulating HEXIM1 in suppressing breast cancer (Ketchart et al., 2013; Wittmann et al., 2003, 2005; Yeh et al., 2013) and prostate cancer (Mascareno et al., 2012). Furthermore, LARP7, a component of the 7SK snRNP complex that includes HEXIM1, is frequently mutated in gastric cancer (Cheng et al., 2012b; He et al., 2008; Mori et al., 2002). In these studies, the mechanism

of tumorigenic transformation and progression is the decreased ability of the 7SK snRNP to form, resulting in dysfunctional P-TEFb sequestration and consequently causing an upregulation in transcription elongation at tumorigenic genes. Furthermore, there have been recent efforts to develop inducers of HEXIM1 as anti-cancer drugs (Zhong et al., 2014).

HEXIM1 likely plays an important role in inhibiting cellular transformation to the tumorigenic state in melanoma as well. This is supported by the fact that HEXIM1 expression is significantly downregulated in a significant percentage of human melanoma samples. In addition, overexpressing HEXIM1 *in vivo* can suppress melanoma in our zebrafish melanoma model. By downregulating HEXIM1, tumors can aberrantly transcribe cell proliferation and metastatic genes without the availability of the 7SK snRNP to regulate them.

The ability for HEXIM1 to respond to cellular stress and negatively regulate transcription has great significance in tumorigenesis. Using leflunomide to create a state of cellular stress owing to nucleotide starvation upregulates HEXIM1, resulting in a transcriptional pause at a broad spectrum of genes associated with survival and proliferation. Metabolic drugs such as leflunomide that cause cellular stress and induce HEXIM1 can therefore pause numerous highly expressed genes simultaneously, targeting multiple pathways to halt the progression of cancer. Inducing the HEXIM1 stress pathway could therefore provide a multi-pronged gene expression approach, through modulating transcription elongation directly, to treat cancer. It can be argued that JQ1, a BRD4 inhibitor that causes a more rapid upregulation of HEXIM1 to trigger a transcriptional pause (Bartholomeeusen et al., 2012), might be better suited than leflunomide to treat melanoma. The fact that JQ1 targets BRD4 regardless of cell type (Delmore et al., 2011; Filippakopoulos et al., 2010) means it is much less selective. Each cell type may have an Achilles' heal for stress, and the neural crest seems to be particularly sensitive to low nucleotides, illustrated by patients with Miller's syndrome who harbor mutations in DHOHD and have neural crest defects (Ng et al., 2010). Even though leflunomide possesses slower kinetics in upregulating HEXIM1, possibly

because it takes some time for cells to become nucleotide starved, it seems more useful in targeting neural crest-derived cancers because of the innate sensitivity of the neural crest to nucleotide stress. Other cell types may be susceptible to different cellular stresses, and respond in a similar manner by activating HEXIM1, inducing transcriptional pausing to help the cell repair. It is particularly interesting and worthwhile to study such dependencies in other cancers and utilize the appropriate drugs to target these cell types specifically.

Materials and Methods

Cell Culture

Human A375 malignant melanoma cells (ATCC) are grown on standard tissue culture plates in filter sterilized DMEM (Life Technologies) with 10% heat-inactivated FBS (Atlanta Biologicals), 1X GlutaMAX (Life Technologies) and 1% Penicillin-Streptomycin (Life Technologies).

Drug Treatment

Zebrafish embryos were treated with leflunomide at 50% epiboly in E3 embryo media and fixed at 24 hpf and 2 dpf for further analysis. A375 human melanoma cell lines were treated at various time points. Drugs used were leflunomide (Enzo Life Sciences) and A771726 (Enzo Life Sciences).

Morpholino Injection

Morpholinos were obtained from Gene Tools, LLC, and injected into the yolk of the 1-cell stage embryo. Morpholinos were injected in a volume of 1 nL containing 8 ng of hexim, 8 ng of control, 10 ng of *bcdin3* and 12 ng of *larp7* morpholinos. *Bcdin3* and *larp7* morpholinos were previously published (Barboric et al., 2009). Morpholino sequences are:

hexim TAATAAGCTCCATAACTGCACACTC

hexim control TAATAGGCTCAATACCTGTACAATC

larp7 ATTAATAAAGTTACATACATCCATC

bcdin3 CATGTTTCTGTGGTCTTACCTTAAT

RNA Extraction and Quantitative RT-PCR Analysis

RNA isolation was performed using TRIzol (Life Technologies), and subsequently treated with the TURBO DNA-free kit (Life Technologies). cDNA was synthesized with the SuperScript III

Kit (Life Technologies). Quantitative PCR was performed on the iQ5 real-time PCR machine using the Ssofast EvaGreen Supermix (BioRad). The ΔΔCt method was used for relative quantification. RT-PCR primers are:

hexim forward: 5'-CAAACACGAGATTTGAGTTAAACG-3'

hexim reverse: 5'-CTCGTCCGATAATCTCTCTGC-3'

HEXIM1 forward: 5'-GACCTGGGAAGAGAAGAAAAAG-3'

HEXIM1 reverse: 5'-GAGGAACTGCGTGGTGTTATAG-3'

gapdh forward: 5'-GTGGAGTCTACTGGTGTCTTC-3'

gapdh reverse: 5'-GTGCAGGAGGCATTGCTTACA-3'

GAPDH forward: 5'-AAGGTGAAGGTCGGAGTCAA-3'

GAPDH reverse: 5'-AATGAAGGGGTCATTGATGG-3'

Antibodies

The HEXIM1 antibody from Abcam (ab25388) was used for western blots, co-immunoprecipitation and immunohistochemistry. IgG normal rabbit control antibody for Co-IP was from Millipore (12-370). Western blot antibodies used were BCDIN3 (ab139562), LARP7 (ab105682), CDK9 (ab76320), CCNT1 (ab2098) and RNAPII Ser-2 phosphorylation (ab 5095) from Abcam, as well as RNAPII (sc-899X) from Santa Cruz Biotechnology and β-Actin (A2228) from Sigma. Western antibodies used in the glycerol gradients were CDK9 (C-20) (sc-484) and CCNT1 (sc-10750) from Santa Cruz.

Glycerol Gradients

Glycerol gradients (10%-30%) were established by pipetting 2 mL of each glycerol fraction (10, 15, 20, 25 and 30% v/v) in MS buffer A into centrifugation tubes (Beckman 331372). Gradients were formed by standing for 6 s at 4° C. A375 cells (106) were untreated or treated

with A771726 for indicated periods of time and lysed in 0.6 mL of buffer A (20 mM HEPES-KOH, pH7.8, 0.2 M KCl, 0.2 mM EDTA, 0.5% NP40) containing protease inhibitors (Pierce) and RNase OUT (Invitrogen) for 30 mins at 4°C. Lysates were centrifuged at 14,000 rpm for 10 minutes and supernatants were loaded into tubes with preformed glycerol gradients. Protein complexes were then fractionated by centrifugation in an SW40T1 rotor (Beckman) at 38,000 rpm for 21 hrs. Ten fractions (1 mL) were collected, precipitated with trichloracetic acid and analyzed with the indicated antibodies by western blotting.

HEXIM1 Co-immunoprecipitation

Co-IP was performed using the Dynabeads Protein G Immunoprecipitation Kit with the DynaMag-2 Magnet (Life Technologies). Adherent cells plated on 10 cm culture plates were placed on ice and washed twice with ice-cold 1X PBS. 1 mL of ice-cold RIPA lysis and extraction buffer (Thermo Scientific), containing protease (Sigma) and phosphatase (Thermo Scientific) inhibitor cocktails, was added to each plate. Cells were scraped into the RIPA buffer and allowed to rotate in microfuge tubes at 4°C for 30 mins. Cell suspensions were then centrifuged at 12,000 rpm at 4°C for 10 mins to pellet cell debris. Protein concentrations of cell lysates were then measured by the DC Protein Assay (Bio-rad) to normalize all samples. Beads were prepared by washing 3 times with 5% Bovine Serum Albumin (Sigma) in 1X PBS on the magnetic stand. For 2 mg total protein, 33 µL of beads and 8 µg of antibody were used. Cell lysates were pre-cleared with beads for 1 hr rotating at 4°C. Beads used for pre-clearing were isolated by magnet and the pre-cleared cell lysate were transferred to a new microfuge tube. This is followed by overnight incubation of the cell lysate with either the HEXIM1 antibody (Abcam) or IgG control (Millipore) at 4°C. Next, fresh beads were added to the lysate-antibody mix for a 2 hr to overnight incubation at 4°C. Protein-bead complexes were then washed 4 times with ice-cold lysis buffer, which consisted of cycles of resuspending beads in wash buffer and isolating beads on the magnet. The final wash

is then removed from the beads and the beads were boiled in 50 µL Laemmli Buffer (Bio-rad) to elute proteins. Eluates were analyzed by western blotting.

Melanoma Immunohistochemical H-scoring

The human melanoma tissue microarray ME1004b (Biomax) used for IHC contains 62 cases of malignant melanoma, 20 cases of metastatic malignant melanoma and 18 cases of nevus tissue. In an attempt to accurately describe the extent of immunohistochemical staining of a tumor, the degree of IHC staining, if any, in each sub-cellular compartment in tumor cells is captured for each analyte. This algorithm includes capturing the percentage of tumor cells stained at each intensity level. A semi-quantitative intensity scale ranging from 0 for no staining to 3+ for the most intense staining is used. All of this information can be analyzed separately or used to calculate a variable, more continuous than simply Positive versus Negative, called the H-Score (McClelland et al., 1990). This score is more representative of the staining of the entire tumor on the section. Although given sections may share the same simple intensity score, there clearly is a difference between a 3+ case with only 10% of the cells staining as compared to a 3+ case where greater than 90% of the cells are staining. This difference is easily picked up using the H-Score method. An H-Score is typically calculated for staining of each sub-cellular compartment for both normal and tumor cells using the following formula; H-Score = (% at 0) * 0 + (% at 1+) * 1 + (% at 2+) * 2 + (% at 3+) * 3. Thus, this score produces a continuous variable that ranges from 0 to 300.

MiniCoopR Assay

The miniCoopR vector sequence and construction was previously described (Ceol et al., 2011). Human *HEXIM1* and zebrafish *hexim* miniCoopR clones were created by MultiSite Gateway recombination (Invitrogen) using full-length open reading frames. *HEXIM1-4A* and *-4D* clones were created by site-directed mutagenesis using the QuikChange II XL Mutagenesis Kit

(Agilent). 25 pg of each miniCoopR clone and 25 pg of mRNA encoding the Tol2 transposase were microinjected into one-cell zebrafish embryos generated from an incross of *Tg(mitfa:BRAF^{V600E}); p53$^{-/-}$; mitfa$^{-/-}$* zebrafish. Rescued animals were scored weekly for the presence of visible tumors.

Zebrafish Genotyping

Adult transgenic zebrafish for WT *HEXIM1*, *HEXIM1-4A* and *-4D* were genotyped by tail fin clipping. Genomic DNA was extracted by incubating fin clips in 25 µL of alkaline lysis buffer (25 mM NaOH, 0.2 mM disodium EDTA) for 1 hr at 95°C. The mixture was then quenched on ice with 25 µL of neutralization solution (Tris-HCL 40 mM) added and mixed by pipetting. Insoluble debris was pelleted by centrifuging for 5 min at 1,000 rpm. The supernatant containing genomic DNA was subjected to PCR with primers: *HEXIM1* forward: 5'-CTCAAAACCGGCCTGTACTC-3', *HEXIM1* reverse: 5'-TCCTTGATGAGCTCCTGCTT-3' to amplify a 212 bp region of human *HEXIM1* which contains the 4A and 4D mutations. PCR products were then sent for sequencing.

GRO-seq Sample Preparation and Sequencing

GRO-seq was performed as previously described (Kim et al., 2013), except conditions were optimized to A375 cells, and libraries were multiplexed to conduct high-throughput sequencing in one lane. One million A375 cells per condition were treated with DMSO, 25 µM leflunomide, or 25 µM A771726 in duplicate. After a 48 hr treatment, cells were washed, swelled, and lysed in lysis buffer with a reduced amount of IGEPAL detergent (composition: 10 mM Tris-Cl pH 7.5, 2 mM MgCl2, 3 mM CaCl2, 10% glycerol, 2 U/mL SUPERasin (Ambion), and 0.25% IGEPAL). Cells were frozen down, nuclear run-on reaction was performed, and nascent RNA was isolated. Adaptors were ligated the same as before, however, TruSeq small RNA sample prep kit adapters and primers (Illumina) were used to make the samples suitable for multiplexing (indexes 1 and 2, 3 and 4, and 5 and 6 were used for DMSO, leflunomide, and A771726 treated nascent RNA

libraries, respectively). The PCR reaction was run for 18 cycles. The indexed libraries were purified on a 6% native polyacrylamide gel, and were cut out between 150 and 300 bp. The concentration of the isolated libraries was estimated with a high-sensitivity DNA chip from Agilent according to the manufacturer's protocol and libraries were mixed in equal quantities and sequenced on Illumina Hi-Seq2000. Index sequences from multiplexed primers were used to identify treatment group and reads were demultiplexed using a perl script.

GRO-seq Data Analysis

GRO-seq data were processed as described in (Sigova et al., 2013). Briefly, for each replicate of DMSO (control), Leflunomide and A771762 treated samples, reads were trimmed at the 3′ends to remove any linker sequence contamination. Trimmed reads for each sample were aligned to the hg18 version of the human genome using Bowtie 0.12.9 with parameters -k 1 -m 10 -n 2 --best --strata. RNA repeats were then filtered out from the alignments using bedtools. Total number of sequenced, mapped, and filtered reads are shown in Table 2.3. Metagenes were created using the method described in (White et al., 2011). The average density of reads was calculated from the two biological replicates using respectively 5 fixed bins for the TSS -2 kb to TSS and TTS to TTS +2 kb regions, and 50 variable bins equally dividing the lengths of each gene. For each sample, the mean densities of reads were normalized to the read density at the promoter of the beta-Actin gene, which transcription is not modified by Leflunomide treatment, and expressed as a fraction of millions of mapped reads per base pair (rpm/bp). Read density at the promoters and within the gene bodies were respectively calculated as the read density within 300 bp of the TSS, and the read density within the TSS +300 bp to the TTS +3 kb. Densities were normalized to the read density at the beta-Actin promoter for each sample. RNA Polymerase II Travelling ratios (TR) were calculated as described in (Rahl et al., 2010; White et al., 2011) as the ratio of read densities at the promoters over the read densities within the gene bodies for

each transcript in each sample. Average TRs were calculated from the TRs calculated in two experimental replicates. To quantify the effects of the drug treatment on the TRs, samples were compared using a Wilcoxon rank sum test. The read densities were calculated on the transcripts which have a TR in the DMSO control condition initially low (TR< 7.5), representing 22442 over 47021 transcripts. For examples of affected and unaffected genes, the GRO-Seq read density profiles for single genes were plotted from -2 kb to TSS to TTS +2 kb. The y-axes shows the average reads per base per million total sample reads. The profile of DMSO, Leflunomide and A771726 treated samples are normalized based on the read density of the peak at the promoter region.

Table 2.3 Number of Reads in the GRO-seq Datasets

Sample	Sequenced	Mapped	Filtered
DMSO_a	12174743	6235753	1314438
DMSO_b	15400969	6907706	1561337
Leflunomide_a	17119601	8792723	1970152
Leflunomide_b	20658238	9441667	1817574
A771762_a	27873749	14033458	2840767
A771762_b	24780556	11104376	2183387

HEXIM1 siRNA Knockdown in Cell Culture

200,000 A375 cells were plated in 6-well plates in complete media and rested for 24 hrs. 50 ng of HEXIM1 SMARTpool siRNAs (Thermo Scientific Bio) were then transfected into the cells via DharmaFECT 1 reagent (Fisher Scientific) following the recommended protocol accompanying the DharmaFECT reagent. Cells were incubated in transfection media containing 60 μM A771726 for 48 hrs before protein was harvested for western blot.

Generation of Neural Crest Gene List

Vertebrate neural crest-associated genes were identified by gene expression and gene ontology analyses. The zebrafish whole-mount mRNA expression database (http://zfin.org/cgi-bin/webdriver?MIval=aa-xpatselect.apg) and the gene ontology database AmiGO (Carbon et al., 2009) (http://amigo.geneontology.org) were queried for 'neural crest' search terms (databases were accessed by EvR on 10 September 2012). High-confidence human orthologs were predicted using the DRSC Integrative Ortholog Prediction Tool DIOPT (Hu et al., 2011) (http://www.flyrnai.org/cgi-bin/DRSC_orthologs.pl). Only orthologs with the highest weighted prediction score were included on the neural crest-associated gene list.

GRO-seq Gene Motif Analysis

Transcripts having a TR fold change > 1.3 were considered as paused and transcripts having a TR fold change < 0.7 were considered as unpaused. TSS +-300bp sequences of each list of transcript for each of the Leflunomide or A771762 drug treated condition were extracted. 1500 randomly picked promoter sequences in each list were used as input for the Transcription Factor Affinity Prediction (TRAP) program using TRANSFAC vertebrates set of motifs, human promoters as the background model, and Benjamini-Hochberg as the multiple test for p-value correction (Thomas-Chollier et al., 2011). The transcription factor binding sequence motifs that were enriched with a corrected p-value < 1e-4 in the paused list of transcripts but not in the unpaused list of transcripts were selected and their motif logo were recovered from the TRANSFAC database (Matys et al., 2006).

ChIP-seq Sample Preparation and Sequencing

ChIP-seq was performed as previously described (Lee et al., 2006), except growth conditions were optimized to A375 cells, and libraries were multiplexed to conduct high-throughput

sequencing in one lane. One hundred million A375 cells per condition were treated with DMSO or 25 μM A771726. After a 48 hr treatment, cells were fixed in 11% formaldehyde and subjected to chromatin immunoprecipitation with HEXIM1 antibody (Abcam) or Cdk9 (C-20) antibody (Santa Cruz). 10 μL of input DNA and the entire volume of ChIP DNA samples were prepared for sequencing. The End-It DNA End-Repair Kit (Epicentre) was used to turn DNA overhangs into phosphorylated blunt ends and the Agencourt AMPure XP PCR Purification Kit (Beckman Coulter) was used to purify the resulting samples using a 1.8X ratio of beads to sample. Next, a single A in the 3' end was added to samples using the Klenow Fragment enzyme (NEB) to allow for directional ligation and the AMPure Kit was again used to purify samples. Illumina adaptor oligos (1:10 dilution) were added to samples using the Quick Ligation Kit (NEB) and NEBNext Multiplex Oligos for Illumina Kit (NEB), and samples were purified with the AMPure Kit. Samples were then size-selected with the AMPure beads with a 0.9X bead to sample ratio. Multiplexing primers from the NEBNext Multiplex Oligos Kit were added during the 18-cycle PCR enrichment step, which utilized the Phusion High-Fidelity PCR Master Mix (NEB), to generate indexed libraries (multiplex indexes used were: 3 – DMSO Input, 4 – A771726 Input, 5 – DMSO Cdk9 IP, 6 – A771726 Cdk9 IP, 9 – DMSO HEXIM1 IP, 10 – A771726 HEXIM1 IP). Indexed libraries were separated on a 2% agarose gel. Products between 150-350 base pairs were excised and gel purified using the QIAquick Gel Extraction Kit (Qiagen). The concentration of the isolated libraries was estimated with a high-sensitivity DNA chip from Agilent according to manufacturer's protocol and libraries were mixed in equal quantities and sequenced on Illumina Hi-Seq2000. Index sequences from multiplexed primers were used to identify treatment group and reads were demultiplexed using a perl script.

ChIP-seq Data Analysis

All ChIP-seq data sets were aligned using Bowtie (version 0.12.2) (Langmead et al., 2009) to build version hg19 of the human genome with parameters “-k 2 -m 2 -n 2”. We used the MACS version 1.4.1 (Model-based analysis of ChIP-seq) (Zhang et al., 2008) peak finding algorithm to identify regions of ChIP-seq enrichment over background. A p-value threshold of enrichment of 1e-9 was used for all data sets with parameters “--keep-dup=2”. To obtain the normalized read density of ChIP-seq data sets in any region, ChIP-seq reads aligning to each region were extended automatically by MACS, and the density of reads per bp was calculated. The density of reads in each region was normalized to the total number of million mapped reads producing read density in units of reads per million mapped reads per bp (r.p.m./bp).

Heatmap Representation of ChIP-seq Read Density Profiles

The merged regions of CDK9 DMSO control and HEXIM1 DMSO control were aligned at the center in the composite view of signal density profile. The enriched regions of CDK9 DMSO and HEXIM1 DMSO were first merged together if overlapping by 1 bp, resulting in a total of 9,230 merged regions. The average ChIP-seq read density (r.p.m./bp) around 5 kb centered on the centers in 50 bp bin was next calculated and displayed.

Meta Representation of ChIP-seq Read Density Profiles

We first created density vectors for the list of transcribed genes with initial TR < 7.5 from the GRO-seq experiment. The densities in the promoter, gene body, and gene end region were placed into 320 bins to create a density vector. 60 fixed width bins for the -3000 to 0 promoter region, 200 variable bins equally dividing the length of the gene, and 60 fixed bins for the 0 to +3 kb after transcript end region. The average ChIP-seq read density (r.p.m./bp) for each bin was next averaged and displayed.

Chapter 3:

HEXIM1 Pauses Transcription in Response to Nucleotide Starvation

Justin L. Tan[1,2], Rachel D. Fogley[1,2], Cristina Santoriello[1,2], John M. Asara[3], and Leonard I. Zon[1,2] *

[1]Howard Hughes Medical Institute, Stem Cell Program and Division of Pediatric Hematology/ Oncology, Boston Children's Hospital, Dana-Farber Cancer Institute, Harvard Medical School, Boston MA 02115, USA. [2]Department of Stem Cell and Regenerative Biology, Harvard Stem Cell Institute, Cambridge, MA 02138, USA. [3]Department of Medicine, Division of Signal Transduction, Beth Israel Deaconess Medical Center and Harvard Medical School, Boston, MA 02215, USA.

*To whom correspondence should be addressed
Address: 300 Longwood Ave, Boston, MA 02115
Email: zon@enders.tch.harvard.edu

Attributions

I conceived the idea to perform metabolite profiling on leflunomide-treated A375 cells to determine changes in metabolism. In addition, I performed cell culture and metabolite extraction. M. Yuan and J. M. Asara ran my samples on the mass spectrometer utilizing the liquid chromatography-based tandem mass spectrometry (LC-MS/MS) methodology. After which, I normalized the raw data and analyzed the processed data in Microsoft Excel and on the Metaboanalyst web server to generate the metabolite heatmap, fold changes, time course analysis and metabolite set enrichment analysis (MSEA). C. S. Santoriello optimized the nucleotide rescue experiment and performed the crystal violet cell number assay. I performed the real time RT-PCR analysis for the nucleotide rescue experiment and the western blots for HEXIM1 and ACTB, with technical assistance from R. D. Fogley.

Introduction

The primary function of leflunomide is to bind and inhibit DHODH, leading to a block in pyrimidine biosynthesis and a subsequent decrease in proliferation of neural crest and melanoma. Since leflunomide targets a metabolic process, we investigated how metabolism is affected by drug treatment by metabolite profiling. Metabolite profiling is highly analogous to microarray gene expression analysis, where the relative amounts of a number of metabolites in a cell are measured via targeted mass spectrometry under various conditions, in our case, with and without leflunomide. One can examine significant differences in metabolites with online tools in the Metaboanalyst web server (Xia et al., 2009, 2012). In addition to metabolite profiling, we examined how *HEXIM1* expression is regulated by primary metabolic changes induced by leflunomide.

Results

Leflunomide Primarily Targets Pyrimidine Biosynthesis

Leflunomide targets a key metabolic pathway, so we explored the changes in metabolism caused by the drug. We employed liquid chromatography-based tandem mass spectrometry (LC-MS/MS) (Yuan et al., 2012) to perform metabolite profiling on A771726 treated A375 cells at various time points. From the heatmap profile, metabolites are unchanged by DMSO treatment at various time points, while A771726 treatment causes significant changes in multiple metabolites, particularly from 24 hrs onwards (Figure 3.1, Tables 3.1 and 3.2). The cut-off for a significant altered metabolite is at least a 2-fold change in relative levels with an accompanying p-value of less than 0.05 (Student's two-tailed t-test). Metabolite Set Enrichment Analysis (MSEA) of significantly altered metabolites at the various time points indicates that pyrimidine biosynthesis and RNA transcription are significantly dysregulated at the 24, 48 and 72 hr time points (Figure 3.2). These results demonstrate that the drug is specifically targeting pyrimidine biosynthesis as expected.

Further analysis of pyrimidine biosynthesis and purine biosynthesis alone also reflects the specificity of the drug. Significant upregulation of the pyrimidine intermediate N-carbamoyl-L-aspartate upstream of DHODH is already seen with 1 hr of drug treatment (Figure 3.3A). At later time points, there is significant upregulation of all metabolites upstream of DHODH and significant downregulation of metabolites downstream of DHODH (Figure 3.3A). Purine biosynthesis intermediates are hardly affected until 72 hrs of treatment. Furthermore, significant metabolite changes are primarily limited to pyrimidine intermediates before 48 hrs, after which secondary effects are observed (Figure 3.1, Tables 3.1 and 3.2). These metabolite profiles highlight the high degree of specificity of A771726 to pyrimidine biosynthesis.

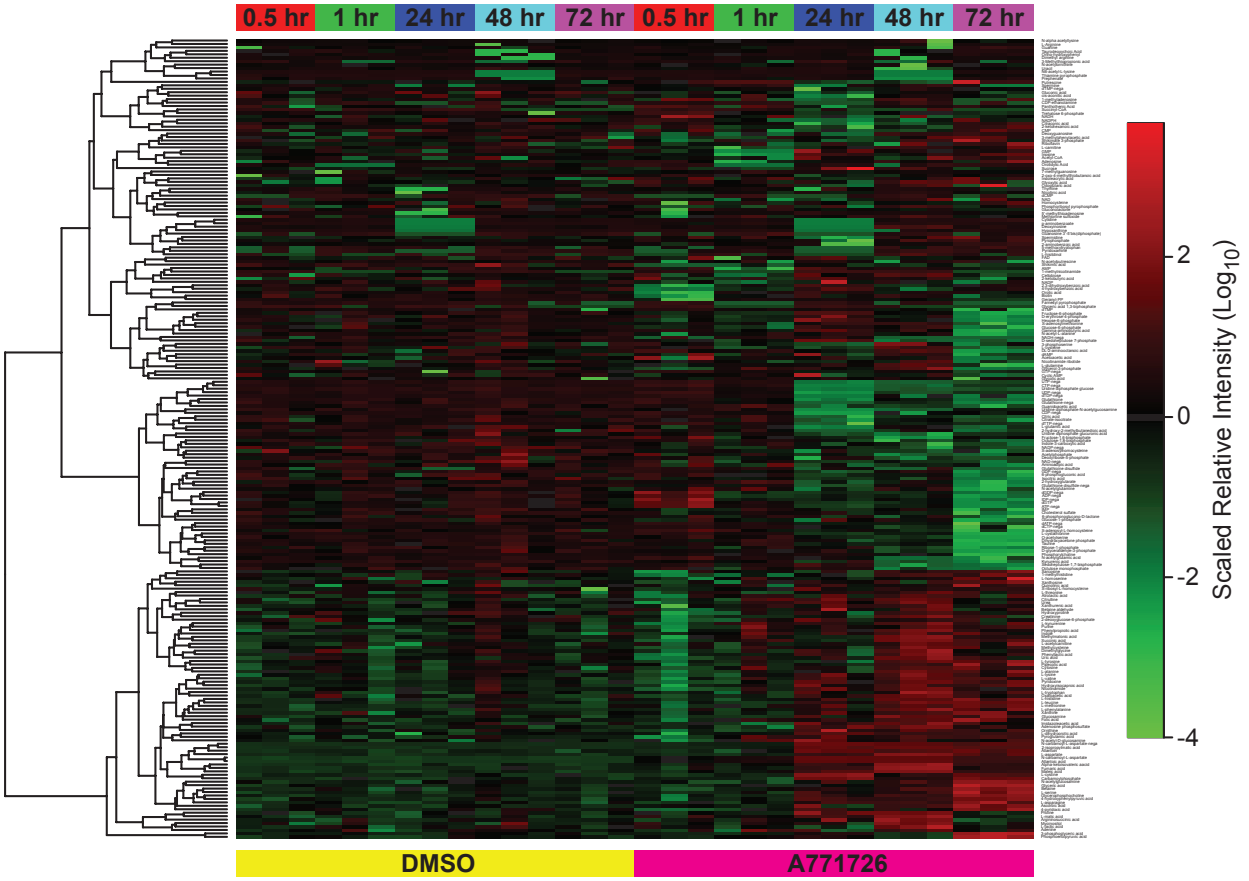

Figure 3.1 Metabolite Profiling of DHODH Inhibition in A375 Cells

LC-MS/MS metabolite profile of the A375 cell line treated with DMSO or 25μM A771726 over various time points.

Table 3.1 List of Metabolites Significantly Upregulated by A771726 Treatment

Time Point	Metabolite	Fold Change	P-value
0.5 hr	N-carbamoyl-L-aspartate	6.53	1.88E-05
	dTTP	2.32	6.45E-03
	Trehalose-6-Phosphate	2.32	9.12E-03
1 hr	N-carbamoyl-L-aspartate	14.95	7.92E-03
	Putrescine	3.15	5.74E-03
24 hr	N-carbamoyl-L-aspartate	187.36	2.42E-03
	Dihydroorotate	57.33	1.29E-03
	2-Isopropylmalic acid	19.13	9.91E-03
	Cystine	10.26	6.72E-03
	Methylnicotinamide	3.73	2.85E-02
	Aspartate	3.00	2.56E-03
	Carbamoyl phosphate	2.94	7.27E-04
	Allantoin	2.50	2.36E-03
	dCDP	2.06	6.78E-04
	Maleic acid	2.06	9.95E-04
48 hr	N-carbamoyl-L-aspartate	180.62	1.52E-03
	2-Isopropylmalic acid	21.28	1.05E-03
	Dihydroorotate	15.70	5.85E-04
	Aspartate	6.71	1.68E-03
	N-acetyl spermidine	4.89	4.25E-03
	Deoxyinosine	4.71	1.91E-02
	Adenosine 5-phosphosulfate	2.87	2.20E-02
	Fumarate	2.82	4.56E-04
	2-keto-isovalerate	2.75	1.35E-03
	Maleic acid	2.70	1.37E-04
	Guanosine	2.22	1.91E-02
	Allantoin	2.16	7.16E-03
	Imidazole	2.08	4.87E-02
72 hr	N-carbamoyl-L-aspartate	64.62	7.85E-04
	Dihydroorotate	24.13	3.65E-03
	2-Isopropylmalic acid	15.87	1.01E-03
	Cystine	5.60	6.44E-03
	Phosphoenolpyruvate	5.19	1.98E-02
	Aspartate	4.32	1.29E-02
	2,3-Diphosphoglyceric acid	4.15	6.07E-03
	3-phosphoglycerate	3.87	8.01E-03
	Ascorbic acid	3.53	1.82E-02
	Glycerate	3.40	2.20E-04
	Carbamoyl phosphate	3.02	2.27E-04
	Asparagine	2.83	4.97E-02
	Allantoin	2.62	5.23E-04
	Anthranilate	2.59	7.70E-03
	N-acetyl-glucosamine-1-phosphate	2.41	2.03E-03
	Guanine	2.23	4.95E-02

Table 3.2 List of Metabolites Significantly Downregulated by A771726 Treatment

Table 3.2 (Continued)

Time Point	Metabolite	Fold Change	P-value
0.5 hr	2,3-dihydroxybenzoic acid	-6.04	1.34E-02
	Shikimate	-2.00	1.46E-02
1 hr	Adenosine	-2.76	4.10E-02
	Inosine	-2.50	1.24E-02
24 hr	UDP	-28.75	1.38E-02
	UTP	-16.92	6.94E-03
	CTP	-16.39	8.69E-03
	UDP-D-glucose	-6.90	4.72E-03
	UDP-N-acetyl-glucosamine	-5.24	3.18E-03
	Trehalose-6-Phosphate	-3.97	2.52E-02
	Cystathionine	-2.96	5.44E-03
	GTP	-2.62	1.01E-02
	Guanidoacetic acid	-2.17	5.87E-03
	3-phospho-serine	-2.10	9.23E-03
	Citraconic acid	-2.07	8.32E-03
	dATP	-2.06	2.64E-02
48 hr	UTP	-10.92	1.02E-02
	CTP	-9.43	1.20E-02
	UDP	-7.93	8.80E-03
	dCTP	-4.95	4.28E-02
	UDP-D-glucose	-4.67	3.55E-03
	UDP-N-acetyl-glucosamine	-3.68	6.13E-04
	Kynurenic acid	-3.44	1.93E-03
	dTTP	-3.30	4.52E-03
	N-acetyl-glutamate	-3.04	1.67E-02
	Coenzyme A	-2.63	1.09E-02
	Glutathione	-2.60	3.53E-02
	UMP	-2.59	7.28E-03
	Fructose-1,6-bisphosphate	-2.40	3.81E-03
	dTMP	-2.35	3.45E-02
	Glutathione	-2.32	2.22E-02
	Geranyl-PP	-2.27	7.95E-03
	O-acetyl-L-serine	-2.08	3.85E-02
	Putrescine	-2.06	3.07E-02
	Sedoheptulose-1,7-bisphosphate	-2.02	3.93E-03

Table 3.2 (Continued)

Time Point	Metabolite	Fold Change	P-value
72 hr	Aminoimidazole carboxamide ribonucleotide	-10.55	1.66E-03
	Cystathionine	-10.35	2.37E-04
	Glutathione	-6.53	9.09E-04
	UTP	-6.07	2.07E-05
	Phosphorylcholine	-5.08	1.72E-06
	dTTP	-5.05	1.69E-02
	dihydroxy-acetone-phosphate	-4.96	4.28E-02
	Geranyl-PP	-4.47	1.53E-02
	Kynurenic acid	-4.47	6.76E-03
	UDP	-4.40	1.36E-02
	O-acetyl-L-serine	-4.19	1.00E-02
	CTP	-4.12	5.36E-03
	GTP	-3.95	4.67E-02
	UDP-D-glucose	-3.89	1.71E-03
	4-aminobutyrate	-3.52	1.40E-02
	Trehalose-6-Phosphate	-3.17	3.47E-02
	N-acetyl-glutamate	-3.09	1.64E-02
	Taurine	-2.78	3.05E-03
	D-glyceraldehdye-3-phosphate	-2.72	1.49E-02
	Glucono-δ-lactone	-2.48	1.03E-01
	Glutathione disulfide	-2.39	1.98E-02
	2-hydroxygluterate	-2.37	7.52E-04
	Guanidoacetic acid	-2.32	1.19E-02
	Biotin	-2.28	2.28E-02
	IDP	-2.16	2.98E-02
	Fructose-6-phosphate	-2.15	1.23E-02
	Glutathione disulfide	-2.13	2.27E-05
	ATP	-2.12	4.72E-02
	Glucose-6-phosphate	-2.07	9.97E-03
	Cholesteryl sulfate	-2.04	6.55E-03

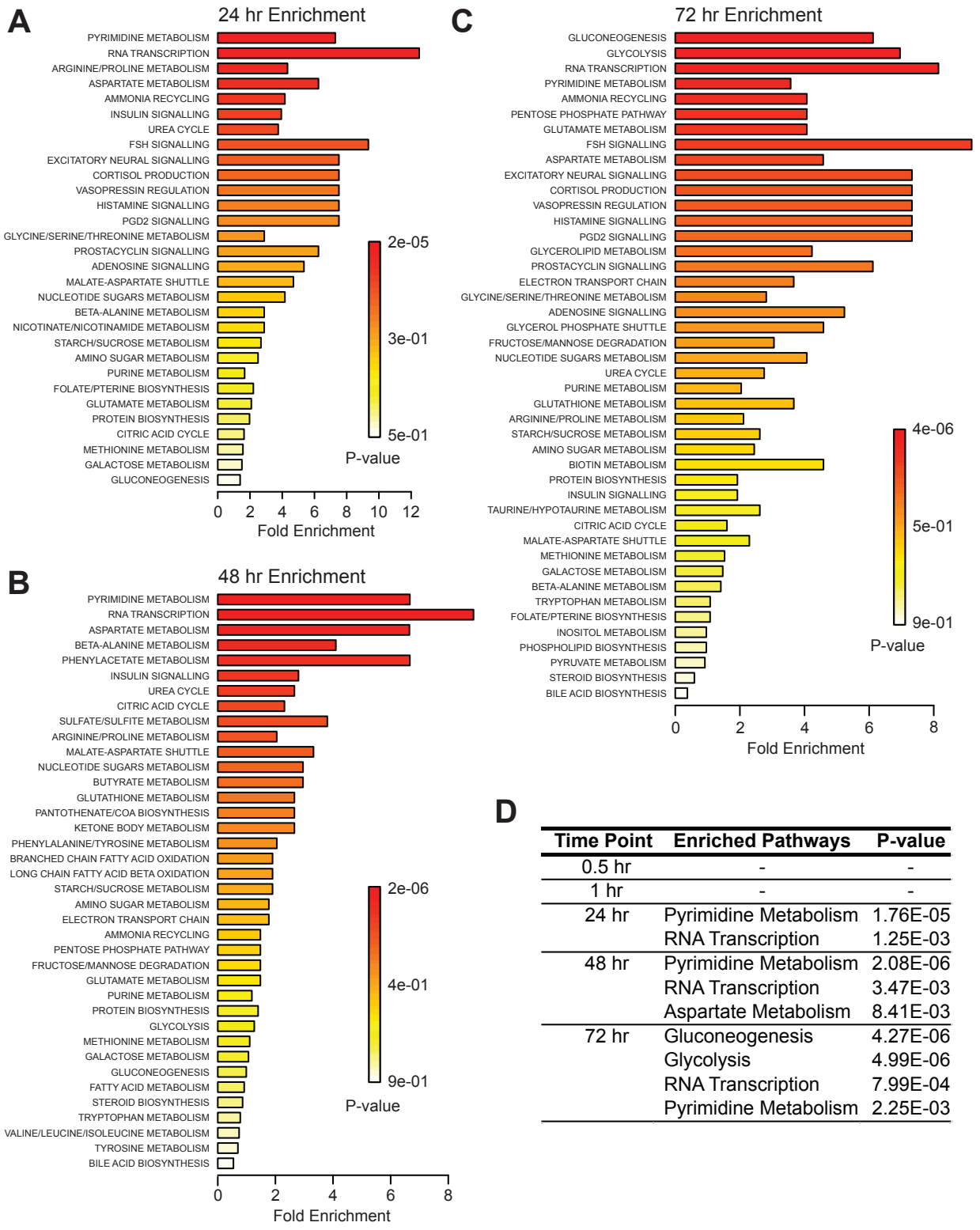

Time Point	Enriched Pathways	P-value
0.5 hr	-	-
1 hr	-	-
24 hr	Pyrimidine Metabolism	1.76E-05
	RNA Transcription	1.25E-03
48 hr	Pyrimidine Metabolism	2.08E-06
	RNA Transcription	3.47E-03
	Aspartate Metabolism	8.41E-03
72 hr	Gluconeogenesis	4.27E-06
	Glycolysis	4.99E-06
	RNA Transcription	7.99E-04
	Pyrimidine Metabolism	2.25E-03

Figure 3.2 Pyrimidine Biosynthesis is Primarily Affected by Leflunomide

(A) Metabolite Set Enrichment Analysis (MSEA) was performed on a list of significantly altered

(Continued) metabolites (> 2-fold change, p-value < 0.05) from A771726-treated A375 cells compared to DMSO controls at a 24 hr time point. The graph shows rank ordered metabolic pathways by p-value that are enriched by drug treatment. (B) MSEA performed after 48 hr of A771726 treatment. (C) MSEA performed after 72 hr of A771726 treatment. (D) Summary of significantly altered metabolic pathways (p-value < 0.01).

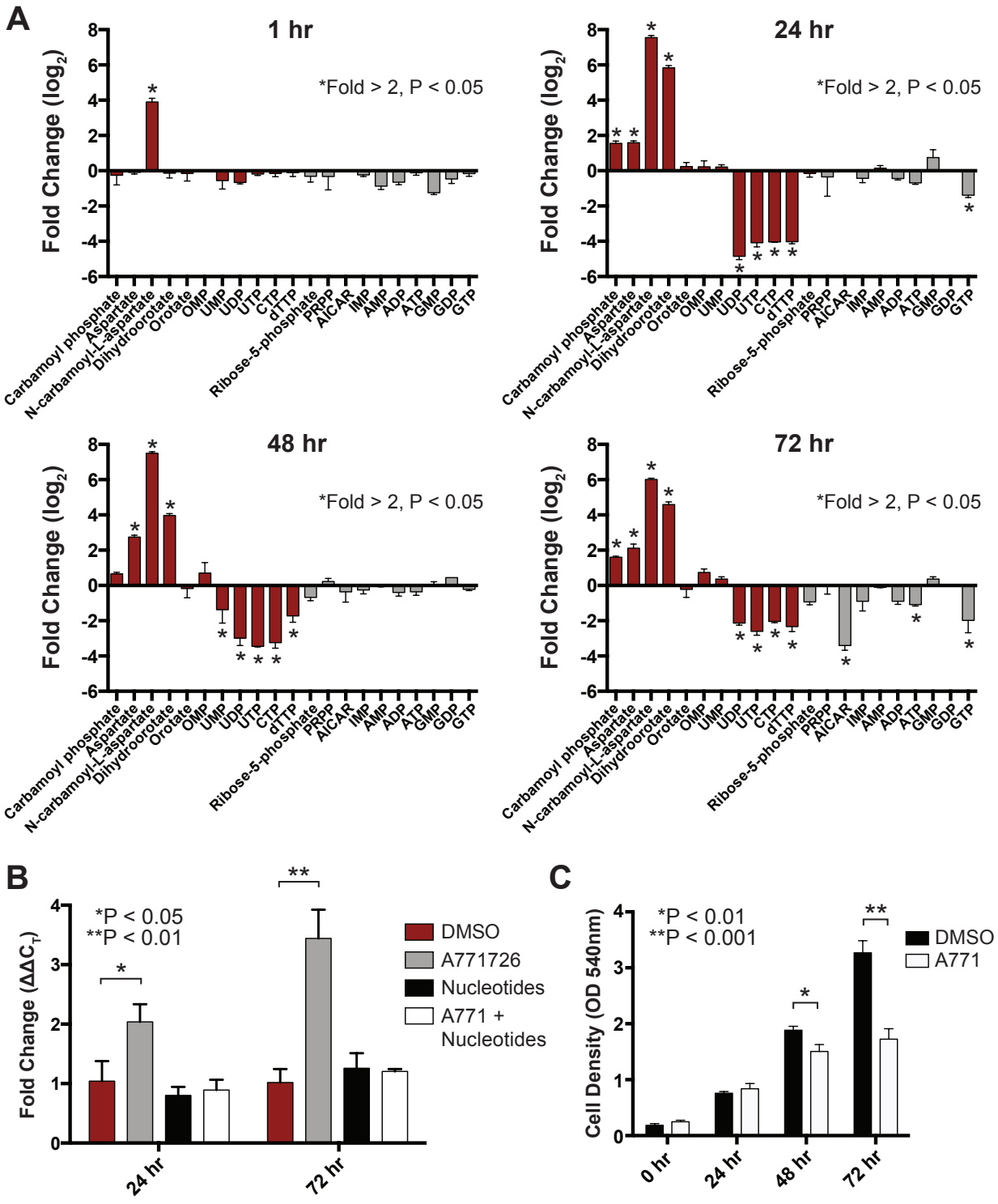

Figure 3.3 HEXIM1 is Upregulated in Response to Low Nucleotide Levels Induced by DHODH Inhibition

(A) Profiling of pyrimidine and purine biosynthesis metabolites in A375 cells treated with 25 μM A771726 at 1 hr, 24 hr, 48 hr and 72 hr time points. (B) Real time RT-PCR on A375 cells treated

(Continued) with 25 μM A771726, a cocktail of 10 μg/mL pyrimidine nucleotides (UMP and CMP) and a combination of both A771726 and nucleotides to examine *HEXIM1* expression at the 24 hr and 72 hr time point. Data is normalized to *GAPDH*. (C) Quantification of cell number changes at various time points of A375 cells treated as in (A).

HEXIM1 is Upregulated in Response to a Low Nucleotide State Induced by DHODH Inhibition

Since leflunomide primarily perturbs pyrimidine biosynthesis, we examined if HEXIM1 responds to this perturbation. A *HEXIM1*-luciferase reporter assay (Liu et al., 2014b) in A375 cells demonstrates that *HEXIM1* is increasingly transcribed over time with the addition of A771726, with HMBA as a positive control for *HEXIM1* induction (Figure 2.4E). In addition, the accompanying westerns show that HEXIM1 is only significantly unregulated 48 hrs after treatment (Figure 3.4). We also show that increased *HEXIM1* expression induced by A771726 can be rescued by the addition of pyrimidine nucleotides to the cells (Figure 3.3B). Adding nucleotides alone does not alter *HEXIM1* expression, suggesting that the role of HEXIM1 in transcriptional regulation is prominent in times of starvation and not in times of nucleotide excess.

The effects on cell proliferation correlate with HEXIM1 expression, where a 50% reduction in cell number is observed only at the 72 hr time point where HEXIM1 protein is most differentially increased (Figures 3.3B and 3.3C). Taken together, these results indicate that the cells have to be sufficiently starved of nucleotides before HEXIM1 is activated to regulate transcription with a corresponding decrease in cell proliferation.

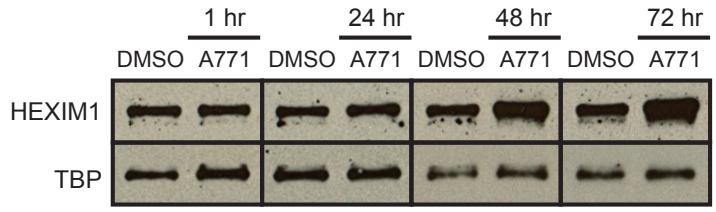

Figure 3.4 HEXIM1 is Upregulated After Significant Nucleotide Depletion Following DHODH Inhibition

Western blot of HEXIM1 and TBP in nuclear extract of A375 cells treated with 25 μM A771726 at 1 hr, 24 hr, 48 hr and 72 hr time points.

Discussion

HEXIM1 Regulates Transcription in Response to Low Nucleotide Levels

When cells are nucleotide starved, they are likely to slow their rate of transcription in order to conserve nucleotides till homeostasis returns. We suggest that one mechanism in which cells conserve nucleotides is to repress transcription elongation, which involves an upregulation of HEXIM1 to bind and sequester P-TEFb. Sequestration of P-TEFb prevents P-TEFb from phosphorylating RNA Pol II at its CTD Ser-2 sites. As a result, more RNA Pol II molecules remain paused at the initiation step of transcription. *HEXIM1* expression is tightly linked to nucleotide levels, with decreasing levels triggering an increase in *HEXIM1* expression. Cells can therefore take advantage of the transcriptional reprieve, provided by HEXIM1 inhibition of elongation, until nucleotides return to sufficient levels. After which, HEXIM1 returns to homeostatic levels, allowing transcription to return to normal. This suggests an elegant feedback mechanism, where cells are able to control transcription based on the amount of mRNA precursors available. Cells prefer to slow their growth rate via HEXIM1 downregulation of genes associated with cell cycle and proliferation in times of starvation, therefore conserving cellular resources until conditions become favorable for proliferation.

Regulating Transcription Elongation in Response to Cellular Stress

Gene expression can be regulated at the level of chromatin structure, transcription initiation and elongation, but there are a number of advantages if transcription elongation is regulated as a direct consequence of nucleotide starvation or other cellular stresses. Studies have shown that a number of genes in the Drosophila embryo involved in key developmental pathways as well as heat shock genes are held in a paused state before induction as reviewed by Levine (Levine, 2011). At these genes, transcription has already been initiated as RNA Pol II has been successfully recruited to the promoters. However, RNA Pol II does not immediately transition to a

productive elongation phase and instead, remains paused on these promoters before receiving signals to induce productive elongation (Chopra et al., 2009; Levine, 2011; Muse et al., 2007; Zeitlinger et al., 2007). This allows RNA Pol II to be poised at genes that require rapid induction, saving the time needed for RNA Pol II to be recruited to the promoters to initiate transcription (Levine, 2011). In addition, chromatin can remain in an open state before elongation is induced (Levine, 2011). This sets up a system where cellular stress can induce a rapid and coordinated upregulation of genes to respond effectively to the stress.

Such a system is highly beneficial to the organism as a quick and concerted response could limit the damage done by the stress. In the case of nucleotide starvation, unfavorable effects might include DNA damage, mis-expression of mRNA and protein, and possibly bioenergetic issues due to the lack of ATP and GTP. An immediate repression of non-essential genes by halting elongation through HEXIM1 sequestration of P-TEFb will allow for stress response genes to be expressed properly utilizing the remaining nucleotides available. In addition, once the stress is alleviated, the cell can return to homeostasis more rapidly, as RNA Pol II remains poised in a paused state at genes that were expressed before the stress. Inhibiting transcription elongation temporarily as a response to nucleotide starvation is therefore a viable mechanism to ensure a quick turnaround in terms of response to and recovery from cellular stress.

Materials and Methods

Targeted Mass Spectrometry

Samples were re-suspended using 20 µL HPLC grade water for mass spectrometry. 5 µL were injected and analyzed using a hybrid 5500 QTRAP triple quadrupole mass spectrometer (AB/SCIEX) coupled to a Prominence UFLC HPLC system (Shimadzu) via selected reaction monitoring (SRM) of a total of 256 endogenous water soluble metabolites for steady-state analyses of samples (Yuan et al., 2012). Some metabolites were targeted in both positive and negative ion mode for a total of 289 SRM transitions using positive/negative ion polarity switching. ESI voltage was +4900 V in positive ion mode and –4500 V in negative ion mode. The dwell time was 3 ms per SRM transition and the total cycle time was 1.55 seconds. Approximately 10-14 data points were acquired per detected metabolite. Samples were delivered to the mass spectrometer via hydrophilic interaction chromatography (HILIC) using a 4.6 mm i.d x 10 cm Amide XBridge column (Waters) at 400 µL/min. Gradients were run starting from 85% buffer B (HPLC grade acetonitrile) to 42% B from 0-5 minutes; 42% B to 0% B from 5-16 minutes; 0% B was held from 16-24 minutes; 0% B to 85% B from 24-25 minutes; 85% B was held for 7 minutes to re-equilibrate the column. Buffer A was comprised of 20mM ammonium hydroxide/20 mM ammonium acetate (pH=9.0) in 95:5 water:acetonitrile. Peak areas from the total ion current for each metabolite SRM transition were integrated using MultiQuant v2.0 software (AB/SCIEX).

Metabolite Profile Analyses

Relative intensities of metabolites were first normalized to the row average of the DMSO 0.5 hr time point, followed by normalization to the median of the entire dataset. Heat map generation and clustering were performed on the MetaboAnalyst web server with Log transformation and Autoscaling (mean-centered and divided by the standard deviation of each variable) (Xia et al., 2009, 2012). MSEA was also performed on the MetaboAnalyst web server with lists of metabolites

with fold change more than or equal to 2 in drug treatment compared to DMSO, with a Student's two-tailed t-test p-value of less than 0.05 (Xia and Wishart, 2010).

Nucleotide Rescue Experiment

A375 cells were seeded in a 6 well plate. The following day culture media was replaced with fresh media containing 25 μM A771726 and/or a cocktail of 10 μg/mL uridine 5′-monophosphate (UMP, Sigma) and 10 μg/mL cytidine 5′-monophosphate (CMP, Sigma), or the combination of A771726 and UMP/CMP. RNA extraction was performed after 24 and 72 hrs after treatment.

Crystal Violet Staining

10,000 cells were seeded per well in a 96 well plate in quadruplicate. Cells were fixed at different time point using 4% PFA (USB, Affymetrix) for 15 mins. Fixative was washed out with 1X PBS and cells were stained with 100 μL of 0.05% Crystal Violet (Sigma) in 20% ethanol for 15 mins. Crystal Violet was collected and plates were rinsed 3 times by immerging plates in a basin full of dH2O. Once plates were dried cells were dissolved by adding 100 mL of 1% SDS (in H2O). Absorbance was read at 540 nm by using a plate reader (SpectraMax M5, Molecular Devices)

Cell Line Nuclear Protein Extraction

Nuclear protein was extracted from the A375 cells using the NE-PER Nuclear and Cytoplasm Extraction Kit (Thermo Scientific) following the prescribed protocol.

Chapter 4:

Concluding Discussion and

Future Directions

Justin L. Tan[1,2], Rachel D. Fogley[1,2] and Leonard I. Zon[1,2]*

[1]Howard Hughes Medical Institute, Stem Cell Program and Division of Pediatric Hematology/ Oncology, Boston Children's Hospital, Dana-Farber Cancer Institute, Harvard Medical School, Boston MA 02115, USA. [2]Department of Stem Cell and Regenerative Biology, Harvard Stem Cell Institute, Cambridge, MA 02138, USA.

*To whom correspondence should be address
Address: 300 Longwood Ave, Boston, MA 02115
Email: zon@enders.tch.harvard.edu

Attributions

I conceived the idea to assess protein phosphorylation changes and potential mRNA-mediated HEXIM1 regulation in response to leflunomide in the A375 cells. I performed the protein phosphorylation array with technical assistance from R. D. Fogley. In addition, I performed the analysis of the array results. I performed the real time RT-PCR analysis for *CAD* mRNA changes in response to leflunomide.

Concluding Discussion

DHODH Inhibition Suppresses Melanoma Through *HEXIM1*

Leflunomide can act as an efficient anti-melanoma drug, both on its own and in synergy with vemurafenib (White et al., 2011). A combination therapy of these two drugs is currently in a clinical trial for metastatic melanoma. Leflunomide is a DHODH inhibitor that affects pyrimidine biosynthesis, resulting in the induction of a transcriptional pause. A significant pause is induced in genes involved in cell proliferation and cell cycle, thereby slowing the growth and proliferation of the neural crest and melanoma. However, the mechanism of how a shortage of nucleotides through DHODH inhibition can eventually lead to a transcriptional pause is unclear.

Our work presented here demonstrates an important role for *HEXIM1* in regulating this pause in transcription in melanoma in response to DHODH inhibition (Figure 4.1). We show that HEXIM1, as part of the 7SK snRNP, is bound to the promoter regions of genes (Figure 4.1A). This possibly poises P-TEFb at the promoters to allow rapid induction of transcription elongation when required. Leflunomide treatment induces a transient release of P-TEFb from the 7SK snRNP, releasing the transcriptional pause at a number of genes including *HEXIM1* (Figure 4.1B). This results in an upregulation of HEXIM1 to sequester P-TEFb away from chromatin, thus preventing P-TEFb from phosphorylating RNA Pol II and other pausing factor (Figure 4.1C). Hence, RNA Pol II can no longer efficiently transition from a paused state into a productive elongation state. As a result, a large number of cell cycle and proliferative genes are downregulated and this in turn suppresses melanoma *in vivo*. Transcription elongation is an important step for highly regulated genes in development, as reviewed by Levine (Levine, 2011). Having RNA Pol II recruited to promoters prior to expression allows for rapid and concerted gene expression, which is crucial for proper gene expression at the appropriate developmental stage as well as during a stress response.

The significance of elongation in development might explain why HEXIM1 is downregulated in human melanoma. Tumorigenesis is often characterized by dedifferentiation and melanoma has been shown to express neural crest stem cell marker *SOX10*, which is typically not expressed in differentiated melanocytes (Shakhova, 2014; Shakhova et al., 2012). In addition, HEXIM1 and the 7SK snRNP have been shown to regulate differentiation, possibly by controlling gene expression at the appropriate developmental stages to determine the cellular decision between proliferation and differentiation (Zhou and Yik, 2006). The fact that melanoma reverts to a dedifferentiated, proliferative state might therefore require HEXIM1 to be downregulated to maintain this tumorigenic state. We affirm the role of HEXIM1 in suppressing melanoma in our zebrafish melanoma model where even without induction by leflunomide, overexpressing human HEXIM1 can effectively suppress melanoma *in vivo*.

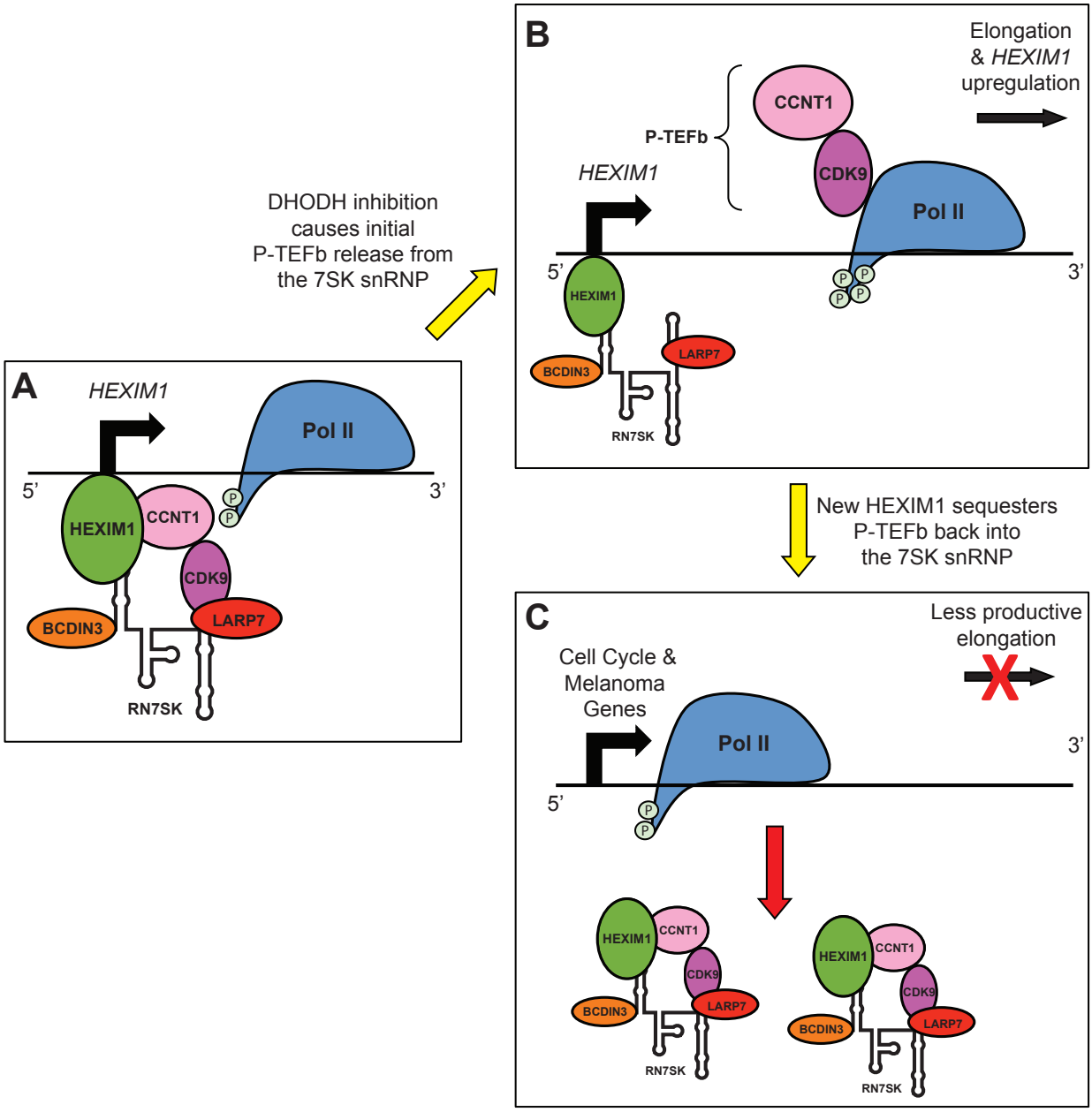

Figure 4.1 A Model for DHODH Induced Melanoma Suppression by Upregulation of HEXIM1

(A) The 7SK snRNP poises P-TEFb at promoters such as the *HEXIM1* promoter in preparation for transcription elongation at the appropriate time. (B) DHODH inhibition triggers P-TEFb release from the 7SK snRNP at a number of loci, including at *HEXIM1*. The free P-TEFb results in a transient release of pausing at the *HEXIM1* gene, upregulating *HEXIM1* transcription. (C) Newly synthesized HEXIM1 sequesters P-TEFb back into the 7SK snRNP away from chromatin, inhibiting transcription elongation at cell cycle and melanoma genes.

Upregulating HEXIM1 might prove to be a practical way of targeting melanoma. We discovered that leflunomide is a novel inducer of *HEXIM1* expression other than JQ1 (Bartholomeeusen et al., 2012b) and bipolar compounds such as HMBA (Zhong et al., 2014). Leflunomide targets a stress-related aspect of melanoma, where a shortage of pyrimidine nucleotides triggers a proliferation defect. The neural crest lineage seems to be particularly sensitive to nucleotide starvation, possibly due to an inactive nucleotide salvage pathway. As a result, leflunomide-induced *HEXIM1* induction in the early, undifferentiated neural crest in zebrafish embryos causes an artificial growth-suppressive transcriptional response before the later stages of differentiation. This ablates the neural crest and its downstream lineages. Such an effect is mirrored in leflunomide treatment of melanoma since melanoma possesses characteristics of the undifferentiated neural crest. Hence, treating patients with leflunomide might induce *HEXIM1* in many cell types, but the induction might have a more profound effect in melanoma because of its sensitivity to nucleotide starvation. The anti-proliferative effect of leflunomide will specifically be felt in melanoma more than in healthy tissues. This suggests that HEXIM1 is a major component of the anti-proliferative response caused by leflunomide.

Our work here demonstrates a novel mechanism to target melanoma other than existing targeted therapies that modulate the MAPK pathway. BRAF and MEK inhibitors currently improve the standard of care for melanoma patients, but the rapid evolution of resistance mechanisms to these drugs means that their effect is short-lived. Exploiting a more general pathway such as cellular stress to repress melanoma might be preferential since cancer cells will need to spend more resources to overcome the stress response. In the case of leflunomide, a drug-induced nucleotide shortage results in the inhibition of productive elongation by HEXIM1 at numerous proliferation and cell cycle genes. It might prove difficult for the melanomas to develop resistance mechanisms to overcome the transcriptional pause, as many components of the elongation mechanism such as HEXIM1 are essential for survival. Although the cancer might be able to

mutate DHODH so that leflunomide can no longer bind, mutating a gene involved in an essential cellular process might prove deleterious. More has to be done in characterizing other melanoma dependencies that can be targeted by drugs to modulate the proliferation and survival program in melanoma.

Inducers of HEXIM1 as Cancer Therapeutics

There are currently four classes of compounds that induce HEXIM1 and have been investigated as possible cancer therapies. They are the bipolar compounds such as hexamethylene bisacetamide (HMBA) and dimethyl sulfoxide (DMSO) with unknown targets (Contreras et al., 2007; Marks and Rifkind, 1989; Zhong et al., 2014), histone deacetylase (HDAC) inhibitors like suberoylanilide hydroxamic acid (SAHA) (Liu et al., 2014b; Richon et al., 1998), bromodomain and extra-terminal (BET) bromodomain inhibitor JQ1 (Bartholomeeusen et al., 2012b; Filippakopoulos et al., 2010; Liu et al., 2014b) and DHODH inhibitor leflunomide (based on our current study). These compounds have different targets but what is interesting is why they converge on the induction of HEXIM1 and modulation of the 7SK snRNP.

HMBA and other bipolars compounds tested showed the distinct ability to induce terminal differentiation in a variety of cancer cell lines as reviewed by Marks and Rifkind (Marks and Rifkind, 1989). While the mechanism of how HMBA induces these changes is not well understood, studies in mouse erythroleukemia (MEL) cells demonstrated that HMBA caused multiple cellular changes, including transient cyclic AMP induction (Gazitt et al., 1978), protein kinase C activation (Melloni et al., 1987) and alteration of gene expression of *c-myb*, *c-myc*, *c-fos* and *p53* (Lachman and Skoultchi, 1984; Ramsay et al., 1986; Todokoro and Ikawa, 1986). All of which resulted in the consequent expression of differentiation markers such as globins and heme biosynthesis enzymes, as well as changes in morphology of the MEL cells. These studies provide evidence that HMBA and other bipolar compounds either target multiple factors in different pathways or

one factor that affects multiple downstream pathways. However, the direct targets of bipolar compounds remain elusive. HMBA had previously been tested in a clinical trial for myelo-dysplastic syndrome and acute myelogenous leukemia (Andreeff et al., 1992). Although the drug induced remission in patients, it is not currently utilized in the clinic because of the high dose needed and toxic side effects such as thrombocytopenia (Andreeff et al., 1992). There are currently efforts to design more potent HMBA analogues with longer half-lives for disease treatment (Zhong et al., 2014). More has to be done to identify the targets of HMBA to develop more potent drugs to these targets.

HDAC inhibitors like SAHA were synthesized as the second generation of bipolar compounds (newly termed “hybrid polar compounds” based on chemical modifications) and were designed based on HMBA to achieve more potent induction of cellular differentiation (Richon et al., 1996). They are up to 2000-fold more active than HMBA in inducing differentiation in MEL cells (Richon et al., 1996). These hybrid polar compounds were thought to target the same pathways as HMBA, and might therefore lead to the discovery of what HMBA targets in cells. Fortunately for hybrid polar compounds, they where found to specifically inhibit HDACs, resulting in hyper-acetylation of histones which induced gene expression changes responsible for the differentiation phenotype (Richon et al., 1998). Unfortunately for HMBA, it was not found to target HDACs like hybrid polar compounds (Richon et al., 1998), so its targets still remain a mystery. The ability of HDAC inhibitors to induce cellular differentiation and apoptosis has been particularly useful in treating cancer, as reviewed by Wagner et. al. (Wagner et al., 2010). A number of HDAC inhibitors have been or are currently being tested in clinical trials for a wide array of cancers, with compounds Vorinostat and Romedepsin having already been FDA approved for treatment of refractory T-cell lymphoma (Wagner et al., 2010). Not much has been investigated in terms of how HEXIM1 induction by HDAC inhibition is responsible for the anti-tumorigenic effect, and further study could prove useful in understanding the complex cellular changes that occur to induce

differentiation or apoptosis in cancer.

BET domain inhibition is a more recent published discovery of a novel way to target cancer. A study in multiple myeloma found that the BET domain-containing gene *BRD4* locus was frequently amplified in patients with this disease (Delmore et al., 2011). BET domain inhibitor JQ1 was developed to target BRD4 (Filippakopoulos et al., 2010), and this drug results in a pronounced anti-proliferative effect in multiple myeloma (Delmore et al., 2011). BRD4 was shown to be a transcriptional activator of oncogenic *MYC* expression (Delmore et al., 2011). Thus, inhibition of BRD4 by JQ1 suppresses *MYC*, resulting in an anti-proliferative state that suppresses the cancer. Interestingly, gene expression data from JQ1 inhibition in multiple myeloma revealed that HEXIM1 is significantly upregulated (Delmore et al., 2011). Biochemical analysis of JQ1 in Jurkat cells revealed that BET domain inhibition caused identical effects on the 7SK snRNP as with SAHA and HMBA (Bartholomeeusen et al., 2012b). JQ1 treatment causes an initial release of P-TEFb from the 7SK snRNP followed by increased HEXIM1 expression and subsequent re-sequestration of P-TEFb by newly synthesized HEXIM1 (Bartholomeeusen et al., 2012b). These three drugs that represent different classes cause an initial transient release of P-TEFb from the 7SK snRNP, followed by HEXIM1 upregulation and subsequent reassembly of the 7SK snRNP (Bartholomeeusen et al., 2012b).

We have identified a novel pathway that induces HEXIM1 and modulates the 7SK snRNP through DHODH inhibition by leflunomide. Leflunomide employs a transient release of P-TEFb from the 7SK snRNP and subsequent HEXIM1 induction similar to the aforementioned mechanism of bipolar compounds, HDAC inhibitors and BET domain inhibitor JQ1. We demonstrate that HEXIM1 and the 7SK snRNP are necessary for the anti-melanoma effect of leflunomide, and that HEXIM1 itself can functionally suppress tumorigenesis. Leflunomide seems to induce HEXIM1 in a different manner from the other three compound classes, as it creates a state of nucleotide starvation in the cell. This stress state is what drives the cell to induce HEXIM1 to suppress its

proliferation and cell cycle program, and induction of this stress by leflunomide can be exploited to treat cancer. It is evident that there are a number of pathways that can induce HEXIM1 and modulate the 7SK snRNP. Further comprehension of these pathways could result in novel combination therapies to induce HEXIM1 through modulation of these convergent pathways to achieve highly potent tumor suppression.

HEXIM1 Responds to Nucleotide Stress

Other than its ability to suppress melanoma, *HEXIM1* also plays an important role in nucleotide metabolism. DHODH inhibition by leflunomide creates a state of cellular stress caused by pyrimidine nucleotide starvation. We demonstrate that *HEXIM1* expression is responsive to perturbations in pyrimidine nucleotide levels. This fits with a model where the cell senses low nucleotides and upregulates HEXIM1. This upregulation inhibits productive elongation on a large number of genes, giving the cell an opportunity to either synthesize nucleotides *de novo* or salvage them from other metabolites before transcription can return to homeostatic levels. Hence, HEXIM1 provides an elegant mechanism where nucleotide biosynthesis is linked with transcription elongation so that there are always sufficient pools of mRNA precursors.

Linking nucleotide regulation with transcription elongation also has a number of benefits. Halting productive elongation temporarily means that RNA Pol II remains bound to the promoter regions of genes, albeit in a paused state. This allows for a rapid return to homeostatic gene expression once nucleotide levels returns to normal, since RNA Pol II remains poised for transcription without the initiation step being required again. Initiation first requires the formation of euchromatin by chromatin factors, followed by stochastic binding of RNA Pol II recruitment factors that brings RNA Pol II to the promoters. After which, pausing factors are recruited to the promoters to hold RNA Pol II in position to await Cdk9 phosphorylation, which ultimately triggers the transition from a paused state to productive elongation. This chain of events takes time and

would not benefit the cell if the cycle has to be repeated every time nucleotide levels return to normal after starvation. It seems more efficient to regulate transcription by increased HEXIM1 sequestration of P-TEFb, thus inhibiting productive elongation at a stage in transcription that can rapidly return to normalcy once the stress is alleviated.

The *HEXIM1* gene falls into a category of genes that are not paused by leflunomide. It is interesting that nucleotide starvation induced by leflunomide does not cause a transcriptional pause in all genes. The pause is preferential for cell cycle and proliferative genes while genes such as *HEXIM1* that maintain the paused state are unaffected or upregulated. There might exist a mechanism where nucleotide starvation causes cells to preferentially upregulate genes that will conserve nucleotide precursors, salvage them or synthesize them. HEXIM1 seems to be responsible for the conservation of nucleotides by inhibiting the transition from a paused state to productive elongation. It would be interesting to investigate the mechanism behind these differences in gene expression due to nucleotide stress.

Future Directions

Introduction

From our work thus far, we have uncovered how leflunomide acts through HEXIM1 in order to inhibit productive elongation to suppress melanoma. We also demonstrate that HEXIM1 suppresses tumorigenesis and is downregulated in melanoma for the tumors to proliferate. There remain a number of questions about this mechanism. Although leflunomide prevents the transition from a paused state to a productive elongation state at many genes, there are still a number of genes like *HEXIM1* that are induced to elongate. This observation hints at a complex mechanism upstream of HEXIM1 induction and downstream of nucleotide biosynthesis that has yet to be identified. Some clues of how a shortage of nucleotides can directly influence transcription can be found in yeast. Ppr1p is a DNA binding yeast protein that can induce the transcription of the *URA* pyrimidine biosynthesis genes upon the addition of pyrimidine precursors dihydroorotate or orotate (Flynn and Reece, 1999). This posits an interesting mechanism where a build up of pyrimidine precursors (dihydroorotate and/or orotate) activates a transcription factor (Ppr1p) possibly by binding to it, resulting in an upregulation of downstream pyrimidine biosynthesis genes (*URA* genes) by the activated transcription factor. Since leflunomide causes an upregulation of pyrimidine precursors upstream of DHODH, these precursors might potentially bind to activate or deactivate proteins that have a direct impact on transcription.

Our next step would be to uncover the factors upstream of HEXIM1-mediated inhibition of elongation in response to low nucleotide levels. One can envision cellular mechanisms that regulate either *HEXIM1* expression or HEXIM1 functioning in the 7SK snRNP. We have determined that leflunomide upregulates HEXIM1 mRNA and protein levels in mammalian melanoma cells and in zebrafish. To examine how alterations in *HEXIM1* expression are achieved by leflunomide, we will first generate a list of candidate transcription factors that have been shown to bind the *HEXIM1* locus from current literature. We can then knock down these factors via small-interfering RNA

(siRNA) technology in a mini-screen to determine which transcription factor(s) is/are responsible for *HEXIM1* induction by leflunomide. Once we have positive hits, we can perform downstream assays to see if they respond to nucleotide starvation or other cellular stresses to induce *HEXIM1* expression. Discovering the transcription factors involved in regulating *HEXIM1* expression in nucleotide stress conditions will help piece together a feedback mechanism where nucleotide levels directly control and regulate transcription.

In addition to transcriptional regulation of *HEXIM1*, leflunomide probably induces biochemical changes in the 7SK snRNP that causes the initial release and subsequent re-sequestration of P-TEFb we have shown. HEXIM1 is phosphorylated at a number of potential sites in order to regulate P-TEFb binding (Contreras et al., 2007; Fujinaga et al., 2012). Hence, we will perform phosphorylation site mapping of HEXIM1 via mass spectrometry to determine if leflunomide causes changes in the phosphorylation state of HEXIM1 and which phosphorylation sites specifically are affected. We can then examine the sites modified for amino acid motifs recognized by kinases and phosphatases to shortlist candidate enzymes that potentially modify HEXIM1 at these sites. We can complement this study with a phosphorylated protein array on leflunomide-treated A375 cells, where we can examine changes in phosphorylation state of a wide variety of signal transduction proteins due to drug. These experiments will allow us to compare hits and shortlist potential kinases and phosphatases that modify HEXIM1 in response to DHODH inhibition. Once we determine which site(s) on HEXIM1 is/are modified by which enzyme, we can then proceed to validate our results in downstream cell-based or zebrafish assays. Determining how HEXIM1 is biochemically modified will identify upstream signal transduction pathways that feed into the downstream regulation of transcription during nucleotide deficiency.

Other than direct biochemical modification of HEXIM1, a third avenue we will pursue is the discovery of factors that physically modify the 7SK snRNP or recruit it to target genes in response to DHODH inhibition. Firstly, there is evidence for factors such as PP2B and PP1α that induce a

conformational change in the 7SK snRNP to disrupt the complex (Chen et al., 2008). Secondly, it is possible that factors exist to selectively recruit the 7SK snRNP to chromatin in order to inhibit transcription at specific loci. Thirdly, there is evidence that HEXIM1 can bind RNA species other than the 7SK RNA (Fujimoto et al., 2012). To address if leflunomide treatment elicits protein factors to modify the function of the 7SK snRNP, we will co-immunoprecipitate HEXIM1 with its binding partners to identify these partners by mass spectrometry. By comparing mass spectrometry results in DMSO- and leflunomide-treated cells, we can ascertain changes in binding partners caused by the drug. Candidate proteins that modulate the function of the 7SK snRNP can be tested in biochemical and genetic assays to validate their relevance to leflunomide-induced changes in the 7SK snRNP. To address novel RNA species that might bind and affect HEXIM1 function, we will perform high-throughput sequencing of RNA isolated by cross-linking immunoprecipitation (HTS-CLIP) (Licatalosi et al., 2008) to identify strong RNA binders of HEXIM1. After which, we will validate the ability of candidate RNAs to activate HEXIM1 in downstream assays. Identifying factors that modulate the 7SK snRNP with DHODH inhibition will further develop our understanding of transcriptional regulation in response to cellular stress.

Finally, we hope to discover novel therapeutics that can exploit stress pathways that induce HEXIM1 to target melanoma and other cancers. We demonstrate that HEXIM1 can robustly suppress melanoma. In addition, previous studies have implicated the importance of *HEXIM1* and *LARP7* in a variety of other cancers (Cheng et al., 2012b; He et al., 2008; Ketchart et al., 2013; Mascareno et al., 2012; Mori et al., 2002; Wittmann et al., 2003, 2005; Yeh et al., 2013). Thus far, bipolar compounds such as HMBA, HDAC inhibitor SAHA, BRD4 inhibitor JQ1 and our DHODH inhibitor leflunomide have been shown to induce HEXIM1 to target tumorigenesis. However, the detailed mechanism of how these drugs activate HEXIM1 is not well understood. To address this question, we intend to conduct a chemical screen on the A375 *HEXIM1*-Luciferase reporter cell line. This will allow us to obtain hit compounds of drugs with either known or unknown

mechanisms-of-action. With the list of drugs with known targets, we can discern potential pathways that upregulate *HEXIM1* and test them in future assays. As an additional benefit, all hits obtained are potential cancer therapeutics that function through the 7SK snRNP and should be validated for anti-tumor activity. A screen for chemical modulators of *HEXIM1* expression will aid the discovery of novel cancer therapeutics and refinement of the upstream mechanisms that govern *HEXIM1* expression and function.

Transcription Factor Screen on *HEXIM1*

We demonstrate that DHODH inhibition causes a transient release of P-TEFb from the 7SK snRNP, which causes an upregulation of HEXIM1. There might be other factors that mediate HEXIM1 upregulation other than a transient release of P-TEFb alone. Hence, we examined the ENCODE database of ChIP-seq experiments performed with different transcription factors on a variety of cell lines within the UCSC Genome Browser. From this, we created a list of candidate transcription factors that seemingly bind the *HEXIM1* promoter under various contexts. With this list, we intend to perform a transcription factor siRNA screen to determine which factor(s) is (are) responsible for HEXIM1 upregulation by leflunomide. The candidates we will test are *CTCF*, *EGR1*, *ELF1*, *HEY1*, *cMYC*, *SP1*, *USF1* and *YY1* and the controls are scrambled siRNA, *HEXIM1* and *GAPDH*. A375 cells treated with DMSO or A771726 will be subjected to siRNA knockdown for each of the factors listed. RNA will be isolated for real time RT-PCR for *ACTB*, *GAPDH* and *HEXIM1* and protein will be isolated for western blotting of ACTB and HEXIM1.

We hypothesize that this screen will discover potential activators or repressors of HEXIM1. Knockdown of one or more of these factors will either block *HEXIM1* upregulation by A771726 (activators) or unblock *HEXIM1* upregulation in the DMSO control (repressors). DHODH inhibitors can therefore upregulate *HEXIM1* expression either by increasing recruitment of transcriptional activators or reducing the occupancy of transcriptional repressors at the *HEXIM1* locus. We can

validate how these factors respond to DHODH inhibition by performing ChIP-PCR using the *HEXIM1* promoter region as readout for binding. In addition, we can mutate the predicted binding motifs of the shortlisted factors on the *HEXIM1* promoter and determine if this has any effect on the ability of leflunomide to induce *HEXIM1* transcription.

Mass Spectrometry Analysis on the 7SK snRNP

We have shown that HEXIM1 is transcriptionally induced by DHODH inhibition to achieve inhibition of productive elongation. However, there is a biochemical level of 7SK snRNP regulation that we have yet to examine. The 7SK snRNP has been shown to be phosphorylated, dephosphorylated and structurally modified at a number of sites that modulate its ability to sequester and inhibit P-TEFb (Chen et al., 2008; Cho et al., 2009; Contreras et al., 2007; Fujinaga et al., 2012). We would like to establish the homeostatic HEXIM1 phosphorylation state in human melanoma by performing protein mass spectrometry on HEXIM1 protein that is immunoprecipitated from the A375 cell lines. This method will allow us to validate the literature in terms of which sites are phosphorylated *in vivo*. Furthermore, we can perform mass spectrometry on cells treated with DMSO and A771726 to determine if the drug causes any changes in the phosphorylation state of HEXIM1.

In addition to phosphorylation state, protein mass spectrometry can also give us an additional readout of HEXIM1 binding partners. There is evidence that other factors can bind HEXIM1, such as the glucocorticoid receptor (Shimizu et al., 2005), and it would be insightful to examine if leflunomide causes any changes in the association of factors with the 7SK snRNP. These factors could potentially affect 7SK snRNP nucleation or localization in the nucleus in response to DHODH inhibition. We hypothesize that one or more phosphorylation events on HEXIM1 will be changed in response to leflunomide and that we will find binding partners that are either responsible for localizing the 7SK snRNP to chromatin (transcription factors) or for

modifying its phosphorylation state (kinases and phosphatases).

Protein Phosphorylation Array on A771726-Treated A375 Cells

We have subjected DMSO and A771726-treated A375 cells to a human protein phosphorylation array to determine which signal transduction pathways are modified in terms of phosphorylation state in response to drug (Figure 4.2A). By visual inspection, focal adhesion kinase (FAK) and STAT6 phosphorylation are downregulated by A771726. FAK is a cytoplasmic tyrosine kinase that is co-activated by integrin and VEGFR-2 receptors to control vascular permeability, and seems to be responsible for tumor metastasis (Chen et al., 2012). Its expression and activation is elevated in malignant astrocytomas and ovarian cancer (Halder et al., 2007; Haskell et al., 2003). In addition, its inhibition or knockdown has been shown to suppress non-small cell lung cancer and ovarian cancer (Halder et al., 2007; Li et al., 2013a). STAT6 is a member of the JAK-STAT pathway which is activated in a number of cancers, such as breast, ovarian and prostate cancer, as reviewed by Furqan et. al. (Furqan et al., 2013). STAT inhibitors are currently being developed and tested for tumor suppression activity (Furqan et al., 2013). In addition to FAK and STAT6 downregulation of phosphorylation, tumor suppressor p53 is significantly upregulated at three different phosphorylation sites by A771726.

Further analysis of the blots was performed in ImageJ and this confirmed more candidate proteins that are significantly altered by drug (Figure 4.2B). Based on the cut-off of > 1.5 fold up- or downregulation of phosphorylation and a p-value of < 0.05, we further shortlisted proteins that we considered significantly altered (Figure 4.2C). Interestingly, only p53 phosphorylation is significantly upregulated and on all three sites probed (Figures 4.3A and 4.3C). We also shortlisted FAK and STAT6 phosphorylation as being downregulated, which we previously observed by eye. Other interesting proteins which experience a downregulation of phosphorylation by DHODH inhibition include c-Jun N-terminal kinases (JNKs) and platelet-derived growth factor (PDGF),

both of which are implicated in cancer (Alvarez et al., 2006; Song et al., 2014). A771726 seems to inhibit a number of tumor oncogenes and activate tumor suppressor p53 to achieve its tumor-suppressive function.

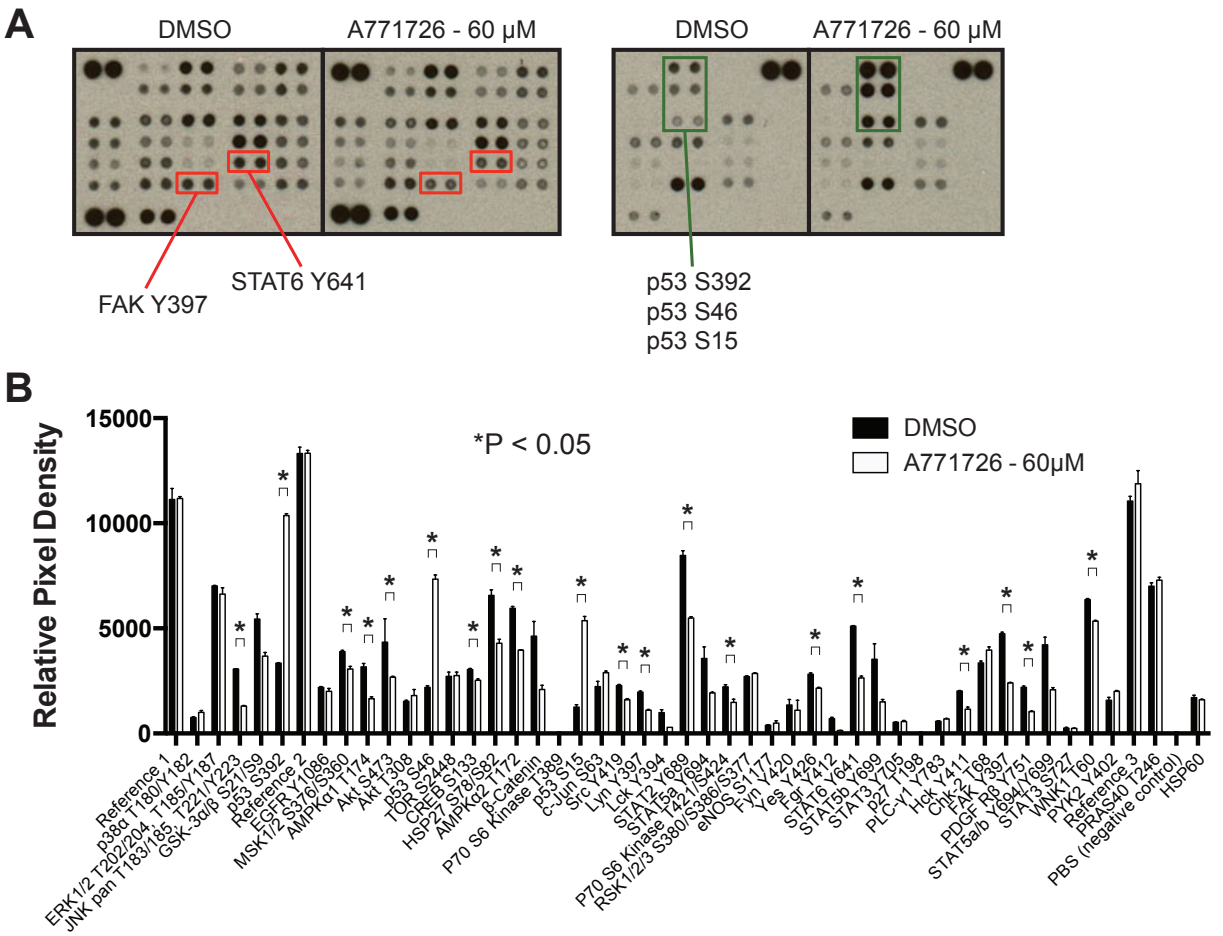

C

Phosphorylation Event	Fold Change	P-value
p53 S15	4.28	4.74E-03
p53 S46	3.35	6.90E-03
p53 S392	3.10	2.80E-03
HSP 27 S78/S82	-1.52	1.44E-02
STAT2 Y689	-1.54	2.15E-02
Hck Y411	-1.74	3.81E-02
Lyn Y397	-1.78	3.53E-03
STAT6 Y641	-1.93	7.78E-03
AMPKα1 T174	-1.94	2.09E-02
FAK Y397	-1.97	5.85E-03
PDGF Rβ Y751	-2.11	1.07E-02
JNK Pan T183/Y185, T221/Y223	-2.35	1.56E-04

Figure 4.2 Signal Transduction Pathways Affected by DHODH Inhibition

(A) Lysates from A375 cells treated with DMSO or 60 μM A771726 for 72 hrs were applied to a human phospho kinase antibody array. (B) ImageJ was used to determine the relative changes in pixel density for each antibody signal in the DMSO condition compared to A771726. (C) Significantly altered protein phosphorylation events are tabulated based on a relative fold change in pixel density of > 1.5-fold increase or decrease, and a Student's two-tailed t-test p-value cut-off of < 0.05.

Now that we have obtained candidates for signal transduction pathways that either directly or indirectly affect the 7SK snRNP, the next step is to test the appropriate kinase inhibitors or protein knockdowns to determine which ones are responsible for the changes to the 7SK snRNP caused by leflunomide. There are a number of proteins on the array that are expressed at a low levels, so it might be worth purchasing antibodies to determine if the phosphorylation state of these proteins is affected by DHODH inhibition as well. Once we have validated which pathways are responsible for the changes in 7SK snRNP phosphorylation, we can develop a clearer upstream mechanistic network of how transcription elongation is affected by various signals.

Investigation of Alternative RNA Binders to HEXIM1

There is evidence that HEXIM1 can bind RNA species other than the 7SK RNA (Fujimoto et al., 2012). One mRNA candidate that potentially binds to HEXIM1 is the *CAD* gene, which expresses the gate-keeper enzyme of pyrimidine biosynthesis (Jones, 1980). Since DHODH inhibition blocks pyrimidine biosynthesis, there might be some relevance to HEXIM1 regulation by *CAD* mRNA in order to regulate transcription. We previously showed that N-carbamoyl-L-aspartate is the earliest metabolite to be significantly upregulated with DHODH inhibition in the A375 cells, and this metabolite is an intermediate synthesized by CAD. In addition, *cad* mRNA expression is increased in zebrafish treated with leflunomide at a similar level to *hexim* mRNA, while melanocyte markers *mitfa* and *dct* are downregulated (White et al., 2011) as previously published (Figure 4.3). To investigate the possible relationship between *CAD* mRNA and HEXIM1 function, we will perform high-throughput sequencing of RNA isolated by cross-linking immunoprecipitation (HTS-CLIP) (Licatalosi et al., 2008) on A375 cells treated with DMSO or A771726 to determine if HEXIM1 indeed binds *CAD* mRNA and if there is any alteration of binding with drug.

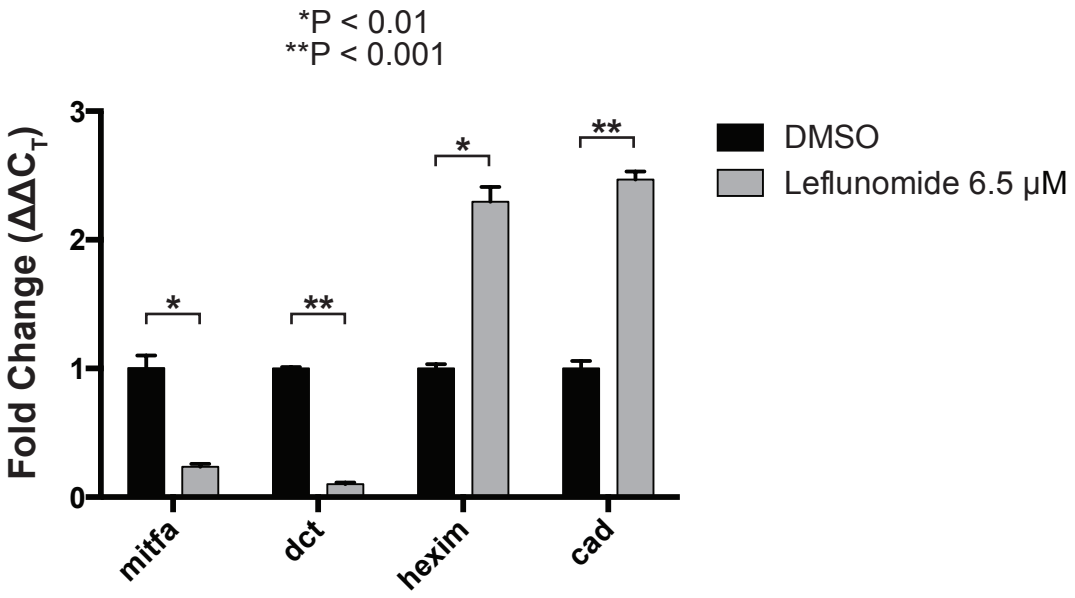

Figure 4.3 DHODH Inhibition Upregulates cad mRNA

Real time RT-PCR was performed on zebrafish embryos treated with leflunomide from 50% epiboly to 24 hpf. Genes examined were *mitfa*, *dct*, *hexim* and *cad*. Data is normalized to *gapdh*.

We hypothesize that *CAD* mRNA will be induced to bind HEXIM1 in a state of nucleotide starvation caused by leflunomide (Figure 4.4). This will activate HEXIM1 regardless of 7SK RNA binding to inhibit productive elongation, thus halting cell proliferation and the cell cycle until nucleotide levels return to normal. From HTS-CLIP, we can also discover potential novel interactions that act like *CAD* mRNA to regulate transcription in nucleotide level sensing.

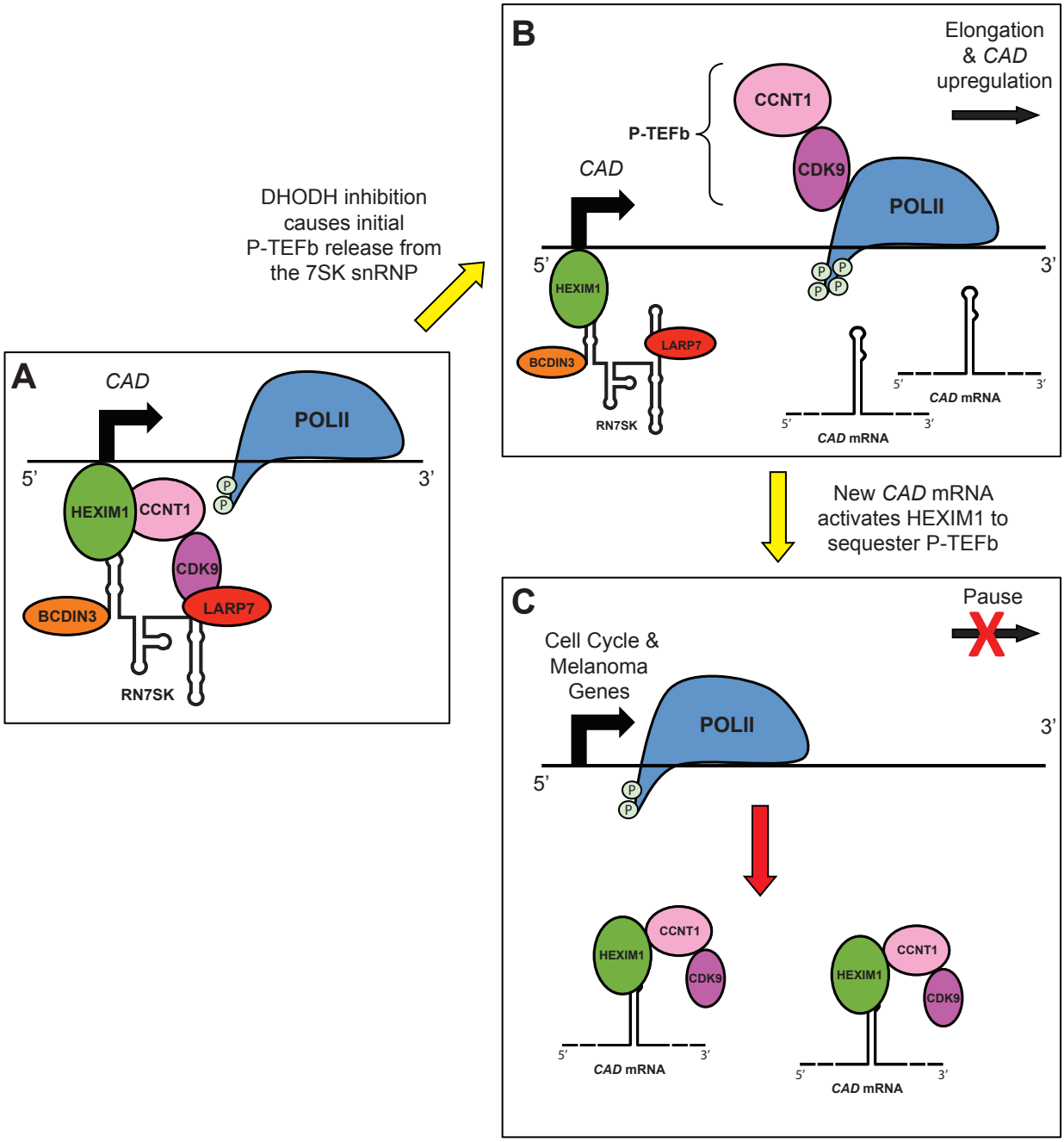

Figure 4.4 A Model for DHODH Induced *CAD* mRNA Expression to Inhibit Elongation via HEXIM1

(A) The 7SK snRNP poises P-TEFb at the *CAD* promoter in preparation for transcription elongation at the appropriate time. (B) DHODH inhibition triggers P-TEFb release from the 7SK snRNP at the *CAD* locus. The free P-TEFb results in a transient release of pausing at the *CAD* gene, upregulating *CAD* transcription. (C) Newly synthesized *CAD* mRNA binds HEXIM1, activating it to sequester P-TEF and consequently inhibiting transcription elongation at proliferation and cell cycle genes.

Chemical Screen for Novel Inducers of HEXIM1

There are already a number of drugs that are known to upregulate *HEXIM1*, including leflunomide that we show here. Since HEXIM1 has demonstrated strong tumor suppressing potential in a number of cancers, it might be prudent to discover more pathways that can modulate *HEXIM1* expression to target melanoma. We can perform a high-throughput chemical screen on our *HEXIM1*-Luciferase reporter A375 line to rapidly detect compounds that significantly upregulate *HEXIM1* expression. This screen will generate chemical probes to further comprehend HEXIM1 biology as well as potential targeted therapies for melanoma and other cancers. Since this is a cell-based screen, we can easily plate cells into 48- or 96-well format and deliver chemical libraries to these cells via robot. The luciferase reporter system will allow automated collection of plate images after the addition of fluorescent substrate. In addition, we can design algorithms to quantify fluorescence intensities in the images to further expedite the determination of hit compounds. Performing a secondary luciferase assay with a dose-response curve will validate chemical hits. After hits are verified, we will assign them to categories either through a literature search or with online tools such as Discovery Gate (Accelrys). Further cell culture, biochemical and zebrafish assays will be performed on hits-of-interest to discover their basis of *HEXIM1* induction.

Materials and Methods

Human Phospho-kinase Array

We treated A375 cells with DMSO or 60 μM A771726 for 72 hrs and obtained lysates as recommended by the manufacturer's protocol in the protein array (RnD Systems). We normalized total protein levels in the supernatants using the DC Protein Assay (Bio-rad). We then applied the lysates to the proteome profiler human phospho-kinase array ARY003B (RnD Systems) and imaged the blots with a traditional western film developer. Pixel densitometry analysis was performed in ImageJ (NIH).

RNA Extraction and Quantitative RT-PCR Analysis

RNA isolation was performed using TRIzol (Life Technologies), and subsequently treated with the TURBO DNA-free kit (Life Technologies). cDNA was synthesized with the SuperScript III Kit (Life Technologies). Quantitative PCR was performed on the iQ5 real-time PCR machine using the Ssofast EvaGreen Supermix (BioRad). The ΔΔCt method was used for relative quantification. RT-PCR primers are:

hexim forward: 5'-CAAACACGAGATTTGAGTTAAACG-3'

hexim reverse: 5'-CTCGTCCGATAATCTCTCTGC-3'

cad forward: 5'-ATGGAGGAAATCAACGAGCA-3'

cad reverse: 5'-GACCAGAACCGGATAACCAA-3'

mitfa forward: 5'-GGCGGTTTAATATCAATGACAGA-3'

mitfa reverse: 5'-GGTGCCTTTATTCCACCTCA-3'

dct forward: 5'-CACCTGGCACAGATATCACCT-3'

dct reverse: 5'-CGGCGAAGTTCTCATTACCT-3'

gapdh forward: 5'-GTGGAGTCTACTGGTGTCTTC-3'

gapdh reverse: 5'-GTGCAGGAGGCATTGCTTACA-3'

Bibliography

Adelman, K., and Lis, J.T. (2012). Promoter-proximal pausing of RNA polymerase II: emerging roles in metazoans. Nat. Rev. Genet. 13, 720–731.

Alvarez, R.H., Kantarjian, H.M., and Cortes, J.E. (2006). Biology of platelet-derived growth factor and its involvement in disease. Mayo Clin. Proc. 81, 1241–1257.

Andreeff, M., Stone, R., Michaeli, J., Young, C.W., Tong, W.P., Sogoloff, H., Ervin, T., Kufe, D., Rifkind, R.A., and Marks, P.A. (1992). Hexamethylene bisacetamide in myelodysplastic syndrome and acute myelogenous leukemia: a phase II clinical trial with a differentiation-inducing agent. Blood 80, 2604–2609.

Ascierto, P.A., Berking, C., Agarwala, S.S., Schadendorf, D., Herpen, C.V., Queirolo, P., Blank, C.U., Hauschild, A., Beck, J.T., Zubel, A., et al. (2012). Efficacy and safety of oral MEK162 in patients with locally advanced and unresectable or metastatic cutaneous melanoma harboring BRAFV600 or NRAS mutations. J. Clin. Oncol. 30. 8511.

Baldwin, C.T., Hoth, C.F., Amos, J.A., da-Silva, E.O., and Milunsky, A. (1992). An exonic mutation in the HuP2 paired domain gene causes Waardenburg's syndrome. Nature 355, 637–638.

Barboric, M., Kohoutek, J., Price, J.P., Blazek, D., Price, D.H., and Peterlin, B.M. (2005). Interplay between 7SK snRNA and oppositely charged regions in HEXIM1 direct the inhibition of P-TEFb. EMBO J. 24, 4291–4303.

Barboric, M., Lenasi, T., Chen, H., Johansen, E.B., Guo, S., and Peterlin, B.M. (2009). 7SK snRNP/P-TEFb couples transcription elongation with alternative splicing and is essential for vertebrate development. Proc. Natl. Acad. Sci. 106, 7798–7803.

Bardeesy, N., Kim, M., Xu, J., Kim, R.-S., Shen, Q., Bosenberg, M.W., Wong, W.H., and Chin, L. (2005). Role of epidermal growth factor receptor signaling in RAS-driven melanoma. Mol. Cell. Biol. 25, 4176–4188.

Bartholomeeusen, K., Xiang, Y., Fujinaga, K., and Peterlin, B.M. (2012a). Bromodomain and extra-terminal (BET) bromodomain inhibition activate transcription via transient release of positive transcription elongation factor b (P-TEFb) from 7SK small nuclear ribonucleoprotein. J. Biol. Chem. 287, 36609–36616.

Bartholomeeusen, K., Xiang, Y., Fujinaga, K., and Peterlin, B.M. (2012b). BET bromodomain inhibition activates transcription via a transient release of P-TEFb from 7SK snRNP. J. Biol. Chem.
Beeram, M., Patnaik, A., and Rowinsky, E.K. (2005). Raf: a strategic target for therapeutic development against cancer. J. Clin. Oncol. Off. J. Am. Soc. Clin. Oncol. 23, 6771–6790.

Berger, M.F., Hodis, E., Heffernan, T.P., Deribe, Y.L., Lawrence, M.S., Protopopov, A., Ivanova, E., Watson, I.R., Nickerson, E., Ghosh, P., et al. (2012). Melanoma genome sequencing reveals frequent PREX2 mutations. Nature 485, 502–506.

Blazek, D., Barboric, M., Kohoutek, J., Oven, I., and Peterlin, B.M. (2005). Oligomerization of HEXIM1 via 7SK snRNA and coiled-coil region directs the inhibition of P-TEFb. Nucleic Acids Res. 33, 7000–7010.

Boiko, A.D., Razorenova, O.V., van de Rijn, M., Swetter, S.M., Johnson, D.L., Ly, D.P., Butler, P.D., Yang, G.P., Joshua, B., Kaplan, M.J., et al. (2010). Human melanoma-initiating cells express neural crest nerve growth factor receptor CD271. Nature 466, 133–137.

Bollag, G., Hirth, P., Tsai, J., Zhang, J., Ibrahim, P.N., Cho, H., Spevak, W., Zhang, C., Zhang, Y., Habets, G., et al. (2010). Clinical efficacy of a RAF inhibitor needs broad target blockade in BRAF-mutant melanoma. Nature 467, 596–599.

Carbon, S., Ireland, A., Mungall, C.J., Shu, S., Marshall, B., Lewis, S., AmiGO Hub, and Web Presence Working Group (2009). AmiGO: online access to ontology and annotation data. Bioinforma. Oxf. Engl. 25, 288–289.

Ceol, C.J., Houvras, Y., Jane-Valbuena, J., Bilodeau, S., Orlando, D.A., Battisti, V., Fritsch, L., Lin, W.M., Hollmann, T.J., Ferré, F., et al. (2011). The histone methyltransferase SETDB1 is recurrently amplified in melanoma and accelerates its onset. Nature 471, 513–517.

Chapman, P.B., Hauschild, A., Robert, C., Haanen, J.B., Ascierto, P., Larkin, J., Dummer, R., Garbe, C., Testori, A., Maio, M., et al. (2011). Improved survival with vemurafenib in melanoma with BRAF V600E mutation. N. Engl. J. Med. 364, 2507–2516.

Chen, J., Abi-Daoud, M., Wang, A., Yang, X., Zhang, X., Feilotter, H.E., and Tron, V.A. (2013). Stathmin 1 is a potential novel oncogene in melanoma. Oncogene 32, 1330–1337.

Chen, R., Liu, M., Li, H., Xue, Y., Ramey, W.N., He, N., Ai, N., Luo, H., Zhu, Y., Zhou, N., et al. (2008). PP2B and PP1alpha cooperatively disrupt 7SK snRNP to release P-TEFb for transcription in response to Ca2+ signaling. Genes Dev. 22, 1356–1368.

Chen, X.L., Nam, J.-O., Jean, C., Lawson, C., Walsh, C.T., Goka, E., Lim, S.-T., Tomar, A., Tancioni, I., Uryu, S., et al. (2012). VEGF-induced vascular permeability is mediated by FAK. Dev. Cell 22, 146–157.

Cheng, B., Li, T., Rahl, P.B., Adamson, T.E., Loudas, N.B., Guo, J., Varzavand, K., Cooper, J.J., Hu, X., Gnatt, A., et al. (2012a). Functional association of Gdown1 with RNA polymerase II poised on human genes. Mol. Cell 45, 38–50.

Cheng, Y., Jin, Z., Agarwal, R., Ma, K., Yang, J., Ibrahim, S., Olaru, A.V., David, S., Ashktorab, H., Smoot, D.T., et al. (2012b). LARP7 is a potential tumor suppressor gene in gastric cancer. Lab. Invest. 92, 1013-1019.

Cho, S., Schroeder, S., Kaehlcke, K., Kwon, H.-S., Pedal, A., Herker, E., Schnoelzer, M., and Ott, M. (2009). Acetylation of cyclin T1 regulates the equilibrium between active and inactive P-TEFb in cells. EMBO J. 28, 1407–1417.

Chopra, V.S., Hong, J.-W., and Levine, M. (2009). Regulation of Hox gene activity by transcriptional elongation in Drosophila. Curr. Biol. CB 19, 688–693.

Civenni, G., Walter, A., Kobert, N., Mihic-Probst, D., Zipser, M., Belloni, B., Seifert, B., Moch, H., Dummer, R., van den Broek, M., et al. (2011). Human CD271-positive melanoma stem cells associated with metastasis establish tumor heterogeneity and long-term growth. Cancer Res. 71, 3098–3109.

Contreras, X., Barboric, M., Lenasi, T., and Peterlin, B.M. (2007). HMBA Releases P-TEFb from HEXIM1 and 7SK snRNA via PI3K/Akt and Activates HIV Transcription. PLoS Pathog. 3, 1459-1469.

Contreras, X., Schweneker, M., Chen, C.-S., McCune, J.M., Deeks, S.G., Martin, J., and Peterlin, B.M. (2009). Suberoylanilide hydroxamic acid reactivates HIV from latently infected cells. J. Biol. Chem. 284, 6782–6789.

Coulie, P.G., Brichard, V., Van Pel, A., Wölfel, T., Schneider, J., Traversari, C., Mattei, S., De Plaen, E., Lurquin, C., Szikora, J.P., et al. (1994). A new gene coding for a differentiation antigen recognized by autologous cytolytic T lymphocytes on HLA-A2 melanomas. J. Exp. Med. 180, 35–42.

Curtin, J.A., Fridlyand, J., Kageshita, T., Patel, H.N., Busam, K.J., Kutzner, H., Cho, K.-H., Aiba, S., Bröcker, E.-B., LeBoit, P.E., et al. (2005). Distinct sets of genetic alterations in melanoma. N. Engl. J. Med. 353, 2135–2147.

Davies, H., Bignell, G.R., Cox, C., Stephens, P., Edkins, S., Clegg, S., Teague, J., Woffendin, H., Garnett, M.J., Bottomley, W., et al. (2002). Mutations of the BRAF gene in human cancer. Nature 417, 949–954.

Delmore, J.E., Issa, G.C., Lemieux, M.E., Rahl, P.B., Shi, J., Jacobs, H.M., Kastritis, E., Gilpatrick, T., Paranal, R.M., Qi, J., et al. (2011). BET Bromodomain Inhibition as a Therapeutic Strategy to Target c-Myc. Cell 146, 904–917.

Eggermont, A.M.M., Spatz, A., and Robert, C. (2014). Cutaneous melanoma. Lancet 383, 816–827.

Filippakopoulos, P., Qi, J., Picaud, S., Shen, Y., Smith, W.B., Fedorov, O., Morse, E.M., Keates, T., Hickman, T.T., Felletar, I., et al. (2010). Selective inhibition of BET bromodomains. Nature 468, 1067–1073.

Flaherty, K.T., Robert, C., Hersey, P., Nathan, P., Garbe, C., Milhem, M., Demidov, L.V., Hassel, J.C., Rutkowski, P., Mohr, P., et al. (2012). Improved survival with MEK inhibition in BRAF-mutated melanoma. N. Engl. J. Med. 367, 107–114.

Flynn, P.J., and Reece, R.J. (1999). Activation of transcription by metabolic intermediates of the pyrimidine biosynthetic pathway. Mol. Cell. Biol. 19, 882–888.

Fujimoto, Y., Nakamura, Y., and Ohuchi, S. (2012). HEXIM1-binding elements on mRNAs identified through transcriptomic SELEX and computational screening. Biochimie 94, 1900-1909.

Fujinaga, K., Irwin, D., Huang, Y., Taube, R., Kurosu, T., and Peterlin, B.M. (2004). Dynamics of human immunodeficiency virus transcription: P-TEFb phosphorylates RD and dissociates negative effectors from the transactivation response element. Mol. Cell. Biol. 24, 787–795.

Fujinaga, K., Barboric, M., Li, Q., Luo, Z., Price, D.H., and Peterlin, B.M. (2012). PKC phosphorylates HEXIM1 and regulates P-TEFb activity. Nucleic Acids Res. 40, 9160-9170.

Furqan, M., Akinleye, A., Mukhi, N., Mittal, V., Chen, Y., and Liu, D. (2013). STAT inhibitors for cancer therapy. J. Hematol. Oncol.J Hematol Oncol 6, 90.

Gazitt, Y., Reuben, R.C., Deitch, A.D., Marks, P.A., and Rifkind, R.A. (1978). Changes in cyclic adenosine 3':5'-monophosphate levels during induction of differentiation in murine erythroleukemia cells. Cancer Res. 38, 3779–3783.

Guo, J., and Price, D.H. (2013). RNA polymerase II transcription elongation control. Chem. Rev. 113, 8583–8603.

Halder, J., Lin, Y.G., Merritt, W.M., Spannuth, W.A., Nick, A.M., Honda, T., Kamat, A.A., Han, L.Y., Kim, T.J., Lu, C., et al. (2007). Therapeutic efficacy of a novel focal adhesion kinase inhibitor TAE226 in ovarian carcinoma. Cancer Res. 67, 10976–10983.

Haskell, H., Natarajan, M., Hecker, T.P., Ding, Q., Stewart, J., Jr, Grammer, J.R., and Gladson, C.L. (2003). Focal adhesion kinase is expressed in the angiogenic blood vessels of malignant astrocytic tumors *in vivo* and promotes capillary tube formation of brain microvascular endothelial cells. Clin. Cancer Res. Off. J. Am. Assoc. Cancer Res. 9, 2157–2165.

He, N., Jahchan, N.S., Hong, E., Li, Q., Bayfield, M.A., Maraia, R.J., Luo, K., and Zhou, Q. (2008). A La-related protein modulates 7SK snRNP integrity to suppress P-TEFb-dependent transcriptional elongation and tumorigenesis. Mol. Cell 29, 588–599.

Hong, S.-K., Tsang, M., and Dawid, I.B. (2008). The mych gene is required for neural crest survival during zebrafish development. PloS One 3, e2029.

Hu, Y., Flockhart, I., Vinayagam, A., Bergwitz, C., Berger, B., Perrimon, N., and Mohr, S.E. (2011). An integrative approach to ortholog prediction for disease-focused and other functional studies. BMC Bioinformatics 12, 357.

Huang, F., Wagner, M., and Siddiqui, M.A.Q. (2004). Ablation of the CLP-1 gene leads to down-regulation of the HAND1 gene and abnormality of the left ventricle of the heart and fetal death. Mech. Dev. 121, 559–572.

Huang, W.-Y., Xie, W., Guo, X., Li, F., Jose, P.A., and Chen, S.-Y. (2011). Smad2 and PEA3 cooperatively regulate transcription of response gene to complement 32 in TGF-β-induced smooth muscle cell differentiation of neural crest cells. Am. J. Physiol. Cell Physiol. 301, C499–506.

Jakob, J.A., Bassett, R.L., Jr, Ng, C.S., Curry, J.L., Joseph, R.W., Alvarado, G.C., Rohlfs, M.L., Richard, J., Gershenwald, J.E., Kim, K.B., et al. (2012). NRAS mutation status is an independent prognostic factor in metastatic melanoma. Cancer 118, 4014–4023.

Jeronimo, C., Forget, D., Bouchard, A., Li, Q., Chua, G., Poitras, C., Thérien, C., Bergeron, D., Bourassa, S., Greenblatt, J., et al. (2007). Systematic analysis of the protein interaction network for the human transcription machinery reveals the identity of the 7SK capping enzyme. Mol. Cell 27, 262–274.

Ji, X., Zhou, Y., Pandit, S., Huang, J., Li, H., Lin, C.Y., Xiao, R., Burge, C.B., and Fu, X.-D. (2013). SR proteins collaborate with 7SK and promoter-associated nascent RNA to release paused polymerase. Cell 153, 855–868.

Jones, M.E. (1980). Pyrimidine nucleotide biosynthesis in animals: genes, enzymes, and regulation of UMP biosynthesis. Annu. Rev. Biochem. 49, 253–279.

Joseph, E.W., Pratilas, C.A., Poulikakos, P.I., Tadi, M., Wang, W., Taylor, B.S., Halilovic, E., Persaud, Y., Xing, F., Viale, A., et al. (2010). The RAF inhibitor PLX4032 inhibits ERK signaling and tumor cell proliferation in a V600E BRAF-selective manner. Proc. Natl. Acad. Sci. U. S. A. 107, 14903–14908.

Kaplan, M.J. (2001). Leflunomide Aventis Pharma. Curr. Opin. Investig. Drugs Lond. Engl. 2000 2, 222–230.

Kawakami, Y., Eliyahu, S., Delgado, C.H., Robbins, P.F., Sakaguchi, K., Appella, E., Yannelli, J.R., Adema, G.J., Miki, T., and Rosenberg, S.A. (1994). Identification of a human melanoma antigen recognized by tumor-infiltrating lymphocytes associated with *in vivo* tumor rejection. Proc. Natl. Acad. Sci. U. S. A. 91, 6458–6462.

Keegan, B.R., Feldman, J.L., Lee, D.H., Koos, D.S., Ho, R.K., Stainier, D.Y.R., and Yelon, D. (2002). The elongation factors Pandora/Spt6 and Foggy/Spt5 promote transcription in the zebrafish embryo. Dev. Camb. Engl. 129, 1623–1632.

Ketchart, W., Smith, K.M., Krupka, T., Wittmann, B.M., Hu, Y., Rayman, P.A., Doughman, Y.Q., Albert, J.M., Bai, X., Finke, J.H., et al. (2013). Inhibition of metastasis by HEXIM1 through effects on cell invasion and angiogenesis. Oncogene 32, 3829–3839.

Kim, Y.J., Greer, C.B., Cecchini, K.R., Harris, L.N., Tuck, D.P., and Kim, T.H. (2013). HDAC inhibitors induce transcriptional repression of high copy number genes in breast cancer through elongation blockade. Oncogene 32, 2828–2835.

Kollias, N., Sayre, R.M., Zeise, L., and Chedekel, M.R. (1991). Photoprotection by melanin. J. Photochem. Photobiol. B 9, 135–160.

Lachman, H.M., and Skoultchi, A.I. (1984). Expression of c-myc changes during differentiation of mouse erythroleukaemia cells. Nature 310, 592–594.

Langmead, B., Trapnell, C., Pop, M., and Salzberg, S.L. (2009). Ultrafast and memory-efficient alignment of short DNA sequences to the human genome. Genome Biol. 10, R25.

Lee, T.I., Johnstone, S.E., and Young, R.A. (2006). Chromatin immunoprecipitation and microarray-based analysis of protein location. Nat. Protoc. 1, 729–748.

Lenasi, T., Contreras, X., and Peterlin, B.M. (2008). Transcriptional interference antagonizes proviral gene expression to promote HIV latency. Cell Host Microbe 4, 123–133.

Levine, M. (2011). Paused RNA polymerase II as a developmental checkpoint. Cell 145, 502–511.
Levy, C., Khaled, M., and Fisher, D.E. (2006). MITF: master regulator of melanocyte development and melanoma oncogene. Trends Mol. Med. 12, 406–414.

Li, C., Zhang, X., Cheng, L., Dai, L., Xu, F., Zhang, J., Tian, H., Chen, X., Shi, G., Li, Y., et al. (2013a). RNA interference targeting human FAK and EGFR suppresses human non-small-cell lung cancer xenograft growth in nude mice. Cancer Gene Ther. 20, 101–108.

Li, Q., Price, J.P., Byers, S.A., Cheng, D., Peng, J., and Price, D.H. (2005). Analysis of the large inactive P-TEFb complex indicates that it contains one 7SK molecule, a dimer of HEXIM1 or HEXIM2, and two P-TEFb molecules containing Cdk9 phosphorylated at threonine 186. J. Biol. Chem. 280, 28819–28826.

Li, S., Huang, X., Zhang, D., Huang, Q., Pei, G., Wang, L., Jiang, W., Hu, Q., Tan, R., and Hua, Z.-C. (2013b). Requirement of PEA3 for transcriptional activation of FAK gene in tumor metastasis. PloS One 8, e79336.

Licatalosi, D.D., Mele, A., Fak, J.J., Ule, J., Kayikci, M., Chi, S.W., Clark, T.A., Schweitzer, A.C., Blume, J.E., Wang, X., et al. (2008). HITS-CLIP yields genome-wide insights into brain alternative RNA processing. Nature 456, 464–469.

Lin, H., Wong, R.P.C., Martinka, M., and Li, G. (2010). BRG1 expression is increased in human cutaneous melanoma. Br. J. Dermatol. 163, 502–510.

Lin, W.M., Baker, A.C., Beroukhim, R., Winckler, W., Feng, W., Marmion, J.M., Laine, E., Greulich, H., Tseng, H., Gates, C., et al. (2008). Modeling genomic diversity and tumor dependency in malignant melanoma. Cancer Res. 68, 664–673.

Liu, P., Xiang, Y., Fujinaga, K., Bartholomeeusen, K., Nilson, K.A., Price, D.H., and Peterlin, B.M. (2014a). Release of Positive Transcription Elongation Factor b (P-TEFb) from 7SK Small Nuclear Ribonucleoprotein (snRNP) Activates Hexamethylene Bisacetamide-inducible Protein (HEXIM1) Transcription. J. Biol. Chem. 289, 9918–9925.

Liu, P., Xiang, Y., Fujinaga, K., Bartholomeeusen, K., Nilson, K., Price, D.H., and Peterlin, B.M. (2014b). Release of P-TEFb from 7SK snRNP Activates HEXIM1 Transcription. J. Biol. Chem.
Löffler, M., Jöckel, J., Schuster, G., and Becker, C. (1997). Dihydroorotat-ubiquinone oxidoreductase links mitochondria in the biosynthesis of pyrimidine nucleotides. Mol. Cell. Biochem. 174, 125–129.

Long, G.V., Menzies, A.M., Nagrial, A.M., Haydu, L.E., Hamilton, A.L., Mann, G.J., Hughes, T.M., Thompson, J.F., Scolyer, R.A., and Kefford, R.F. (2011). Prognostic and clinicopathologic associations of oncogenic BRAF in metastatic melanoma. J. Clin. Oncol. Off. J. Am. Soc. Clin. Oncol. 29, 1239–1246.

Luo, R., An, M., Arduini, B.L., and Henion, P.D. (2001). Specific pan-neural crest expression of zebrafish Crestin throughout embryonic development. Dev. Dyn. Off. Publ. Am. Assoc. Anat. 220, 169–174.

Magne, D., Mézin, F., Palmer, G., and Guerne, P.-A. (2006). The active metabolite of leflunomide, A77 1726, increases proliferation of human synovial fibroblasts in presence of IL-1beta and TNF-alpha. Inflamm. Res. Off. J. Eur. Histamine Res. Soc. Al 55, 469–475.

Marks, P.A., and Rifkind, R.A. (1989). Induced differentiation of erythroleukemia cells by hexamethylene bisacetamide: a model for cytodifferentiation of transformed cells. Environ. Health Perspect. 80, 181–188.

Marquette, A., André, J., Bagot, M., Bensussan, A., and Dumaz, N. (2011). ERK and PDE4 cooperate to induce RAF isoform switching in melanoma. Nat. Struct. Mol. Biol. 18, 584–591.

Marshall, N.F., Peng, J., Xie, Z., and Price, D.H. (1996). Control of RNA polymerase II elongation potential by a novel carboxyl-terminal domain kinase. J. Biol. Chem. 271, 27176–27183.

Mascareno, E.J., Belashov, I., Siddiqui, M.A.Q., Liu, F., and Dhar-Mascareno, M. (2012). Hexim-1 modulates androgen receptor and the TGF-β signaling during the progression of prostate cancer. The Prostate 72, 1035–1044.

Matys, V., Kel-Margoulis, O.V., Fricke, E., Liebich, I., Land, S., Barre-Dirrie, A., Reuter, I., Chekmenev, D., Krull, M., Hornischer, K., et al. (2006). TRANSFAC and its module TRANSCompel: transcriptional gene regulation in eukaryotes. Nucleic Acids Res. 34, D108–110.

McClelland, R.A., Finlay, P., Walker, K.J., Nicholson, D., Robertson, J.F., Blamey, R.W., and Nicholson, R.I. (1990). Automated quantitation of immunocytochemically localized estrogen receptors in human breast cancer. Cancer Res. 50, 3545–3550.

Melloni, E., Pontremoli, S., Michetti, M., Sacco, O., Cakiroglu, A.G., Jackson, J.F., Rifkind, R.A., and Marks, P.A. (1987). Protein kinase C activity and hexamethylenebisacetamide-induced erythroleukemia cell differentiation. Proc. Natl. Acad. Sci. U. S. A. 84, 5282–5286.

Michels, A.A., and Bensaude, O. (2008). RNA-driven cyclin-dependent kinase regulation: When CDK9/cyclin T subunits of P-TEFb meet their ribonucleoprotein partners. Biotechnol. J. 3, 1022–1032.

Montano, M.M., Doughman, Y.Q., Deng, H., Chaplin, L., Yang, J., Wang, N., Zhou, Q., Ward, N.L., and Watanabe, M. (2008). Mutation of the HEXIM1 Gene Results in Defects During Heart and Vascular Development Partly Through Downregulation of Vascular Endothelial Growth Factor. Circ. Res. 102, 415–422.

Mori, Y., Sato, F., Selaru, F.M., Olaru, A., Perry, K., Kimos, M.C., Tamura, G., Matsubara, N., Wang, S., Xu, Y., et al. (2002). Instabilotyping reveals unique mutational spectra in microsatellite-unstable gastric cancers. Cancer Res. 62, 3641–3645.

Muse, G.W., Gilchrist, D.A., Nechaev, S., Shah, R., Parker, J.S., Grissom, S.F., Zeitlinger, J., and Adelman, K. (2007). RNA polymerase is poised for activation across the genome. Nat. Genet. 39, 1507–1511.

Ng, S.B., Buckingham, K.J., Lee, C., Bigham, A.W., Tabor, H.K., Dent, K.M., Huff, C.D., Shannon, P.T., Jabs, E.W., Nickerson, D.A., et al. (2010). Exome sequencing identifies the cause of a mendelian disorder. Nat. Genet. 42, 30–35.

Nguyen, V.T., Kiss, T., Michels, A.A., and Bensaude, O. (2001). 7SK small nuclear RNA binds to and inhibits the activity of CDK9/cyclin T complexes. Nature 414, 322–325.

Ogba, N., Chaplin, L.J., Doughman, Y.Q., Fujinaga, K., and Montano, M.M. (2008). HEXIM1 regulates 17beta-estradiol/estrogen receptor-alpha-mediated expression of cyclin D1 in mammary cells via modulation of P-TEFb. Cancer Res. 68, 7015–7024.

Ohshima, Y., Yajima, I., Takeda, K., Iida, M., Kumasaka, M., Matsumoto, Y., and Kato, M. (2010). c-RET molecule in malignant melanoma from oncogenic RET-carrying transgenic mice and human cell lines. PloS One 5, e10279.

Ouchida, R., Kusuhara, M., Shimizu, N., Hisada, T., Makino, Y., Morimoto, C., Handa, H., Ohsuzu, F., and Tanaka, H. (2003). Suppression of NF-kappaB-dependent gene expression by a hexamethylene bisacetamide-inducible protein HEXIM1 in human vascular smooth muscle cells. Genes Cells Devoted Mol. Cell. Mech. 8, 95–107.

Patton, E.E., Widlund, H.R., Kutok, J.L., Kopani, K.R., Amatruda, J.F., Murphey, R.D., Berghmans, S., Mayhall, E.A., Traver, D., Fletcher, C.D.M., et al. (2005). BRAF mutations are sufficient to promote nevi formation and cooperate with p53 in the genesis of melanoma. Curr. Biol. CB 15, 249–254.

Peng, J., Zhu, Y., Milton, J.T., and Price, D.H. (1998). Identification of multiple cyclin subunits of human P-TEFb. Genes Dev. 12, 755–762.

Pollock, P.M., Harper, U.L., Hansen, K.S., Yudt, L.M., Stark, M., Robbins, C.M., Moses, T.Y., Hostetter, G., Wagner, U., Kakareka, J., et al. (2003). High frequency of BRAF mutations in nevi. Nat. Genet. 33, 19–20.

Rahl, P.B., Lin, C.Y., Seila, A.C., Flynn, R.A., McCuine, S., Burge, C.B., Sharp, P.A., and Young, R.A. (2010). c-Myc regulates transcriptional pause release. Cell 141, 432–445.

Ramsay, R.G., Ikeda, K., Rifkind, R.A., and Marks, P.A. (1986). Changes in gene expression associated with induced differentiation of erythroleukemia: protooncogenes, globin genes, and cell division. Proc. Natl. Acad. Sci. U. S. A. 83, 6849–6853.

Raskin, L., Fullen, D.R., Giordano, T.J., Thomas, D.G., Frohm, M.L., Cha, K.B., Ahn, J., Mukherjee, B., Johnson, T.M., and Gruber, S.B. (2013). Transcriptome profiling identifies HMGA2 as a biomarker of melanoma progression and prognosis. J. Invest. Dermatol. 133, 2585–2592.

Richon, V.M., Webb, Y., Merger, R., Sheppard, T., Jursic, B., Ngo, L., Civoli, F., Breslow, R., Rifkind, R.A., and Marks, P.A. (1996). Second generation hybrid polar compounds are potent inducers of transformed cell differentiation. Proc. Natl. Acad. Sci. U. S. A. 93, 5705–5708.

Richon, V.M., Emiliani, S., Verdin, E., Webb, Y., Breslow, R., Rifkind, R.A., and Marks, P.A. (1998). A class of hybrid polar inducers of transformed cell differentiation inhibits histone deacetylases. Proc. Natl. Acad. Sci. U. S. A. 95, 3003–3007.

Sauter, E.R., Yeo, U.-C., von Stemm, A., Zhu, W., Litwin, S., Tichansky, D.S., Pistritto, G., Nesbit, M., Pinkel, D., Herlyn, M., et al. (2002). Cyclin D1 is a candidate oncogene in cutaneous melanoma. Cancer Res. 62, 3200–3206.

Schadendorf, D., and Hauschild, A. (2014). Melanoma in 2013: Melanoma-the run of success continues. Nat. Rev. Clin. Oncol. 11, 75-76.

Schatton, T., Murphy, G.F., Frank, N.Y., Yamaura, K., Waaga-Gasser, A.M., Gasser, M., Zhan, Q., Jordan, S., Duncan, L.M., Weishaupt, C., et al. (2008). Identification of cells initiating human melanomas. Nature 451, 345–349.

Shakhova, O. (2014). Neural crest stem cells in melanoma development. Curr. Opin. Oncol. 26, 215–221.

Shakhova, O., Zingg, D., Schaefer, S.M., Hari, L., Civenni, G., Blunschi, J., Claudinot, S., Okoniewski, M., Beermann, F., Mihic-Probst, D., et al. (2012). Sox10 promotes the formation and maintenance of giant congenital naevi and melanoma. Nat. Cell Biol. 14, 882–890.

Shimizu, N., Ouchida, R., Yoshikawa, N., Hisada, T., Watanabe, H., Okamoto, K., Kusuhara, M., Handa, H., Morimoto, C., and Tanaka, H. (2005). HEXIM1 forms a transcriptionally abortive complex with glucocorticoid receptor without involving 7SK RNA and positive transcription elongation factor b. Proc. Natl. Acad. Sci. U. S. A. 102, 8555–8560.

Sigova, A.A., Mullen, A.C., Molinie, B., Gupta, S., Orlando, D.A., Guenther, M.G., Almada, A.E., Lin, C., Sharp, P.A., Giallourakis, C.C., et al. (2013). Divergent transcription of long noncoding RNA/mRNA gene pairs in embryonic stem cells. Proc. Natl. Acad. Sci. U. S. A. 110, 2876–2881.

Sloane, B.F., Honn, K.V., Sadler, J.G., Turner, W.A., Kimpson, J.J., and Taylor, J.D. (1982). Cathepsin B activity in B16 melanoma cells: a possible marker for metastatic potential. Cancer Res. 42, 980–986.

Song, W., Ma, Y., Wang, J., Brantley-Sieders, D., and Chen, J. (2014). JNK signaling mediates EPHA2-dependent tumor cell proliferation, motility, and cancer stem cell-like properties in non-small cell lung cancer. Cancer Res. 74, 2444-2454.

Sullivan, R.J., and Flaherty, K. (2013). MAP kinase signaling and inhibition in melanoma. Oncogene 32, 2373–2379.

Talantov, D., Mazumder, A., Yu, J.X., Briggs, T., Jiang, Y., Backus, J., Atkins, D., and Wang, Y. (2005). Novel genes associated with malignant melanoma but not benign melanocytic lesions. Clin. Cancer Res. Off. J. Am. Assoc. Cancer Res. 11, 7234–7242.

Tan, J.L., and Zon, L.I. (2011). Chemical screening in zebrafish for novel biological and therapeutic discovery. Methods Cell Biol. 105, 493–516.

Tassabehji, M., Read, A.P., Newton, V.E., Harris, R., Balling, R., Gruss, P., and Strachan, T. (1992). Waardenburg's syndrome patients have mutations in the human homologue of the Pax-3 paired box gene. Nature 355, 635–636.

Thomas, K.R., and Capecchi, M.R. (1987). Site-directed mutagenesis by gene targeting in mouse embryo-derived stem cells. Cell 51, 503–512.

Thomas-Chollier, M., Hufton, A., Heinig, M., O'Keeffe, S., Masri, N.E., Roider, H.G., Manke, T., and Vingron, M. (2011). Transcription factor binding predictions using TRAP for the analysis of ChIP-seq data and regulatory SNPs. Nat. Protoc. 6, 1860–1869.

Todokoro, K., and Ikawa, Y. (1986). Sequential expression of proto-oncogenes during a mouse erythroleukemia cell differentiation. Biochem. Biophys. Res. Commun. 135, 1112–1118.

Trunzer, K., Pavlick, A.C., Schuchter, L., Gonzalez, R., McArthur, G.A., Hutson, T.E., Moschos, S.J., Flaherty, K.T., Kim, K.B., Weber, J.S., et al. (2013). Pharmacodynamic effects and mechanisms of resistance to vemurafenib in patients with metastatic melanoma. J. Clin. Oncol. Off. J. Am. Soc. Clin. Oncol. 31, 1767–1774.

Wada, T., Takagi, T., Yamaguchi, Y., Watanabe, D., and Handa, H. (1998). Evidence that P-TEFb alleviates the negative effect of DSIF on RNA polymerase II-dependent transcription *in vitro*. EMBO J. 17, 7395–7403.

Wagner, J.M., Hackanson, B., Lübbert, M., and Jung, M. (2010). Histone deacetylase (HDAC) inhibitors in recent clinical trials for cancer therapy. Clin. Epigenetics 1, 117–136.

Walker, G.J., Soyer, H.P., Terzian, T., and Box, N.F. (2011). Modelling melanoma in mice. Pigment Cell Melanoma Res. 24, 1158–1176.

Wei, P., Garber, M.E., Fang, S.M., Fischer, W.H., and Jones, K.A. (1998). A novel CDK9-associated C-type cyclin interacts directly with HIV-1 Tat and mediates its high-affinity, loop-specific binding to TAR RNA. Cell 92, 451–462.

White, R., Rose, K., and Zon, L. (2013). Zebrafish cancer: the state of the art and the path forward. Nat. Rev. Cancer 13, 624–636.

White, R.M., Cech, J., Ratanasirintrawoot, S., Lin, C.Y., Rahl, P.B., Burke, C.J., Langdon, E., Matthew L Tomlinson, Mosher, J., Kaufman, C., et al. (2011). DHODH modulates transcriptional elongation in the neural crest and melanoma. Nature 471, 518–522.

Wittmann, B.M., Wang, N., and Montano, M.M. (2003). Identification of a Novel Inhibitor of Breast Cell Growth That Is Down-Regulated by Estrogens and Decreased in Breast Tumors. Cancer Res. 63, 5151–5158.

Wittmann, B.M., Fujinaga, K., Deng, H., Ogba, N., and Montano, M.M. (2005). The breast cell growth inhibitor, estrogen down regulated gene 1, modulates a novel functional interaction between estrogen receptor alpha and transcriptional elongation factor cyclin T1. Oncogene 24, 5576–5588.

Wollnik, B., Tukel, T., Uyguner, O., Ghanbari, A., Kayserili, H., Emiroglu, M., and Yuksel-Apak, M. (2003). Homozygous and heterozygous inheritance of PAX3 mutations causes different types of Waardenburg syndrome. Am. J. Med. Genet. A. 122A, 42–45.

Xia, J., Psychogios, N., Young, N., and Wishart, D.S. (2009). MetaboAnalyst: a web server for metabolomic data analysis and interpretation. Nucleic Acids Res. 37, W652–660.

Xia, J., Mandal, R., Sinelnikov, I.V., Broadhurst, D., and Wishart, D.S. (2012). MetaboAnalyst 2.0--a comprehensive server for metabolomic data analysis. Nucleic Acids Res. 40, W127–133.
Yamada, T., Yamaguchi, Y., Inukai, N., Okamoto, S., Mura, T., and Handa, H. (2006). P-TEFb-mediated phosphorylation of hSpt5 C-terminal repeats is critical for processive transcription elongation. Mol. Cell 21, 227–237.

Yang, Z., Zhu, Q., Luo, K., and Zhou, Q. (2001). The 7SK small nuclear RNA inhibits the CDK9/cyclin T1 kinase to control transcription. Nature 414, 317–322.

Yeh, I.-J., Ogba, N., Bensigner, H., Welford, S.M., and Montano, M.M. (2013). HEXIM1 down-regulates hypoxia-inducible factor-1α protein stability. Biochem. J. 456, 195–204.

Yik, J.H.N., Chen, R., Nishimura, R., Jennings, J.L., Link, A.J., and Zhou, Q. (2003). Inhibition of P-TEFb (CDK9/Cyclin T) kinase and RNA polymerase II transcription by the coordinated actions of HEXIM1 and 7SK snRNA. Mol. Cell 12, 971–982.

Yuan, M., Breitkopf, S.B., Yang, X., and Asara, J.M. (2012). A positive/negative ion-switching, targeted mass spectrometry-based metabolomics platform for bodily fluids, cells, and fresh and fixed tissue. Nat. Protoc. 7, 872–881.

Zeitlinger, J., Stark, A., Kellis, M., Hong, J.-W., Nechaev, S., Adelman, K., Levine, M., and Young, R.A. (2007). RNA polymerase stalling at developmental control genes in the Drosophila melanogaster embryo. Nat. Genet. 39, 1512–1516.

Zhang, Y., Liu, T., Meyer, C.A., Eeckhoute, J., Johnson, D.S., Bernstein, B.E., Nusbaum, C., Myers, R.M., Brown, M., Li, W., et al. (2008). Model-based analysis of ChIP-Seq (MACS). Genome Biol. 9, R137.

Zhong, B., Lama, R., Ketchart, W., Montano, M.M., and Su, B. (2014). Lead optimization of HMBA to develop potent HEXIM1 inducers. Bioorg. Med. Chem. Lett. 24, 1410–1413.

Zhou, Q., and Yik, J.H.N. (2006). The Yin and Yang of P-TEFb Regulation: Implications for Human Immunodeficiency Virus Gene Expression and Global Control of Cell Growth and Differentiation. Microbiol Mol Biol Rev 70, 646–659.

Zhou, Q., Li, T., and Price, D.H. (2012). RNA Polymerase II Elongation Control. Annu. Rev. Biochem. 81, 119-143.

Zhu, Y., Pe'ery, T., Peng, J., Ramanathan, Y., Marshall, N., Marshall, T., Amendt, B., Mathews, M.B., and Price, D.H. (1997). Transcription elongation factor P-TEFb is required for HIV-1 tat transactivation *in vitro*. Genes Dev. 11, 2622–2632.